Climate change is associated with a higher extinction risk of a subshrub in anthropogenic landscapes

A manuscript for consideration as a Research Article for publication in Journal of Ecology

Eva Conquet[1]*, Arpat Ogzul[1], Susana Gómez-González[2,3], Fernando Ojeda[2], Maria Paniw[1,4]

1. Department of Evolutionary Biology and Environmental Studies, University of Zurich, Zurich 8057, Switzerland

2. Departamento de Biología-IVAGRO, Universidad de Cádiz, Campus Río San Pedro, 11510 Puerto Real, Spain

3. Center for Climate and Resilience Research, (CR)2, Santiago, Chile

4. Department of Conservation and Global Change, Doñana Biological Station (EBD-CSIC), Seville 41092, Spain

Author's ORCID IDs:
Eva Conquet: 0000-0002-8047-2635
Arpat Ozgul: 0000-0001-7477-2642
Susana Gómez-González: 0000-0002-3779-8701
Fernando Ojeda: 0000-0001-5480-0925
Maria Paniw: 0000-0002-1949-4448

* Corresponding author's email address: eva.conquet@gmail.com

Word count (abstract through references): 12010
Number of citations: 103
Number of tables in main document: 0
Number of figures in main document: 5

Acknowledgments

We are grateful to all the helpers who have contributed to the data collection. We are thankful to the Parque Natural Los Alcornocolas, who kindly granted authorisation for fieldwork on their premises, and to the Spanish military Campo de Adiestramiento de la Armada in Sierra del Retín (Cádiz), who granted access to some study populations. We acknowledge the E-OBS dataset from the EU-FP6 project UERRA (https://www.uerra.eu) and the Copernicus Climate Change Service, as well as the data providers in the ECA&D project (https://www.ecad.eu). EC was supported by a Swiss National Science Foundation Grant (31003A_182286) to AO. MP was funded by the grant RYC2021-033192-I by MCIN/AEI/10.13039/501100011033 and "European Union NextGenerationEU/PRTR". SG-G was funded by the Agencia Estatal de Investigación (Spain; PID2019-106908RA-I00/AEI/10.13039/501100011033) and ANID/FONDAP (Chile; 1522A0001).

Author Contributions

Eva Conquet: Conceptualization, Methodology, Software, Validation, Formal analysis, Investigation, Data curation, Writing - Original Draft, Writing - Review and Editing, Visualization. **Arpat Ozgul:** Conceptualization, Methodology, Resources, Writing - Review and Editing, Supervision, Project administration, Funding acquisition. **Susana Gómez-González:** Validation, Investigation, Resources, Writing - Review and Editing. **Fernando Ojeda:** Investigation, Resources, Writing - Review and Editing, Supervision, Project administration, Funding acquisition. **Maria Paniw:** Conceptualization, Methodology, Software, Validation, Formal analysis,

Investigation, Data curation, Writing - Original Draft, Writing - Review and Editing, Supervision, Project administration, Funding acquisition.

Data and Code Availability Statement

The data necessary for reproducing results and graphs presented in this study are available on GitHub (https://github.com/EvaCnqt/DewyPinesLandUseClimateChange) and Zenodo 10.5281/zenodo.16370814 (Conquet et al. 2025). Original data can be requested from Maria Paniw (maria.paniw@ebd.csic.es). Code for formatting data, implementing and running models and analyses, and plotting results is available on GitHub: https://github.com/EvaCnqt/DewyPinesLandUseClimateChange. The version of code used for this study is archived on Zenodo 10.5281/zenodo.16370814 (Conquet et al. 2025).

Conflict of Interest Statement

The authors declare no conflict of interest.

Statement on Inclusion

Our work was performed in collaboration with scientists based in the country where the study was initiated and carried out. The perspective of locally based authors who have strong experience with the focal system was paramount to ensure our

conclusions took into account the local context. Additionally, we relied on literature previously published by scientists from the region.

Abstract

1. In most ecosystems, the increasingly strong effects of climate change on biodiversity co-occur with other anthropogenic pressures, most importantly land-use change. However, many long-term demographic studies focus on populations monitored in protected areas, and our understanding of how climate change will affect population persistence under anthropogenic land use is still limited.
2. To fill this knowledge gap, we assessed the consequences of co-occurring land-use and climate change on vital rates and population dynamics of a fire-adapted Mediterranean carnivorous subshrub, the dewy pine (*Drosophyllum lusitanicum*). We used seven years of individual data on 4,753 plants monitored in three natural heathland sites that experience primarily fire as a disturbance, and five anthropogenic sites, where fires have been replaced by persistent disturbances from browsing or mechanical vegetation removal as a consequence of land-use change. All sites are projected to experience increasingly hotter summers and drier falls and winters. We used generalised additive models to model non-linear responses of survival, growth, and reproduction to rainfall, temperature, size, density, and time since fire in anthropogenic and natural dewy-pine populations. We then projected population dynamics under climate-change scenarios using an individual-based model.
3. Our findings reveal that vital rates respond differently to climate change in anthropogenic compared to natural habitats. While extinction risks did not change under climate change in natural habitats, future higher summer

temperatures decreased survival and led to population declines and higher extinction probabilities in anthropogenic habitats.

4. *Synthesis*: Our results highlight the possible dramatic effects of climate change on populations largely confined to chronically disturbed, anthropogenic habitats and provide a foundation for devising relevant management strategies aiming towards the protection of species in human-disturbed habitats of the Mediterranean habitat. Overall, our findings emphasise the need for more long-term studies in managed landscapes.

Keywords

plant population and community dynamics, anthropogenic landscape, climate change, land-use change, disturbance regime, fire adaptation, Mediterranean habitat, population persistence

Introduction

Land-use change has been identified as the most important driver of biodiversity declines in most ecosystems (Sala et al., 2000; Díaz et al., 2019; IPBES, 2019). Across the globe, human expansion has caused habitat loss and fragmentation through the modification of lands for urbanisation or agricultural purposes (Foley et al., 2005), with dire consequences on local and regional species persistence (Selwood et al., 2015) and cascading effects at the community and ecosystem levels (Garnier et al., 2007; Kampichler et al., 2012; Alberti, 2015). Meanwhile, the effects of land-use change on species are increasingly compounded

by more severe impacts of climate change on natural systems (Brook et al., 2008; Mantyka-Pringle et al., 2012; Oliver & Morecroft, 2014).

The complex interplay of land-use and climate change is reshaping ecosystems at an unprecedented rate, with profound implications for the persistence of many species (Pereira et al., 2024). Nonetheless, many studies assess the persistence of populations under climate change in protected areas (Murali et al., 2022)—which are generally sheltered from anthropogenic land use and habitat loss (Geldmann et al., 2013; Watson et al., 2014; but see Clark et al., 2013), and where populations are thus overall doing better than those outside protected regions (Geldmann et al., 2013; Gray et al., 2016). This means that, in many studies, the key role of land-use change in shaping the response of populations to changes in climate is omitted (Titeux et al., 2016). Land-use and climate change can have reciprocal effects on each other, leading to non-additive effects of these pressures on populations and communities (Brook et al., 2008; Mantyka-Pringle et al., 2012; Oliver & Morecroft, 2014; Montràs-Janer et al., 2024). Thus, the effects of climate change might differ among land use types, and the consequences of land-use change could depend on the strength of climate change (Mantyka-Pringle et al., 2012). Understanding these dynamics beyond the confines of protected areas is crucial for devising effective conservation strategies.

Land-use, climate change, and their interaction (Brook et al., 2008) can affect populations via changes in key vital rates through multiple mechanisms such as inbreeding depression (Leimu et al., 2010; Bijlsma & Loeschcke, 2012), physiological stress (Selwood et al., 2015), or phenotypic selection (Alberti, 2015). Negative

158 effects of climate change on survival could be exacerbated by anthropogenic land
159 use, as habitat fragmentation could hamper individual dispersal, thereby preventing
160 populations to shift their habitat range to respond to the new conditions arising under
161 climate change (Lawson et al., 2010; Oliver & Morecroft, 2014). Additionally,
162 negative correlations between adaptations to land use and to climate change could
163 cause the selection for the tolerance of one pressure to reduce the capacity to adapt
164 to the other (Chevin et al., 2010; Oliver & Morecroft, 2014). As population sizes
165 decrease, these detrimental effects could be amplified through demographic
166 stochasticity and inbreeding depression (Fagan & Holmes, 2006), as a decrease in
167 genetic variability and its subsequent fitness reduction would lower the capacity of
168 individuals to cope with challenging environmental conditions (Leimu et al., 2010;
169 Bijlsma & Loeschcke, 2012). Nonetheless, in face of the prevalence of negative
170 effects of both anthropogenic land use and climate change, and given their
171 interacting effects on demographic parameters (Brook et al., 2008; Titeux et al.,
172 2016) and biodiversity (Montràs-Janer et al., 2024), exhaustively assessing
173 population persistence under changing climatic conditions requires studying
174 populations in anthropogenic landscapes.
175
176 Mediterranean biomes are among the most sensitive to interacting pressures derived
177 from land-use and climate change (Newbold et al., 2020). In these ecosystems, fire
178 is a recurrent disturbance that has shaped plant traits over evolutionary time (Keeley
179 et al., 2012) and is essential to the functioning of ecosystems (Pausas & Bond,
180 2020). However, many fire-adapted plant species in the Mediterranean Basin are
181 now largely found in anthropized habitats where fire regimes have been substantially
182 altered or suppressed altogether by changes in land use (Pausas & Keeley, 2014;

Ojeda 2020), which can have strong impacts on plant population dynamics (Paniw, Quintana-Ascencio et al., 2017) and wider ecosystem processes, such as nutrient cycling (Pausas & Bond, 2020). Mediterranean plant populations are also increasingly exposed to shorter and drier winters and hotter summers, jeopardising the persistence of shrubland communities (Paniw et al., 2021). While the effects of human activities in fire-disturbed habitats on plant population persistence have previously been studied (e.g. Paniw, Quintana-Ascencio et al., 2017), we still lack a full understanding on population dynamics under the interacting pressures of land-use and climate change.

Here, we use a Mediterranean, fire-adapted subshrub, the dewy pine (*Drosophyllum lusitanicum*), as a case study to investigate the effects of changing climatic conditions on population dynamics in natural and anthropogenic habitats. We used seven years of individual-based data, collected as part of long-term demographic monitoring (since 2011) in natural and anthropogenic (i.e., highly human-dominated permanently disturbed sites) habitats, to parameterize vital-rate responses to interacting climate (temperature and rainfall) and biotic (plant size and intraspecific density) drivers and project resulting population dynamics under climate-change scenarios. We expected higher extinction probabilities in anthropogenic habitats under current climatic conditions, as previous research has shown human disturbances to have a negative effect on population dynamics (Paniw, Quintana-Ascencio et al., 2017; Conquet et al., 2023), and such disturbances are likely to persist in Mediterranean heathlands (Ojeda, 2020). Additionally, given the negative effects of compound anthropogenic pressures on natural systems (Zscheischler et

al., 2018), we expected sharper declines in anthropogenic populations than in natural ones under climate change.

Methods

Study species

Life history

The dewy pine, *Drosophyllum lusitanicum* (Drosophyllaceae), is a rare carnivorous subshrub endemic to the western end of the Mediterranean basin and tightly associated to fire-prone Mediterranean heathlands of southern Spain, Portugal, and northern Morocco (Correia & Freitas, 2002; Garrido et al., 2003; Paniw et al., 2015). As with many species in fire-prone habitats, dewy pines have adapted their life history to persist under recurring fire regimes that remove all aboveground vegetation. Populations rely on a persistent soil seedbank (Fig. 1), whose dynamics strongly vary with time since fire (TSF_t, where t is the number of years after a fire; Paniw, Quintana-Ascencio et al., 2017; Conquet et al., 2023). When a fire occurs (TSF_0), the combined effect of heat and vegetation and litter removal trigger the germination of the major part of seeds stored in the seedbank (Fig. 1; Appendix S1: Table S1; Cross et al., 2017; Paniw, Quintana-Ascencio et al., 2017; Gómez-González et al., 2018). Germination from the seedbank continues in later post-fire years but greatly decreases from TSF_2. New seedlings mostly grow during the first year after a fire (TSF_1) and become reproductive plants from the second year after the population burned (TSF_2; Fig. 1). The majority of seeds produced by these

individuals do not germinate directly but go to the soil seedbank to replenish the population at the next fire (Fig. 1). This occurs because dewy pines are increasingly overgrown by dominant shrub vegetation, which hinders seed germination (Gómez-González et al., 2018) and insect prey capture (Paniw et al., 2018), drastically decreasing the survival of aboveground plants after TSF_4 (Paniw et al., 2015).

Despite being fire-adapted, active fire suppression and general degradation of heathland habitats under land-use change (for instance through vegetation removal for wide firebreaks or pine afforestations) mean that most populations of dewy pines as well as numerous other heathland species persist in highly and permanently human-disturbed (hereafter anthropogenic) habitats (Paniw et al., 2015) (see Appendix 2: Table S1 for details on study populations). In such habitats, periodic mechanical clearing of vegetation or browsing—of surrounding vegetation but not on dewy pines—and trampling by domestic ungulates act as a constant disturbance resembling the effect of fire by the removal of aboveground vegetation, but lasting much longer. This has led to important changes in the demographic processes of dewy pines (Paniw, Quintana-Ascencio et al., 2017; Conquet et al., 2023). Seedbanks in chronically disturbed, anthropogenic populations are likely depleted because the long-term clearance of vegetation means that relatively more seeds germinate immediately instead of going into the seedbank (Appendix S1: Table S1; Gómez-González et al., 2018). Vital rates of aboveground individuals are affected as well; while juvenile survival rapidly decreases after a fire in natural populations, it remains stable across time under human disturbances. However, smaller mature individuals in anthropogenic populations have a lower survival than in natural

populations, and reproduction is decreased as well. Moreover, negative density feedbacks are stronger in anthropogenic populations (Conquet et al., 2023).

Anthropogenic pressures in dewy pine habitats are also increasingly interacting with climate change. Temperatures have been increasing in the last four decades (on average by 0.033 ºC per year) and will continue to do so in the future (Appendix S2: Fig. S1 and S2). Contrastingly, while the recent increase in rainfall variability is predicted to reverse, rainfall is forecasted to be less abundant in the future (-0.16 mm per year on average). Such variations in environmental patterns have already shown to lead to population declines in natural shrublands (Paniw et al., 2023). Dewy pines will therefore likely be increasingly affected by interactions of climate change and human disturbance. Therefore, understanding their response to climate effects will help us discern the joint role of different pressures on plants persisting in anthropogenic habitats.

Demographic data

We used individual demographic data collected on 4753 dewy pines from eight populations of southern Spain, located in two types of habitats: Mediterranean heathlands experiencing recurrent fire regimes and low levels of anthropogenic pressures such as cattle browsing and trampling (natural populations; n = 3); and Mediterranean heathlands that have not burned in the past 40 years but where high anthropogenic pressures constantly remove aboveground vegetation (anthropogenic populations; n = 5) (Appendix S2: Table S1). In each population, we obtained information on size, reproduction (probability of flowering and number of flowers), and

281 survival from individually marked plants located in 40 1×1m plots; all individuals,
282 including new recruits, in a given plot were marked and censused every spring in the
283 last week of April or first week of May (see Appendix S1 for details). The Andalusian
284 Consejería de Medio Ambiente issued the requisite permits to undertake fieldwork
285 (permit number Rs-33/13).

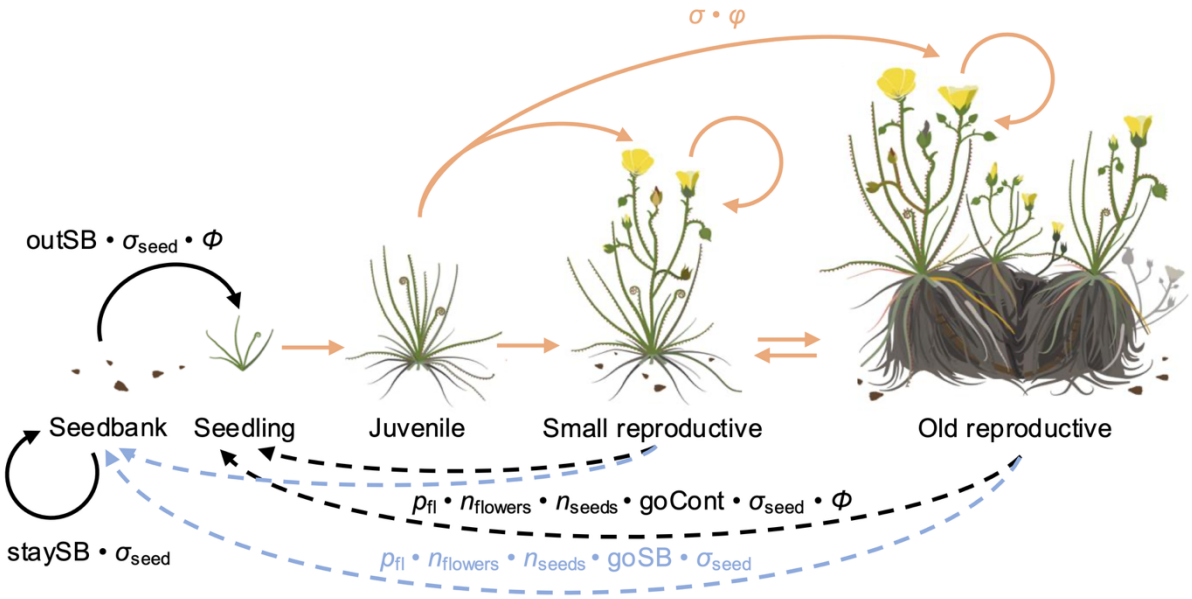

286 **Figure 1 – Dewy-pine life cycle.** Conditional on seed survival (σ_{seed}), seeds in
287 the seedbank germinate, with germination probability outSB, to become seedlings of
288 a given size (Φ), or remain dormant underground (staySB). Aboveground individuals
289 then survive (σ) and grow (φ), depending on their size (size-dependent survival and
290 growth is highlighted in orange); and become reproductive from two years after a fire
291 occurred in natural habitats. Reproductive individuals produce seeds conditional on
292 size-dependent flowering probability (p_{fl}), the number of flowers ($n_{flowers}$), and the
293 number of seeds per flower (n_{seeds}). These seeds, conditional on their survival (σ_{seed}),
294 either germinate directly (goCont; dashed black arrows) and become seedlings of a
295 given size (Φ) or contribute to the underground seedbank (goSB; dashed blue arrow).
296

Estimation of seedbank parameters

To parameterize variation among different habitat types in probabilities of seed germination (goCont for seeds germinating without going to the seedbank and outSB for seeds germinating from the seedbank), dormancy (staySB) and transition to the seedbank (goSB) (Fig. 1), we used published data from seed-burial and greenhouse germination experiments (Paniw, Quintana-Ascencio et al., 2017; Gómez-González et al., 2018). Previous research has shown that in natural populations, most produced seeds (97.4%; 95% confidence interval [96.3%–98.4%]) go to the underground seedbank (Appendix S1: Table S1). While 81% [77.4%-85.2%] of the seeds germinate from the seedbank right after a fire (TSF_0), that proportion greatly decreases in later post-fire habitat stages (6.09% [4.44%–7.75%] in TSF_1 and 3.47% [2.31%–4.63%] in later TSFs). In contrast, in chronically disturbed, anthropogenic populations, a much lower proportion of the produced seeds goes to the seedbank (82.2% [65.3%–97.5%]). In these populations, although 59.8% [56.6%–63.0%] of the underground seeds remain underground, seedbanks are depleted due to the decreased proportion of seeds produced by aboveground plants entering dormancy.

Estimation of aboveground vital rates

We investigated how rainfall, temperature, and density affect the survival, growth, and reproduction of individuals, for natural and anthropogenic dewy-pine populations separately (Appendix 2: Table S1). We used Generalised Additive Models—fitted with the *gam* function of the mgcv package (Wood, 2011; Wood et al., 2016; Wood, 2017)—to estimate (1) survival (σ) and flowering probability (p_{fl}) (using a binomial

distribution), (2) the number of flowers per individual ($n_{flowers}$; using a negative binomial distribution instead of a simple Poisson model as the data were overdispersed), and (3) growth (φ) and seedling size (Φ), with size = log(number of leaves × length of the longest leaf (cm)) (Fig. 1; Paniw, Quintana-Ascencio et al., 2017). We modelled the latter two vital rates using a scaled *t* distribution ("scat" in the family parameter of the *gam* function) instead of a Gaussian distribution to accommodate the heavy-tailed nature of the response variables (see Appendix 1: Table S4). We tested for the nonlinear responses of all vital rates to lag cumulative rainfall and average daily maximum temperature, and aboveground density of large (i.e., size > 4.5) intraspecific neighbours. In addition, to account for effects of post-fire habitat stages, we tested for nonlinear effects of time since fire (TSF) on vital rates of natural populations. We used a cubic spline basis with three dimensions (k = 3) for all these covariates (except for the size effect on the number of flowers, where we used k = 4 to model a decline in the number of flowers of large individuals as has been observed in all populations), and a gamma value of 1.4, as is commonly used to reduce the risk of overfitting (Wood, 2017). We also included random year and population effects on the model intercept in all models using a random-effect spline. We performed all analyses in R 4.2.2 via RStudio (R Core Team, 2022; Posit team, 2023).

Vital-rate responses to climatic variables (cumulative rainfall and average maximum daily temperature)

We chose rainfall and maximum temperatures as climatic predictors based on recent publications showing the importance of these two drivers on vital rates of

Mediterranean plants (García-Callejas et al., 2017; Paniw et al., 2023) and based on our a priori expectations given the biology of the study species (Appendix 1: Table S2). We extracted daily rainfall and maximum temperature data with a resolution of 0.1 degree for all dewy-pine population locations from the E-OBS dataset from the EU-FP6 project UERRA and the Copernicus Climate Change Service (Cornes et al., 2018; see Appendix S2 for details). We obtained the monthly cumulative rainfall and average maximum temperature in each population by averaging the values recorded within a buffer of 0.1×1.5 degrees (i.e. 1.5 times the grid resolution) around the population coordinates. We assessed the presence of rainfall and temperature lag effects on dewy-pine vital rates using GAMs including cumulative rainfall and average maximum daily temperature across several biologically relevant periods. We defined these periods based on prior knowledge of seasonal climatic effects in Mediterranean shrublands (Paniw et al. 2023; Appendix 1, Table S2); and did not use a sliding-window approach to assess lagged effects to avoid spurious correlations (Evers et al., 2021). For survival and growth, we assessed the effect of climate following the annual population census (set to the 1st of May), while for reproductive parameters (i.e., flowering probability, number of flowers, and seedling size), we assessed the effect of climate in periods prior to the census. More specifically, we considered the effect of post-census average maximum temperature in summer (May–September) and of cumulative rainfall in fall (September–November), winter (January–April), or both (September–April), on survival and growth. We tested for the effect of pre-census average maximum daily temperature in winter (January–April), and of cumulative rainfall in fall (September–November) and winter (January–April) on reproductive rates. We considered that the effects of longer lag periods are effectively absorbed by changes in plant size.

Vital-rate responses to large aboveground individual density

To understand how intraspecific interactions affect dewy-pine vital rates, we included in our models the density of aboveground individuals, specific to a 1-m^2 quadrat in a given population. This spatial resolution matches the study design—where plants are censused in four transects of ten 1-m^2 quadrats (Paniw, Quintana-Ascencio et al., 2017)—and corresponds to the observed scale at which the plant-plant interactions affecting the demography of dewy pines occur. We only considered individuals of size > 4.5, which corresponds to the minimum observed size of reproductive plants. Smaller plants are largely seedlings which have relatively weak effects on plant vital rates, as large individuals are unlikely to be affected by small plants and small plants are primarily affected by large shrubs (Brewer et al., 2021). We did not use a spatially explicit formulation of density dependence (e.g. using the crowding approach described in Adler et al., 2010), as such an approach requires knowledge of the spatial distribution of individuals and seeds, which we lacked for some sites and years.

Vital-rate model selection

We selected the best vital-rate models using the Akaike Information Criterion (AIC, using a threshold of $\Delta AIC > 2$ to identify a model as performing better than another; Burnham et al., 2011; Wood, 2017) and the number of degrees of freedom. Prior to model selection, we standardised and checked for correlations between all covariates (see Appendix S1 for more details). We first selected the best lag period

for the effect of rainfall and temperature and then added—in a forward selection framework—density and size to the model selection and, for natural populations, time since last fire (Appendix S1: Table S3 for more details). We considered two-way interactions among the climatic variables, density, size, and TSF as well as site-specific random slopes (e.g., site-specific effects of density or size) in our model selection, using random-effect splines.

Population projections under climate change scenarios

Individual-Based Model definition

We used the estimated vital rates to parameterize an Individual-Based Model (IBM) and project each natural and anthropogenic dewy-pine population under current and predicted climate conditions. The following is a summary of the IBM specificities; a more detailed description of the different modules of the projection model following the ODD (Overview, Design concepts, Details) protocol (Grimm et al., 2006; 2020) can be found in Appendix S3. We performed 500 30-year projections of each dewy-pine population under two scenarios: (1) a control scenario corresponding to current climatic conditions where 30 years—and the corresponding rainfall and temperature values—were sampled at random among the past observed ones (2016–2021); and (2) two climate-change scenario where the rainfall and temperature values corresponded to projected climatic conditions from 2021 to 2050 according to the RCP4.5 and RCP8.5 climate-change scenarios (Riahi et al., 2011). The climate-change scenario comprised 11 sets of 500 population projections, each set corresponding to future rainfall and temperature conditions extracted from 11 global

circulation models (GCM; Appendix S2: Table S2) from the Coupled Model Intercomparison Project 6 (CMIP6; Eyring et al., 2016; Pascoe et al., 2020; Waliser et al., 2020) available from the Earth System Grid Federation's (ESFG; Petrie et al., 2021) web application accessible at https://aims2.llnl.gov/search. These models have been used in several studies on ecological systems (Tredennick et al., 2016; Paniw et al., 2022) and differ in their parameterisation, enabling us to project the dewy-pine populations under a wide range of possible future climatic conditions and thereby reduce bias in our population projections (Sanderson et al., 2015).

Because most GCMs comprised projected rainfall and temperature values beyond the values observed in our populations, we capped these values to the maximum and minimum observed. This approach allowed us to investigate the response of dewy-pine populations to substantial increases in the frequency of extreme climatic conditions, rather than changes in absolute rainfall and temperature values.

Each population projection started with a population vector of z-sized individuals from 2021—the last year used to estimate vital rates—, and the initial population thus comprised individuals observed in the population in that year. This also applies to the initial rainfall and temperature values, and the aboveground density of large individuals. While we assumed no fire occurred in anthropogenic populations, we simulated a sequence of 30 post-fire habitat stages for each projection of natural populations. The first post-fire state corresponded to the one observed in 2021, and the subsequent ones were determined based on a Markov matrix containing the among-TSF transition probabilities based on a fire frequency of 1/30 representing

446 the stochastic fire regime occurring in natural dewy-pine populations (see Appendix
447 S3 for details; see also Conquet et al., 2023).
448
449 We projected each initial population in discrete yearly steps determining which
450 aboveground individuals reproduced, survived, and grew, and how many seeds
451 germinated—from the seedbank or directly after reproduction—or entered or
452 remained in the seedbank. Each of these processes was represented by a sub-
453 model within the general IBM. As annual censuses took place during the flowering
454 period (pre-reproductive census), each projected year started with the reproduction
455 sub-model. This sub-model sampled reproductive individuals (0 or 1) based on a
456 binomial distribution parameterised with the estimated mean flowering probability
457 (p_{fl}). If any individual reproduced, its number of flowers was sampled from a negative
458 binomial distribution based on the estimated mean number of flowers per plant
459 ($n_{flowers}$); and the number of seeds per flower (n_{seeds}) was sampled from a Poisson
460 distribution with a mean of 9.8—the average number of seeds per flower used in
461 Paniw et al. (2017). To avoid excessive reproductive values in natural populations,
462 we capped the number of flowers per individual to the maximum observed number of
463 flowers in each population. In natural populations, where fires could occur, the
464 reproduction sub-model was skipped in the first year after fire, as dewy pine adults
465 are killed by fire and postfire recruits do not reproduce until two years after
466 germination.
467
468 The reproduction sub-model was followed by the survival and growth sub-model,
469 which sampled the surviving individuals from a binomial distribution based on the
470 mean estimated survival rate, and assigned them a size to which they would grow at

471 the next time step by sampling from a scaled *t* distribution (to accommodate for
472 heavy-tailed size values when fitting the growth model) based on the mean, standard
473 deviation, and degrees of freedom of the fitted growth model. Sporadically sampled
474 positive infinite sizes were set to the maximum observed size in the population in the
475 currently projected year, while negative infinite sizes were set to zero.
476
477 Finally, at the end of each projected year, the seedbank sub-model sampled seeds
478 from the seedbank that remained dormant or germinated from binomial distributions
479 based on the respective probabilities (staySB and outSB). The seeds that did not
480 survive—i.e., neither germinated or stayed dormant—were removed from the
481 seedbank. The seeds germinating without going through the seedbank were
482 sampled from a binomial distribution based on the probability of continuous
483 germination (goCont). Some seedbank processes are hidden processes that cannot
484 be easily determined in the field without perturbing the populations. To reduce the
485 resulting bias, we applied a correction factor representing seed survival (σ_{seed}) to the
486 seedbank parameters in anthropogenic populations (see Appendix S1 and Paniw,
487 Quintana-Ascencio et al., 2017 for more details), and further corrected outSB and
488 goCont in Sierra Carbonera Disturbed by reducing them to 40 % of their values. We
489 also capped the number of recruits to the maximum number of seedlings observed in
490 all natural populations as well as in two anthropogenic populations: Bujeo and Sierra
491 Carbonera Disturbed. Ultimately, all recruits were assigned a size by sampling from
492 a scaled *t* distribution based on the estimated mean seedling size as well as its
493 standard deviation and degrees of freedom.
494

At the end of a projected year, we updated the size of individuals that grew during the previous year as well as the aboveground density for each 1-m^2 quadrat in the population. We also calculated and recorded the annual population growth rate (annual log λ), which we used to calculate the stochastic growth rate log λ_S for each projection (see Appendix S3 for more details; see also Conquet et al., 2023). In each projection, the population was considered extinct if it went below the quasi-extinction threshold set at 5 aboveground individuals and 50 seeds in the seedbank.

Model validation

We calibrated our vital-rate and individual-based models by projecting each dewy-pine population from the year it was first censused to 2022. We then compared observed and projected aboveground population sizes and population growth rates, as well as individual size distributions across time. For natural populations, we used the observed post-fire habitat stages and did not simulate fire frequencies. This process enabled us to validate our IBM by assessing its ability to well represent the dynamics of the dewy-pine populations in years that were not used in the model-fitting part of our analysis (i.e., years before 2016 when available, and 2022).

Sensitivity analyses

We assessed which demographic rates contribute most to changes in population dynamics under climate change in anthropogenic and natural populations. To do so, we repeated climate-change projections, as described in the previous section, for each population, but we changed climatic drivers under the RCP 8.5 climate-change

scenario in specific vital rate models only (survival, growth, flowering probability, number of flowers or seedling size), while assuming current climatic conditions in the remaining vital rates. We performed 100 30-year projections, and calculated sensitivities as:

$$\text{Sensitivity} = \frac{\sum_{i=1}^{n=100}(\log \lambda_{S\_perturbed\_i} - \log \lambda_{S\_control\_i})/\log \lambda_{S\_control\_i}}{n},$$

where i = one of 100 log λ_S, and log $\lambda_{S\_control}$ represent population dynamics assuming current climatic conditions in all vital rates. We calculated 500 sensitivity values for each population by randomly sampling 100 log $\lambda_{S\_control}$ from the 500 available and comparing them to the 100 available log $\lambda_{S\_perturbed}$.

Results

Vital-rate responses to habitat disturbance

Dewy-pine vital rates varied between natural and anthropogenic habitats (Fig. 2). Survival was on average higher in anthropogenic (mean = 0.42 and 95% confidence interval = [0.18, 0.70]) than in natural habitats (0.27 [0.17, 0.40]; Fig. 2). In contrast, we found the opposite pattern for growth (i.e., plant size at t+1), which was higher in natural (size 5.0 [4.7, 5.2] at the next time step, calculated as log(number of leaves × length of the longest leaf (cm))) than in anthropogenic sites (4.7 [4.4, 4.9]), as well as flowering probability (0.039 [0.013, 0.11] in natural and 0.025 [0.013, 0.045] in anthropogenic populations), and seedling size (3.4 [3.2, 3.5] and 3.0 [2.8, 3.3], respectively; Fig. 2). However, there was no difference between

habitat types in the number of flowers per individual (6.9 [6.2, 7.7] on average in natural populations and 6.7 [5.8, 7.8] in anthropogenic populations; Fig. 2). Notably, we found more among-site variation in anthropogenic than in natural conditions, possibly because the level of anthropogenic disturbance differed between sites (Appendix S1: Fig. S3).

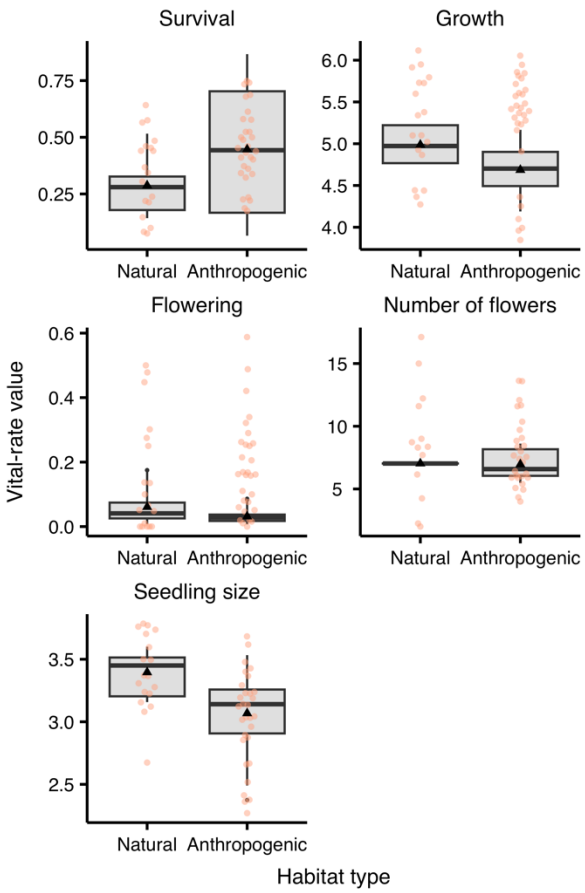

Figure 2 – Predicted and observed average vital-rate values in natural and anthropogenic populations. The boxplots represent the distribution of the predicted average values of habitat-specific survival, growth, i.e., log(number of leaves × length of the longest leaf (cm)), and flowering rates, as well as the number of flowers and seedling size estimated for each population and year from GAMs. The whiskers represent the 2.5th and 97.5th percentiles and the black triangle the mean estimate. We kept covariates at their mean values (scaled value = 0) except for the number of flowers, where we used the mean size of reproducing individuals. The coloured dots represent the observed average vital rates in each population and year.

Vital-rate responses to climatic variables

In both anthropogenic and natural habitats, the variation of most vital rates was associated with changes in at least one of the two climatic variables considered in our analysis: monthly cumulative rainfall (hereafter rainfall) or monthly average daily maximum temperature (hereafter temperature) (Fig. 3; Appendix S1: Table S4). Most vital rates were more strongly associated with the same climatic variable in the same period of the year in both habitats (e.g. variation in survival was associated with changes in summer temperatures and fall rainfall in both natural and anthropogenic populations). Overall, larger variations in vital rates were associated with changes in temperature than with rainfall (Fig. 3; Appendix S1: Table S4).

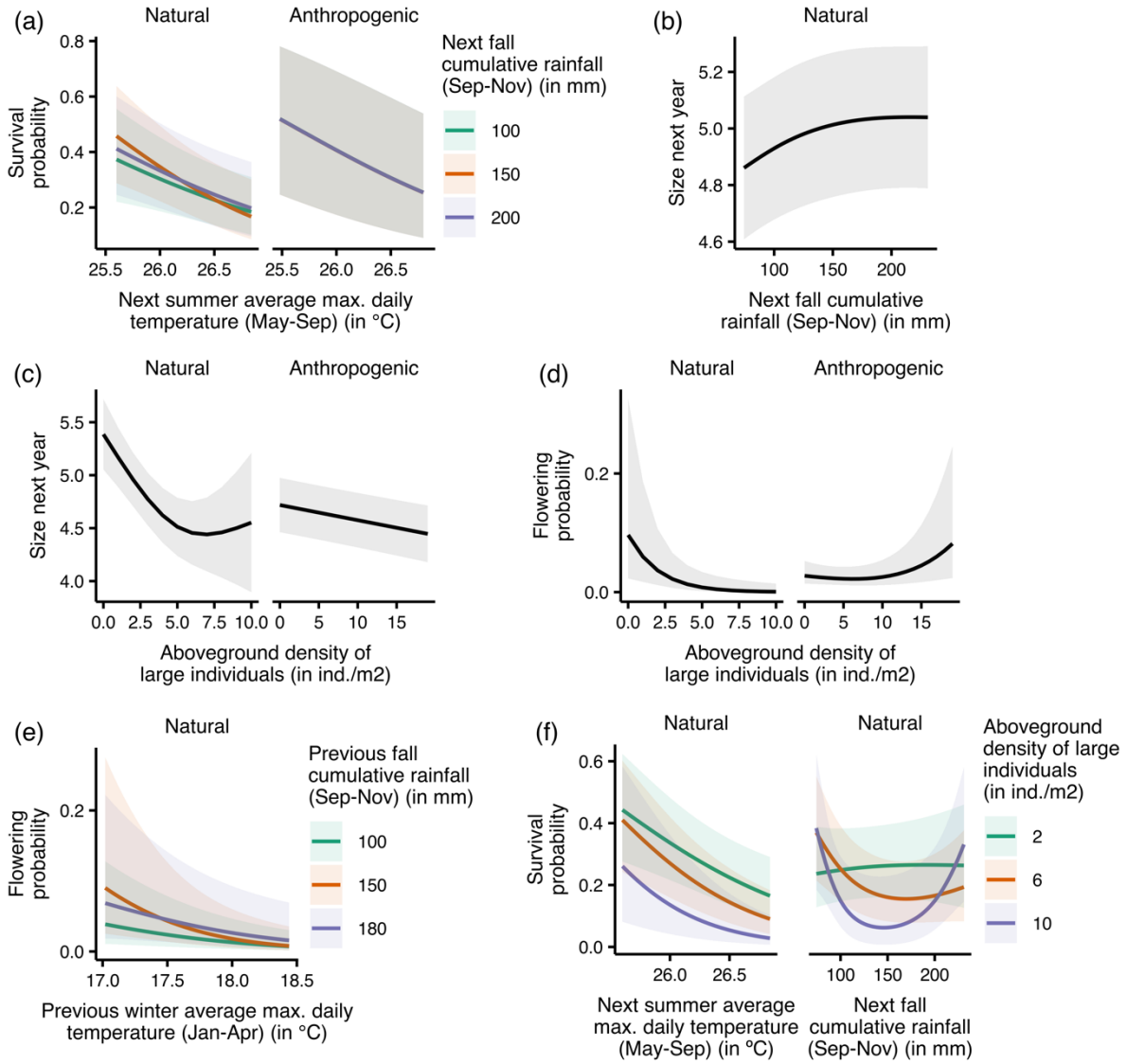

582 **Figure 3 – Relationships between dewy-pine vital rates and climatic**
583 **variables and aboveground density of large individuals.** Predictions from the
584 GAM models show variation in (a) survival and (b) flowering probability with changes
585 in temperature (next summer and previous winter, respectively) and rainfall (next and
586 previous fall), (c) flowering probability with changes in previous fall rainfall and
587 density, and growth, i.e., log(number of leaves × length of the longest leaf (cm)), with
588 (d) changes in next fall rainfall, and (e) aboveground density of large individuals (size
589 > 4.5). Lines show the mean vital-rate values and shaded areas the associated 95%
590 confidence interval.
591

In both natural and anthropogenic populations, survival was the only vital rate for which variation was associated with changes in both rainfall and temperature (i.e., the fixed effects of both climatic variables were retained in the model selection). With all other covariates held constant at their average value in the respective habitat types, survival was negatively associated with an increase in summer temperatures (i.e., average maximum daily temperature from May to September) (Fig. 3a). For example, when temperature increased from 25.5 to 26.5 °C, the average survival rate decreased from 0.47 [0.29, 0.66] to 0.23 [0.14, 0.35] in natural populations, and from 0.51 [0.24, 0.78] to 0.31 [0.12, 0.60] under anthropogenic conditions. In both habitats, variation in survival was also associated with changes in the amount of rainfall in fall (i.e., September–November; Fig. 3a, Appendix S1: Table S4 and Fig. 6e). In natural populations, this association was on average positive (from 0.25 [0.14, 0.39] under 80 mm of rain to 0.28 [0.16, 0.45] under 200 mm). In contrast, in anthropogenic populations, average survival across sites did not change with rainfall, but investigating this relationship at the site level revealed important among-population variability, with positive associations in some sites (e.g. from 0.39 [0.16, 0.67] under 80 mm of rain to 0.46 [0.21, 0.74] under 200 mm in Sierra del Retín Disturbed) and negative associations in others (e.g. from 0.46 [0.21, 0.74] to 0.36 [0.15, 0.65] in Prisioneros; Appendix S1: Fig. S3). Such among-site differences were almost ubiquitous across vital rates in anthropogenic populations (Appendix S1: Fig. S4), but not in natural habitats. For example, on average across all natural sites, individuals grew more with higher amounts of rainfall. More specifically, the longest leaf of an average-sized individual grew from 4.3 to 4.9 [4.6, 5.1] in a year under 80 mm of rain but to 5.0 [4.8, 5.3] under 200 mm (Fig. 3b).

Vital-rate responses to aboveground density of large plants

In both anthropogenic and natural habitats, plants grew less when densities of large individuals increased (Fig. 3c). Under human disturbance, an average-sized individual grew from 4.1 to 4.7 [4.4, 4.9] in a year with 2 large individuals/m^2 but to 4.6 [4.3, 4.8] with 10 ind./m^2 (Fig. 3c). In natural conditions, an individual grew from 4.3 to 5.0 [4.7, 5.2] with a density of 2 ind./m^2 but only to 4.6 [3.9, 5.2] with 10 ind./m^2 (Fig. 3c). Seedling size also decreased with higher numbers of large individuals aboveground (Appendix S1: Fig. S5a). Interestingly, the direction of the association between density and flowering probability differed between habitat types, as the flowering rate was positively associated with density in anthropogenic populations (from 0.50 [0.28, 0.72] with 2 ind./m^2 to 0.65 [0.35, 0.86] with 15 ind./m^2), but strongly negatively in natural ones (from 0.68 [0.41, 0.87] with 2 ind./m^2 to 0.10 [0.013, 0.50] with 7 ind./m^2) (Fig. 3d).

Vital-rate responses to interactions between climate, density, size, and post-fire habitat conditions

In natural—but not in anthropogenic—populations, high amounts of rainfall mitigated the strength of the negative association between temperature and survival, which decreased from 0.48 [0.30, 0.67] at 25.5 ºC to 0.23 [0.14, 0.36] at 26.5 ºC under 150 mm of rainfall but only from 0.43 [0.26, 0.63] at 25.5 ºC to 0.25 [0.13, 0.41] at 26.5 ºC under 200 mm (Fig. 3a). We found a similar pattern for the association between previous winter temperatures and flowering probability, which

641 decreased from 0.72 [0.45, 0.89] at 17.5 ºC to 0.29 [0.076, 0.66] at 18.5 ºC with 150
642 mm of rain but only from 0.73 [0.43, 0.90] to 0.46 [0.15, 0.80] with 180 mm (Fig. 3e).
643
644 Additionally, in natural populations, survival increased with rainfall at low densities
645 (Fig. 3f; from 0.26 [0.16, 0.40] to 0.28 [0.16, 0.44] for 100 and 200 mm of rain at 2
646 ind./m2); but these variables had a u-shaped relationship at high densities, with
647 lowest survival rates reached for about 145 mm of rain (e.g. 0.076 [0.021, 0.24] at 10
648 ind./m2). The decline in survival with increasing summer temperatures was also
649 weaker at low (e.g. from 0.47 [0.29, 0.66] at 25.5 °C to 0.22 [0.14, 0.35] at 26.5 °C
650 with 2 ind./m2) than at high densities (from 0.45 [0.26, 0.65] to 0.14 [0.077, 0.25] with
651 6 ind./m2) (Fig. 3f). We also found density-dependent variation in flowering
652 probability and growth with rainfall and seedling size with temperature (Appendix S1:
653 Fig. S5). Additionally, the strength and direction of the association between survival
654 rates and both rainfall and temperature in natural populations were also size
655 dependent (Appendix S1: Fig. S6g,h).
656
657 ## Individual Based Model
658
659 ### *Population projections*
660
661 The projections of our individual-based model over the observed period
662 showed that our parameterization enabled us to correctly represent the population-
663 specific pattern of changes in mean annual change in aboveground population size
664 and of population abundance (Fig. 4; Appendix S1: Fig. S1). Additionally, observed

665 and projected time-varying size distributions were largely overlapping, with a slight
666 bias towards small individuals in some populations (Appendix S1: Fig. S2).
667 Discrepancies between projection and observed population dynamics
668 occurred both at observed abundance peaks and troughs, and this may in part be
669 explained by the fact that the GAMs parameterized to predict vital rates were
670 smoothed to avoid overfitting to extreme data values. This then constrained
671 estimates of population dynamics (Paniw et al. 2021), but, at the same time, did not
672 extrapolate the latter beyond biologically realistic values. In addition, discrepancies
673 between projection and observed population dynamics may also occur because our
674 models did not consider (due to a lack of data) other processes that may affect vital
675 rates and thus population dynamics, such as density dependent germination of
676 seeds from the seedbank or interspecific interactions (Brewer et al. 2021).
677
678
679
680
681
682
683
684
685
686
687
688
689

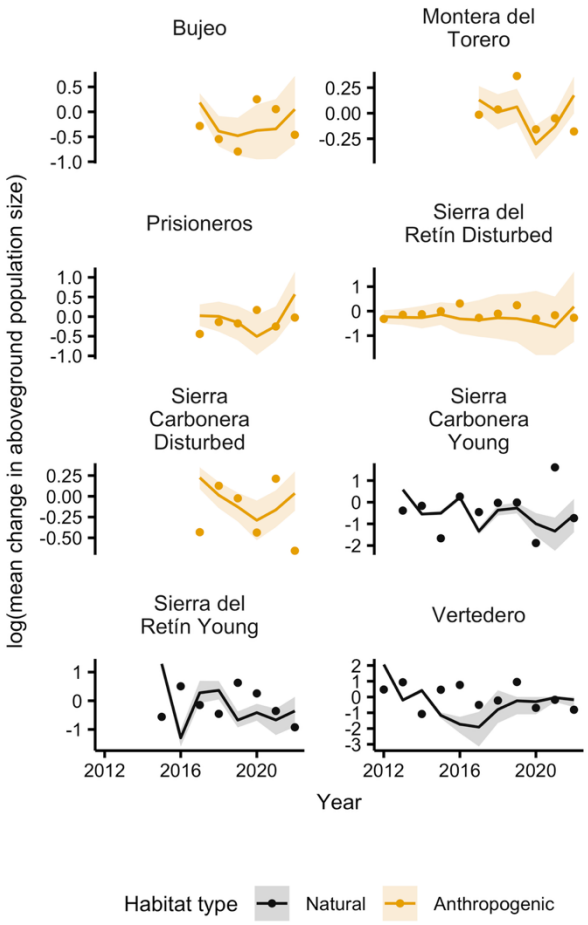

Figure 4 – Observed and projected average change in aboveground population abundance. We projected each natural and anthropogenic population for 500 times across the range of observed years available for each population (maximum range from 2011 to 2022) to perform an out-of-sample validation of our individual-based model parameterization. For each projection, we calculated the log of the average change in aboveground population abundance between years (i.e., $\log(N_t/N_{t-1})$ with N_t the aboveground population size in year t) and obtained the average (line) and 25th and 95th percentile of the population-specific distribution (shaded ribbon). We compared these projected values to the observed ones (dots).

Projecting natural and anthropogenic populations under a control scenario (i.e., assuming similar environmental conditions in the future as currently observed) showed that the average population growth rates (log λ_S) did not vary much between habitat types (mean = -0.15, 2.5 and 97.5% quantiles = [-0.62, 0.33] in natural and -0.19 [-0.89, 0.63] in anthropogenic populations; Fig. 5). On the other hand, the probability of quasi-extinction ($p_{q\text{-}ext}$) was on average higher in anthropogenic (0.56 [0.026, 1.0]) than in natural populations (0.17 [0.062, 0.26]). Extinction probabilities also varied much more among anthropogenic than among natural populations in the control scenario (Fig. 5). In natural populations, the stochastic fire regime in our projections increased the population growth rate substantially after fires, avoiding the quasi-extinction threshold (i.e., 5 aboveground individuals and 50 seeds in the seedbank) in simulations where fires occurred regardless of the population (Conquet et al., 2023). Anthropogenic populations, on the other hand, varied substantially in size, and the high variation in $p_{q\text{-}ext}$ reflects the consistently higher variation in dynamics among populations (Appendix S1: Fig. S7).

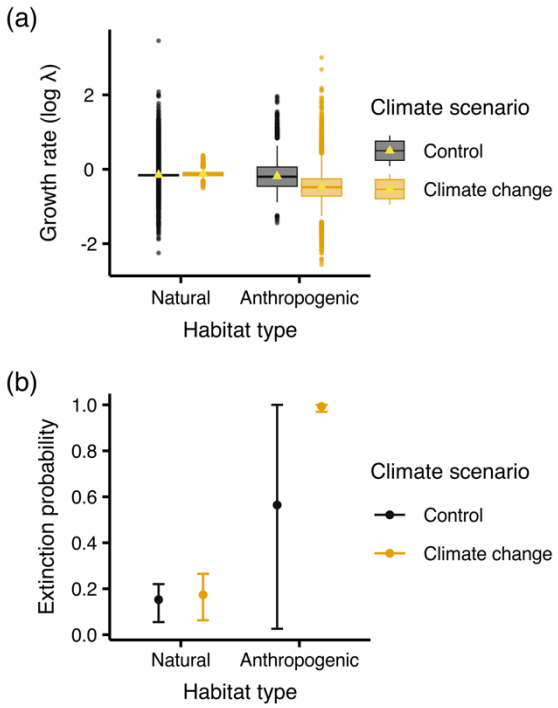

Figure 5 – Demographic consequences of climate change in natural and anthropogenic populations of dewy pines. We projected each natural and anthropogenic population 500 times for 30 years under a control (keeping temperature and rainfall conditions as currently observed) and two climate-change scenarios (RCP4.5 and RCP8.5). Here, results from scenario RCP8.5 are shown. To assess the demographic consequences of climate change in populations experiencing different levels of human disturbance, we computed for each population: (a) the stochastic population growth rate across 30 years for each population projection (log λ_S; including both the seedbank and aboveground individuals) and (b) the probability of quasi-extinction ($p_{q\text{-}ext}$). Here we summarise these metrics per habitat type, and the variability in the values therefore correspond to among-population and among-projection differences.

In contrast with the control scenario, population growth rates differed between habitats under climate change (Fig. 5). While the population growth rate (-0.12 [-0.28, 0.072]) and extinction probability (0.17 [0.070, 0.26]) of natural populations did not vary under climate change, under climate change scenario RCP8.5, our projections show a decrease in log λ_S in anthropogenic sites (-0.47 [-1.3, 0.45]), accompanied by an increase in the extinction probability (0.99 [0.97, 1.0]) (Fig. 5). Results were very similar for scenario RCP4.5 (Appendix S2: Fig. S3), highlighting that anthropogenic populations are at a high risk of local extinction even under moderate climate change. In anthropogenic habitats, changes in population dynamics under climate change were largely driven by the adverse effects of climate change on plant survival (Appendix S4: Figs. S1-S2). In natural habitats, climate change effects on survival and growth increased log λ_S in some populations, likely through compensatory density feedbacks, and only climate change effects on reproduction resulted in consistent decreases in log λ_S compared to the control scenario (Appendix S4: Figs. S1-S2).

Discussion

Our individual-based models projecting natural and anthropogenic populations of dewy pines using habitat-specific survival, growth, and reproductive rates revealed that the current decline of anthropogenic populations will worsen under climate change, leading to increased extinction risk. While the increasing frequency of extreme high summer temperatures affected both natural and anthropogenic populations negatively, occasionally high rainfall and compensatory density dependence greatly reduced this effect in natural populations. Under chronic,

778 anthropogenic disturbance, however, the decline in survival was not compensated by
779 either of these factors. Consequently, with the frequency of extreme climatic
780 conditions increasing under climate change, populations in anthropogenic habitats—
781 which are currently already decreasing—were negatively affected by future climatic
782 conditions. Habitat dynamics shaped by fires also dominated the effects of
783 environmental perturbations in natural habitats, highlighting the importance of fire
784 regimes in Mediterranean heathlands (Ojeda, Pausas, and Verdú, 2010; Keeley et
785 al., 2011). Adaptations to anthropogenic disturbances meanwhile can lead to
786 changes in vital-rate responses to climate and density, with detrimental
787 consequences on population persistence. The implications of our findings extend
788 beyond ecological theory, offering tangible guidance for conservation policies. Under
789 contrasting responses of natural and anthropogenic populations to climate change,
790 management would need to be adapted to allow periodic vegetation clearance (most
791 importantly through burning) in heathlands which would provoke mass germination
792 from the seed bank of dewy pines and other seeder species, increasing local
793 biodiversity (Fernandes et al., 2013; Ojeda, 2020). In anthropogenic habitats, on the
794 other hand, further disturbances should be prevented (Lawson et al. 2010). As our
795 results highlight climate changes drives population dynamics through adverse effects
796 on survival in anthropogenic habitats, management should focus on improving the
797 survival of large plants, for instance by allowing for moderate shrub cover that
798 shields dewy pines from climatic extremes (Brewer et al. 2021).
799
800 Land-use change (e.g. grazing) often has stronger effects on populations than
801 climate change (Sirami et al., 2017). However, few studies assess how interactions
802 between these two environmental pressures affect different vital rates and how such

803 effects then scale to population dynamics, despite evidence of land-use change
804 mediating the effect of climate change on species abundance and diversity
805 (Mantyka-Pringle, Martin, and Rhodes, 2012; Oliver and Morecroft, 2014). Such
806 interactions are likely to be strong drivers of vital-rate responses in habitats such as
807 Mediterranean heathlands, which are among the ecosystems most affected by
808 climate and land-use change (Newbold et al., 2020), the latter leading to changes in
809 disturbance regimes in the habitats. Consequently, interactions between these two
810 pressures might have strong effects on systems such as the dewy pine, where we
811 observe differences among disturbance levels in vital-rate responses to climate,
812 density, and their interactions among natural and highly disturbed habitats.
813
814 Our projections of natural and anthropogenic dewy-pine populations under climate
815 change indicate that future changes in climate will spare populations in natural
816 habitats but will have adverse effects on populations experiencing anthropogenic
817 disturbances, which is the majority of dewy pine populations (Garrido et al., 2003),
818 as well as many other Mediterranean shrublands (Newbold et al., 2020). We also
819 note that we capped the effects of projected climate extremes to the maximum past
820 observed values in order to not project population dynamics outside the observed
821 range of responses to climate (Fronzek et al., 2010). However, climate-change
822 projections show increases in extreme temperature values that are clearly outside
823 the range of past observed values (Fig. S1), indicating that our projections are likely
824 conservative and local extinction risks for this endangered species may be further
825 exacerbated.
826

As previously observed in our study populations, anthropogenic disturbances not only lead to increased continuous seed germination and decreased seed dormancy (Appendix S1), but also allowed aboveground individuals to survive longer in the absence of shrub encroachment (Paniw, Quintana-Ascencio et al., 2017). Consequently, dewy pines in chronically disturbed, anthropogenic habitats reached higher sizes than those in natural habitats. This is contrary to many studies assessing trait-level consequences of land-use change—and more specifically grazing—on plants. In these studies, plants in grazed sites adapted to this disturbance by shrinking over time to avoid being consumed by herbivores (Fischer et al., 2011; Kerns et al., 2011; Völler et al., 2017). However, with their mucilage-covered leaves, dewy pines are not palatable to herbivores (Ojeda et al., 2021), and therefore do not require such an adaptation. On the contrary, the small amount or absence of damage dealt to plants by herbivores along with the removal of other plants and the subsequent release of both intra- and interspecific competition, might allow dewy pines in anthropogenic populations to grow without surrounding vegetation hampering their nutrient acquisition (Paniw et al., 2018) and growth (Grime, 1973; Hjalten et al., 1993; Kambatuku et al., 2011; Fig. 3c).

While anthropogenic disturbances allow dewy pine plants to survive and grow better than in natural conditions, this comes at the cost of reproduction, with flowering probability decreasing in the largest individuals. Although the consequences of land-use change on plant reproduction are clearly species- and site-dependent (Kerns et al., 2011; Völler et al., 2017), tradeoffs similar to those observed in our populations are common across taxa (Stearns, 1989). Such negative correlations between vital rates might be more striking under stressful conditions such as low resource

availability (Villellas & García, 2018). This might be the case in anthropogenic populations of dewy pines particularly. Plants rely almost exclusively on capturing prey invertebrates for nutrient uptake (Paniw, Gil-Cabeza et al., 2017; Skates et al., 2019). In natural populations, invertebrates, especially insect pollinators, are abundant after fires, when many post-fire ephemeral species flower, and dewy pine plants are more conspicuous to insects, thus facilitating prey capture and nutrient uptake (Paniw et al., 2018). In anthropogenic habitats, intense browsing or mechanical vegetation removal are likely to decrease invertebrate abundances with respect to natural sites (Mayer, 2004; Carpio et al., 2014). When shrub cover is chronically low or sparse, dewy pine plants are more conspicuous to prey insects but they may also be more exposed to wind and solar radiation, thus resulting in relatively more stressful environmental conditions (Paniw et al., 2018). In turn, while populations in these chronically disturbed, anthropogenic habitats appear to persist, a low reproductive output may generate an extinction debt, where the population structure is skewed towards old individuals that cannot be replaced in the long term (Matías et al., 2019).

Adverse disturbance effects on vital rates can be exacerbated under unfavourable climatic conditions (e.g. Hindle et al., 2023; see also; Nolan et al., 2021 and references therein). Plants commonly suffer from extreme temperatures and drought, which affect individuals through processes such as heat stress, photosynthesis inhibition, or reduced soil moisture and water resources (e.g. Larcher, 2000; McDowell et al., 2008; Nolan et al., 2021). While dewy pines are somewhat adapted to dry and hot summer conditions (Darwin 1875; Adlassnig et al., 2006; Adamec, 2009), survival greatly decreased with increasing summer temperatures. In addition

877 to the aforementioned processes reducing the survival of plants experiencing high
878 temperatures, such extreme conditions could lead to a great reduction in prey
879 availability. These carnivorous subshrubs indeed rely on droplets of mucilage on
880 their leaves to capture insects, from which they obtain nutrients (Paniw, Gil-Cabeza
881 et al., 2017). However, increasing temperatures and the subsequent decrease in
882 humidity could prevent plants from forming these droplets, and thereby from
883 accessing these resources.
884
885 Rainfall also played an important role in shaping dewy-pine demography. In addition
886 to limiting water resources (McDowell et al., 2008), extremely low amounts of rain do
887 not provide enough moisture for dewy pines to produce mucilage on their leaf-traps
888 (Darwin 1875; Adlassnig et al., 2006; Adamec, 2009). As a result, plants might not
889 get enough nutrients to allocate to the different demographic processes. However, in
890 natural populations, high amounts of rainfall seemed to slightly buffer negative
891 temperature effects, likely by compensating the low humidity and water resources
892 under high temperatures. This process did not seem to occur in anthropogenic
893 populations, where the increased exposure to extreme temperatures due to sparse
894 vegetation cover might be too intense to counterbalance.
895
896 In addition to interactions between climatic variables, density-dependent effects of
897 climate are common across taxa and can play a key role in shaping population
898 dynamics, for example by enhancing or mitigating adverse environmental effects
899 (Gamelon et al., 2017; Paniw et al., 2019). In plant populations, vital-rate density
900 dependence can be attributed to two main biological processes: competition (e.g. for
901 light or pollinators; Craine & Dybzinski, 2013) and facilitation (i.e., the positive effect

902 of neighbours on a focal individual, e.g., through shading or protection from
903 herbivory; Callaway & Pugnaire, 2007; Graff et al., 2007; Le Bagousse-Pinguet et al.,
904 2012). According to the stress-gradient hypothesis, variations in environmental
905 conditions can lead to shifts between these two processes in a given population
906 (Bertness & Callaway, 1994; Maestre et al., 2005), for example under increased
907 levels of disturbance (Graff et al., 2007; Villarreal-Barajas & Martorell, 2009; Le
908 Bagousse-Pinguet et al., 2012) or extreme climatic conditions (Callaway & Pugnaire,
909 2007; Grant et al., 2014; Olsen et al., 2016). This was the case in dewy pines, where
910 intraspecific density had opposite effects on some vital rates between natural—
911 where competition prevailed—and anthropogenic populations—where facilitation
912 was at play.
913
914 As commonly observed in plant communities (Villalobos et al., 2016; Adler et al.,
915 2018), increasing intraspecific densities in natural conditions led to declining
916 survival—with the exception of early post-fire conditions, where facilitation generally
917 predominates in fire-adapted plant communities (Vilà & Sardans, 1999; Paniw et al.,
918 2018). For dewy pines, in addition to the more common resources for which plants
919 compete (e.g. light or pollinators), such negative effects of conspecifics on survival
920 could arise from competition for prey (Craine & Dybzinski, 2013). Contrastingly,
921 individuals in anthropogenic populations benefited from higher intraspecific densities.
922 In addition to the competition release stemming from the removal of surrounding
923 vegetation (Catling et al., 2024), increasing levels of disturbance such as browsing
924 might lead to a shift from competition to facilitation, as neighbours might act as a
925 barrier against browsers (Le Bagousse-Pinguet et al., 2012).
926

In addition to the consequences on vital rates, future increases in temperatures and decreases in rainfall under climate change are expected to lead to higher frequency and intensity of wildfires (Turco et al., 2019; Nolan et al., 2021). In populations where land-use change led to seedbank depletions through increase in continuous germination and dormancy loss, returning fire regimes will likely have strong negative consequences on population persistence, as reduced soil seedbanks will not be enough to replenish populations following the removal of aboveground individuals by fire. Decrease in the ability of fire-adapted plants to germinate or resprout after more frequent and intense fire could have dramatic consequences for the persistence of plant communities in fire-prone habitats (Enright et al., 2015; Nolan et al., 2021).

Overall, our findings highlight the existence of demographic responses to climate and land-use change and call for conservation policies taking into account the detrimental effects of climate change on populations persisting under human alterations to their habitats, more specifically in fire-adapted systems. Moreover, species-specific effects of interactions between climate and land-use change highlight the need for studies assessing these effects at the community level—accounting for the effects of both climate and intra- and inter-specific density—to understand how interactions between these pressures might affect fire-prone and more generally anthropogenic landscapes.

948 ## References

949

950 Adamec, L. (2009). Ecophysiological Investigation on Drosophyllum Lusitanicum:
951 Why Doesn't the Plant Dry Out? *Carnivorous Plant Newsletter*, **38**(3), 71–74.
952 https://doi.org/10.55360/cpn383.la180

953 Adlassnig, W., Peroutka, M., Eder, G., Pois, W., & Lichtscheidl, I. K. (2006).
954 Ecophysiological Observations on Drosophyllum Lusitanicum. *Ecological*
955 *Research*, **21**(2), 255–62. https://doi.org/10.1007/s11284-005-0116-z

956 Adler, P. B., Ellner, S. P., & Levine, J. M. (2010). Coexistence of Perennial Plants:
957 An Embarrassment of Niches. *Ecology Letters*, **13**(8), 1019–29.
958 https://doi.org/10.1111/j.1461-0248.2010.01496.x

959 Adler, P. B., Smull, D., Beard, K. H., Choi, R. T., Furniss, T., Kulmatiski, A., Meiners,
960 J. M., Tredennick, A. T., & Veblen, K. E. (2018). Competition and Coexistence
961 in Plant Communities: Intraspecific Competition Is Stronger than Interspecific
962 Competition. *Ecology Letters*, **21**(9), 1319–29.
963 https://doi.org/10.1111/ele.13098

964 Alberti, M. (2015). Eco-Evolutionary Dynamics in an Urbanizing Planet. *Trends in*
965 *Ecology & Evolution*, **30**(2), 114–26. https://doi.org/10.1016/j.tree.2014.11.007

966 Bertness, M. D., & Callaway, R. (1994). Positive Interactions in Communities. *Trends*
967 *in Ecology & Evolution*, **9**(5), 191–93. https://doi.org/10.1016/0169-
968 5347(94)90088-4

969 Bijlsma, R., & Loeschcke, V. (2012). Genetic Erosion Impedes Adaptive Responses
970 to Stressful Environments. *Evolutionary Applications*, **5**(2), 117–29.
971 https://doi.org/10.1111/j.1752-4571.2011.00214.x

972 Brewer, J. S., Paniw, M., & Ojeda, F. (2021). Plant Behavior and Coexistence: Stem

Elongation of the Carnivorous Subshrub Drosophyllum Lusitanicum within Xerophytic Shrub Canopies. *Plant Ecology*, **222**(11), 1197–1208. https://doi.org/10.1007/s11258-021-01170-0

Brook, B. W., Sodhi, N. S., & Bradshaw, C. J. A. (2008). Synergies among Extinction Drivers under Global Change. *Trends in Ecology & Evolution*, **23**(8), 453–60. https://doi.org/10.1016/j.tree.2008.03.011

Burnham, K. P., Anderson, D. R., & Huyvaert, K. P. (2011). AIC Model Selection and Multimodel Inference in Behavioral Ecology: Some Background, Observations, and Comparisons. *Behavioral Ecology and Sociobiology*, **65**(1), 23–35. https://doi.org/10.1007/s00265-010-1029-6

Callaway, R. M., & Pugnaire, F. I. (2007). Facilitation in Plant Communities. In F. I. Pugnaire, & F. Valladares (Eds.), *Functional Plant Ecology* (2nd ed., pp. 435–55). CRC Press.

Carpio, A. J., Castro–López, J., Guerrero–Casado, J., Ruiz–Aizpurua, L., Vicente, J., & Tortosa, F. S. (2014). Effect of Wild Ungulate Density on Invertebrates in a Mediterranean Ecosystem. *Animal Biodiversity and Conservation*, **37**(2), 115–25. https://doi.org/10.32800/abc.2014.37.0115

Catling, A. A., Mayfield, M. M., & Dwyer, J. M. (2024). Individual Vital Rates Respond Differently to Local-Scale Environmental Variation and Neighbour Removal. *Journal of Ecology*, **112**(6), 1369–82. https://doi.org/10.1111/1365-2745.14308

Chevin, L.-M., Lande, R., & Mace, G. M. (2010). Adaptation, Plasticity, and Extinction in a Changing Environment: Towards a Predictive Theory. *PLOS Biology*, **8**(4), e1000357. https://doi.org/10.1371/journal.pbio.1000357

Clark, N. E., Boakes, E. H., McGowan, P. J. K., Mace, G. M., & Fuller, R. A. (2013).

998 Protected Areas in South Asia Have Not Prevented Habitat Loss: A Study
999 Using Historical Models of Land-Use Change. *PLOS ONE*, **8**(5), e65298.
1000 https://doi.org/10.1371/journal.pone.0065298
1001 Conquet, E., Ozgul, A., Blumstein, D. T., Armitage, K. B., Oli, M. K., Martin, J. G. A.,
1002 Clutton-Brock, T. H., & Paniw, M. (2023). Demographic Consequences of
1003 Changes in Environmental Periodicity. *Ecology*, **104**(3), e3894.
1004 https://doi.org/10.1002/ecy.3894
1005 Conquet, E., Ozgul, A., Gómez-González, S., Ojeda, F., & Paniw, M. (2025). Data
1006 from: Climate change is associated with a higher extinction risk of a subshrub
1007 in anthropogenic landscapes [Data set]. Zenodo.
1008 https://doi.org/10.5281/zenodo.16370815.
1009 Cornes, R. C., van der Schrier, G., van den Besselaar, E. J. M., & Jones, P. D.
1010 (2018). An Ensemble Version of the E-OBS Temperature and Precipitation
1011 Data Sets. *Journal of Geophysical Research: Atmospheres*, **123**(17), 9391–
1012 409. https://doi.org/10.1029/2017JD028200
1013 Correia, E., & Freitas, H. (2002). Drosophyllum Lusitanicum, an Endangered West
1014 Mediterranean Endemic Carnivorous Plant: Threats and Its Ability to Control
1015 Available Resources. *Botanical Journal of the Linnean Society*, **140**(4), 383–
1016 90. https://doi.org/10.1046/j.1095-8339.2002.00108.x
1017 Craine, J. M., & Dybzinski, R. (2013). Mechanisms of Plant Competition for
1018 Nutrients, Water and Light. *Functional Ecology*, **27**(4), 833–40.
1019 https://doi.org/10.1111/1365-2435.12081
1020 Cross, A. T., Paniw, M., Ojeda, F., Turner, S. R., Dixon, K. W., & Merritt, D. J.
1021 (2017). Defining the Role of Fire in Alleviating Seed Dormancy in a Rare
1022 Mediterranean Endemic Subshrub. *AoB PLANTS*, **9**(5), plx036.

https://doi.org/10.1093/aobpla/plx036

Darwin, C. (1875). *Insectivorous Plants*. John Murray, London. https://doi.org/10.1017/CBO9780511694127

Díaz, S., Settele, J., Brondízio, E. S., Ngo, H. T., Agard, J., Arneth, A., Balvanera, P., Brauman, K. A., Butchart, S. H. M., Chan, K. M. A., Garibaldi, L. A., Ichii, K., Liu, J., Subramanian, S. M., Midgley, G. F., Miloslavich, P., Molná,r Z., Obura, D., Pfaff, A., … Polasky, S. (2019). Pervasive Human-Driven Decline of Life on Earth Points to the Need for Transformative Change. *Science*, **366**(6471), eaax3100. https://doi.org/10.1126/science.aax3100

Enright, N. J, Fontaine, J. B, Bowman, D. M. J. S., Bradstock, R. A, & Williams, R. J. (2015). Interval Squeeze: Altered Fire Regimes and Demographic Responses Interact to Threaten Woody Species Persistence as Climate Changes. *Frontiers in Ecology and the Environment*, **13**(5), 265–72. https://doi.org/10.1890/140231

Evers, S. M., Knight, T. M., Inouye, D. W., Miller, T. E. X., Salguero-Gómez, R., Iler, A. M., & Compagnoni, A. (2021). Lagged and Dormant Season Climate Better Predict Plant Vital Rates Than Climate During the Growing Season. *Global Change Biology*, **27**(9), 1927–1941. https://doi.org/10.1111/gcb.15519

Eyring, V., Bony, S., Meehl, G. A., Senior, C. A., Stevens, B., Stouffer, R. J., & Taylor, K. E. (2016). Overview of the Coupled Model Intercomparison Project Phase 6 (CMIP6) Experimental Design and Organization. *Geoscientific Model Development*, **9**(5), 1937–58. https://doi.org/10.5194/gmd-9-1937-2016

Fagan, W. F., & Holmes, E. E. (2006). Quantifying the Extinction Vortex. *Ecology Letters*, **9**(1), 51–60. https://doi.org/10.1111/j.1461-0248.2005.00845.x

Fernandes, P. M., Davies, G. M., Ascoli, D., Fernandez, C., Moreira, F., Rigolot, E.,

1048 Stoof, C. R., Vega, J.A., & Molina, D. (2013). Prescribed Burning in Southern
1049 Europe: Developing Fire Management in a Dynamic Landscape. *Frontiers in*
1050 *Ecology and the Environment*, **11**(s1), e4–e14. https://doi.org/10.1890/120298
1051 Fischer, M., Weyand, A., Rudmann-Maurer, K., & Stöcklin, J. (2011). Adaptation of
1052 Poa Alpina to Altitude and Land Use in the Swiss Alps. *Alpine Botany*, **121**(2),
1053 91–105. https://doi.org/10.1007/s00035-011-0096-2
1054 Foley, J. A., DeFries, R., Asner, G. P., Barford, C., Bonan, G., Carpenter, S. R.,
1055 Chapin, F. S., Coe, M. T., Daily, G. C., Gibbs, H. K., Helkowski, J. H.,
1056 Holloway, T., Howard, E. A., Kucharik, C. J., Monfreda, C., Patz, J. A.,
1057 Prentice, I. C., Ramankutty, N., & Snyder, P. K. (2005). Global Consequences
1058 of Land Use. *Science*, **309**(5734), 570–74.
1059 https://doi.org/10.1126/science.1111772
1060 Fronzek, S., Carter, T. R., Räisänen, J., Ruokolainen, L., & Luoto, M. (2010).
1061 Applying Probabilistic Projections of Climate Change With Impact Models: A
1062 Case Study for sub-Arctic Palsa Mires in Fennoscandia. *Climate Change*, **99**,
1063 515–534. https://doi.org/10.1007/s10584-009-9679-y
1064 Gamelon, M., Grøtan, V., Nilsson, A. L. K., Engen, S., Hurrell, J. W., Jerstad, K.,
1065 Phillips, A. S., Røstad, O. W., Slagsvold, T., Walseng, B., Stenseth, N. C.,
1066 Sæther, B.-E. (2017). Interactions between Demography and Environmental
1067 Effects Are Important Determinants of Population Dynamics. *Science*
1068 *Advances*, **3**(2), e1602298. https://doi.org/10.1126/sciadv.1602298
1069 Garnier, E., Lavorel, S., Ansquer, P., Castro, H., Cruz, P., Dolezal, J., Eriksson, O.,
1070 Fortunel, C., Freitas, H., Golodets, C., Grigulis, K., Jouany, C., Kazakou, E.,
1071 Kigel, J., Kleyer, M., Lehsten, V., Lepš, J., Meier, T., Pakeman, R, … Zarovali,
1072 M. P. (2007). Assessing the Effects of Land-Use Change on Plant Traits,

Communities and Ecosystem Functioning in Grasslands: A Standardized Methodology and Lessons from an Application to 11 European Sites. *Annals of Botany*, **99**(5), 967–85. https://doi.org/10.1093/aob/mcl215

García-Callejas, D., Molowny-Horas, R., & Retana, J. (2017). Projecting the Distribution and Abundance of Mediterranean Tree Species Under Climate Change: A Demographic Approach. *Journal of Plant Ecology*, **10**(5), 731–743. https://doi.org/10.1093/jpe/rtw081

Garrido, B., Hampe, A., Marañón, T., & Arroyo, J. (2003). Regional Differences in Land Use Affect Population Performance of the Threatened Insectivorous Plant Drosophyllum Lusitanicum (Droseraceae). *Diversity and Distributions*, **9**(5), 335–50. https://doi.org/10.1046/j.1472-4642.2003.00029.x

Geldmann, J., Barnes, M., Coad, L., Craigie, I. D., Hockings, M., & Burgess, N. D. (2013). Effectiveness of Terrestrial Protected Areas in Reducing Habitat Loss and Population Declines. *Biological Conservation*, **161**(May), 230–38. https://doi.org/10.1016/j.biocon.2013.02.018

Gómez-González, S., Paniw, M., Antunes, K., & Ojeda, F. (2018). Heat Shock and Plant Leachates Regulate Seed Germination of the Endangered Carnivorous Plant *Drosophyllum Lusitanicum*. *Web Ecology*, **18**(1), 7–13. https://doi.org/10.5194/we-18-7-2018

Graff, P., Aguiar, M. R., & Chaneton, E. J. (2007). Shifts in Positive and Negative Plant Interactions Along a Grazing Intensity Gradient. *Ecology*, **88**(1), 188–99. https://doi.org/10.1890/0012-9658(2007)88[188:SIPANP]2.0.CO;2

Grant, K., Kreyling, J., Heilmeier, H., Beierkuhnlein, C., & Jentsch, A. (2014). Extreme Weather Events and Plant–Plant Interactions: Shifts between Competition and Facilitation among Grassland Species in the Face of Drought

and Heavy Rainfall. *Ecological Research*, **29**(5), 991–1001. https://doi.org/10.1007/s11284-014-1187-5

Gray, C. L., Hill, S. L. L., Newbold, T., Hudson, L. N., Börger, L., Contu, S., Hoskins, A. J., Ferrier, S., Purvis, A., & Scharlemann, J. P. W. (2016). Local Biodiversity Is Higher inside than Outside Terrestrial Protected Areas Worldwide. *Nature Communications*, **7**(1), 12306. https://doi.org/10.1038/ncomms12306

Grime, J. P. (1973). Competitive Exclusion in Herbaceous Vegetation. *Nature*, **242**(5396), 344–47. https://doi.org/10.1038/242344a0

Grimm, V., Berger, U., Bastiansen, F., Eliassen, S., Ginot, V., Giske, J., Goss-Custard, J., Grand, T., Heinz, S. K., Huse, G., Huth, A., Jepsen, J. U., Jørgensen, C., Mooij, W. M., Müller, B., Pe'er, G., Piou, C., Railsback, S. F., Robbins, A. M., … DeAngelis, D. L. (2006). A Standard Protocol for Describing Individual-Based and Agent-Based Models. *Ecological Modelling*, **198**(1), 115–26. https://doi.org/10.1016/j.ecolmodel.2006.04.023

Grimm, V., Railsback, S. F., Vincenot, C. E., Berger, U., Gallagher, C., DeAngelis, D. L., Edmonds, B., Ge, J., Giske, J., Groeneveld, J., Johnston, A. S. A., Milles, A., Nabe-Nielsen, J., Polhill, J. G., Radchuk, V., Rohwäder, M.-S., Stillman, R. A., Thiele, J. C., & Ayllón, D. (2020). The ODD Protocol for Describing Agent-Based and Other Simulation Models: A Second Update to Improve Clarity, Replication, and Structural Realism. *Journal of Artificial Societies and Social Simulation*, **23**(2), 7. https://doi.org/ 10.18564/jasss.4259

Hindle, B. J., Quintana-Ascencio, P. F., Menges, E. S., & Childs, D. Z. (2023). The Implications of Seasonal Climatic Effects for Managing Disturbance Dependent Populations under a Changing Climate. *Journal of Ecology*,

111(8), 1749–61. https://doi.org/10.1111/1365-2745.14143

Hjalten, J., Danell, K., & Ericson, L. (1993). Effects of Simulated Herbivory and Intraspecific Competition on the Compensatory Ability of Birches. *Ecology*, **74**(4), 1136–42. https://doi.org/10.2307/1940483

IPBES. (2019). Global Assessment Report on Biodiversity and Ecosystem Services of the Intergovernmental Science-Policy Platform on Biodiversity and Ecosystem Services. E. S. Brondizio, J. Settele, S. Díaz, & H. T. Ngo (Eds.). IPBES secretariat, Bonn, Germany. https://doi.org/10.5281/zenodo.6417333

Kambatuku, J. R., Cramer, M. D., & Ward, D. (2011). Intraspecific Competition between Shrubs in a Semi-Arid Savanna. *Plant Ecology*, **212**(4), 701–13. https://doi.org/10.1007/s11258-010-9856-0

Kampichler, C., van Turnhout, C. A. M., Devictor, V., & van der Jeugd, H. P. (2012). Large-Scale Changes in Community Composition: Determining Land Use and Climate Change Signals. *PLOS ONE*, **7**(4), e35272. https://doi.org/10.1371/journal.pone.0035272

Keeley, J. E., Bond, W. J., Bradstock, R. A., Pausas, J. G., & Rundel, P. W. (2012). *Fire in Mediterranean Ecosystems: Ecology, Evolution and Management*. Cambridge University Press.

Kerns, B. K., Buonopane, M., Thies, W. G., & Niwa, C. (2011). Reintroducing Fire into a Ponderosa Pine Forest with and without Cattle Grazing: Understory Vegetation Response. *Ecosphere*, **2**(5), art59. https://doi.org/10.1890/ES10-00183.1

Larcher, W. (2000). Temperature Stress and Survival Ability of Mediterranean Sclerophyllous Plants. *Plant Biosystems - An International Journal Dealing with All Aspects of Plant Biology*, **134**(3), 279–95.

https://doi.org/10.1080/11263500012331350455

Lawson, D. M., Regan, H. M., Zedler, P. H., & Franklin, J. (2010). Cumulative Effects of Land Use, Altered Fire Regime and Climate Change on Persistence of Ceanothus Verrucosus, a Rare, Fire-Dependent Plant Species. *Global Change Biology*, **16**(9), 2518–29. https://doi.org/10.1111/j.1365-2486.2009.02143.x

Le Bagousse-Pinguet, Y., Gross, E. M., & Straile, D. (2012). Release from Competition and Protection Determine the Outcome of Plant Interactions along a Grazing Gradient. *Oikos*, **121**(1), 95–101. https://doi.org/10.1111/j.1600-0706.2011.19778.x

Leimu, R., Vergeer, P., Angeloni, F., & Ouborg, N. J. (2010). Habitat Fragmentation, Climate Change, and Inbreeding in Plants. *Annals of the New York Academy of Sciences*, **1195**(1), 84–98. https://doi.org/10.1111/j.1749-6632.2010.05450.x

Maestre, F. T., Valladares, F., & Reynolds, J. F. (2005). Is the Change of Plant–Plant Interactions with Abiotic Stress Predictable? A Meta-Analysis of Field Results in Arid Environments. *Journal of Ecology*, **93**(4), 748–57. https://doi.org/10.1111/j.1365-2745.2005.01017.x

Mantyka-Pringle, C. S., Martin, T. G., & Rhodes, J. R. (2012). Interactions between Climate and Habitat Loss Effects on Biodiversity: A Systematic Review and Meta-Analysis. *Global Change Biology*, **18**(4), 1239–52. https://doi.org/10.1111/j.1365-2486.2011.02593.x

Matías, L., Abdelaziz, M., Godoy, O., & Gómez-Aparicio, L. (2019). Disentangling the Climatic and Biotic Factors Driving Changes in the Dynamics of Quercus Suber Populations across the Species‘ Latitudinal Range. *Diversity and*

Distributions, **25**(4), 524–35. https://doi.org/10.1111/ddi.12873

Mayer, C. (2004). Pollination Services under Different Grazing Intensities. *International Journal of Tropical Insect Science*, **24**(1), 95–103. https://doi.org/10.1079/IJT20047

McDowell, N., Pockman, W. T., Allen, C. D., Breshears, D. D., Cobb, N., Kolb, T., Plaut, J., Sperry, J., West, A., Williams, D. G., & Yepez, E. A. (2008). Mechanisms of Plant Survival and Mortality during Drought: Why Do Some Plants Survive While Others Succumb to Drought? *New Phytologist*, **178**(4), 719–39. https://doi.org/10.1111/j.1469-8137.2008.02436.x

Montràs-Janer, T., Suggitt, A. J., Fox, R., Jönsson, M., Martay, B., Roy, D. B., Walker, K. J., & Auffret, A. G. (2024). Anthropogenic Climate and Land-Use Change Drive Short- and Long-Term Biodiversity Shifts across Taxa. *Nature Ecology & Evolution*, **8**(4), 739–51. https://doi.org/10.1038/s41559-024-02326-7

Murali, G., de Oliveira Caetano, G. H., Barki, G., Meiri, S., & Roll, U. (2022). Emphasizing Declining Populations in the Living Planet Report. *Nature*, **601**(7894), E20–24. https://doi.org/10.1038/s41586-021-04165-z

Newbold, T., Oppenheimer, P., Etard, A., & Williams, J. J. (2020). Tropical and Mediterranean Biodiversity Is Disproportionately Sensitive to Land-Use and Climate Change. *Nature Ecology & Evolution*, **4**(12), 1630–38. https://doi.org/10.1038/s41559-020-01303-0

Nolan, R. H., Collins, L., Leigh, A., Ooi, M. K. J., Curran, T. J. Fairman, T. A., Resco de Dios, V., & Bradstock, R. (2021). Limits to Post-Fire Vegetation Recovery under Climate Change. *Plant, Cell & Environment*, **44**(11), 3471–89. https://doi.org/10.1111/pce.14176

1198 Ojeda, F., Carrera, C., Paniw, M., García-Moreno, L., Barbero, G. F., & Palma, M.
1199 (2021). Volatile and Semi-Volatile Organic Compounds May Help Reduce
1200 Pollinator-Prey Overlap in the Carnivorous Plant Drosophyllum Lusitanicum
1201 (Drosophyllaceae). *Journal of Chemical Ecology*, **47**(1), 73–86.
1202 https://doi.org/10.1007/s10886-020-01235-w
1203 Ojeda, F., Pausas, J. G., & Verdú, M. (2010). Soil Shapes Community Structure
1204 through Fire. *Oecologia*, **163**(3), 729–35. https://doi.org/10.1007/s00442-009-
1205 1550-3
1206 Ojeda, F. (2020). Pine Afforestation, Herriza and Wildfire: A Tale of Soil Erosion and
1207 Biodiversity Loss in the Mediterranean Region. *International Journal of*
1208 *Wildland Fire*, **29**, 1142–1146. https://doi.org/10.1071/WF20097
1209 Oliver, T. H., & Morecroft, M. D. (2014). Interactions between Climate Change and
1210 Land Use Change on Biodiversity: Attribution Problems, Risks, and
1211 Opportunities. *WIREs Climate Change*, **5**(3), 317–35.
1212 https://doi.org/10.1002/wcc.271
1213 Olsen, S. L., Töpper, J. P., Skarpaas, O., Vandvik, V., & Klanderud, K. (2016). From
1214 Facilitation to Competition: Temperature-Driven Shift in Dominant Plant
1215 Interactions Affects Population Dynamics in Seminatural Grasslands. *Global*
1216 *Change Biology*, **22**(5), 1915–26. https://doi.org/10.1111/gcb.13241
1217 Paniw, M., Duncan, C., Groenewoud, F., Drewe, J. A., Manser, M., Ozgul, A., &
1218 Clutton-Brock, T. (2022). Higher Temperature Extremes Exacerbate Negative
1219 Disease Effects in a Social Mammal. *Nature Climate Change*, **12**(3), 284–90.
1220 https://doi.org/10.1038/s41558-022-01284-x
1221 Paniw, M., García-Callejas, D., Lloret, F., Bassar, R. D., Travis, J., & Godoy, O.
1222 (2023). Pathways to Global-Change Effects on Biodiversity: New

Opportunities for Dynamically Forecasting Demography and Species Interactions. *Proceedings of the Royal Society B: Biological Sciences*, **290**(1993), 20221494. https://doi.org/10.1098/rspb.2022.1494

Paniw, M., Gil-Cabeza, E., & Ojeda, F. (2017). Plant Carnivory beyond Bogs: Reliance on Prey Feeding in Drosophyllum Lusitanicum (Drosophyllaceae) in Dry Mediterranean Heathland Habitats. *Annals of Botany*, **119**(6), 1035–41. https://doi.org/10.1093/aob/mcw247

Paniw, M., Maag, N., Cozzi, G., Clutton-Brock, T. H., & Ozgul, A. (2019). Life History Responses of Meerkats to Seasonal Changes in Extreme Environments. *Science*, **363**(6427), 631–35. https://doi.org/10.1126/science.aau5905

Paniw, M., Quintana-Ascencio, P. F., Ojeda, F., & Salguero-Gómez, R. (2017). Interacting Livestock and Fire May Both Threaten and Increase Viability of a Fire-Adapted Mediterranean Carnivorous Plant. *Journal of Applied Ecology*, **54**(6), 1884–94. https://doi.org/10.1111/1365-2664.12872

Paniw, M., de la Riva, E. G., & Lloret, F. (2021). Demographic Traits Improve Predictions of Spatiotemporal Changes in Community Resilience to Drought. *Journal of Ecology*, **109**(9), 3233–45. https://doi.org/10.1111/1365-2745.13597

Paniw, M., Salguero-Gómez, R., & Ojeda, F. (2015). Local-Scale Disturbances Can Benefit an Endangered, Fire-Adapted Plant Species in Western Mediterranean Heathlands in the Absence of Fire. *Biological Conservation*, **187**(July), 74–81. https://doi.org/10.1016/j.biocon.2015.04.010

Paniw, M., Salguero-Gómez, R., & Ojeda, F. (2018). Transient Facilitation of Resprouting Shrubs in Fire-Prone Habitats. *Journal of Plant Ecology*, **11**(3), 475–83. https://doi.org/10.1093/jpe/rtx019

Pascoe, C., Lawrence, B. N., Guilyardi, E., Juckes, M., & Taylor, K. E. (2020). Documenting Numerical Experiments in Support of the Coupled Model Intercomparison Project Phase 6 (CMIP6). *Geoscientific Model Development*, **13**(5), 2149–67. https://doi.org/10.5194/gmd-13-2149-2020

Pausas, J. G., & Bond, W. J. (2020). On the Three Major Recycling Pathways in Terrestrial Ecosystems. *Trends in Ecology and Evolution*, **35**(9), 767–775. https://doi.org/10.1016/j.tree.2020.04.004

Pausas, J. G., & Keeley, J. E. (2014). Abrupt Climate-Independent Fire Regime Changes. *Ecosystems*, **17**(6), 1109–20. https://doi.org/10.1007/s10021-014-9773-5

Pereira, H. M., Martins, I. S., Rosa, I. M. D., Kim, H., Leadley, P., Popp, A., Van Vuuren, D. P., Hurtt, G., Quoss, L., Arneth, A., Baisero, D., Bakkenes, M., Chaplin-Kramer, R., Chini, L., Di Marco, M., Ferrier, S., Fujimori, S., Guerra, C. A., Harfoot, M., … Alkemade, R. (2024). Global trends and scenarios for terrestrial biodiversity and ecosystem services from 1900 to 2050. *Science*, **384**(6694), 458–465. https://doi.org/10.1126/science.adn3441

Petrie, R., Denvil, S., Ames, S., Levavasseur, G., Fiore, S., Allen, C., Antonio, F., Berger, K., Bretonnière P.-A., Cinquini, L., Dart, E., Dwarakanath, P., Drukem, K., Evans, B., Franchistéguy, L., Gardoll, S., Gerbier, E., Greenslade, M., Hassell, D., … Wagner, R. (2021). Coordinating an Operational Data Distribution Network for CMIP6 Data. *Geoscientific Model Development*, **14**(1), 629–44. https://doi.org/10.5194/gmd-14-629-2021

Posit team. (2023). RStudio: Integrated Development Environment for R. Posit Software, PBC, Boston, MA. http://www.posit.co/

R Core Team. (2022). R: A Language and Environment for Statistical Computing.

Vienna, Austria: R Foundation for Statistical Computing. https://www.R-project.org/

Riahi, K., Rao, S., Krey, V., Cho, C., Chirkov, V., Fischer, G., Kindermann, G., Nakicenovic, N., & Rafaj, P. (2011). RCP 8.5—A Scenario of Comparatively High Greenhouse Gas Emissions. *Climatic Change*, **109**(1), 33. https://doi.org/10.1007/s10584-011-0149-y

Sala, O. E., Chapin III, F. S., Armesto, J. J., Berlow, E., Bloomfield, J., Dirzo, R., Huber-Sanwald, E., Huenneke, L. F., Jackson, R. B., Kinzig, A., Leemans, R., Lodge, D. M., Mooney, H. A., Oesterheld, M., Poff, N. L., Sykes, M. T., Walker, B. H., Walker, M., & Wall, D. H. (2000). Global Biodiversity Scenarios for the Year 2100. *Science*, **287**(5459), 1770–74. https://doi.org/10.1126/science.287.5459.1770

Sanderson, B. M., Knutti, R., & Caldwell, P. (2015). A Representative Democracy to Reduce Interdependency in a Multimodel Ensemble. *Journal of Climate*, **28**(13), 5171–94. https://doi.org/10.1175/JCLI-D-14-00362.1

Selwood, K. E., McGeoch, M. A., & Mac Nally, R. (2015). The Effects of Climate Change and Land-Use Change on Demographic Rates and Population Viability. *Biological Reviews*, **90**(3), 837–53. https://doi.org/10.1111/brv.12136

Sirami, C., Caplat, P., Popy, S., Clamens, A., Arlettaz, R., Jiguet, F., Brotons, L., & Martin, J.-L. (2017). Impacts of Global Change on Species Distributions: Obstacles and Solutions to Integrate Climate and Land Use. *Global Ecology and Biogeography*, **26**(4), 385–94. https://doi.org/10.1111/geb.12555

Skates, L. M., Paniw, M., Cross, A. T., Ojeda, F., Dixon, K. W., Stevens, J. C., & Gebauer, G. (2019). An Ecological Perspective on 'Plant Carnivory beyond Bogs': Nutritional Benefits of Prey Capture for the Mediterranean Carnivorous

Plant Drosophyllum Lusitanicum. *Annals of Botany*, **124**(1), 65–76. https://doi.org/10.1093/aob/mcz045

Stearns, S. C. (1989). Trade-Offs in Life-History Evolution. *Functional Ecology*, **3**(3), 259–68. https://doi.org/10.2307/2389364

Titeux, N., Henle, K., Mihoub, J.-B., Regos, A., Geijzendorffer, I. R., Cramer, W., Verburg, P. H., & Brotons, L. (2016). Biodiversity Scenarios Neglect Future Land-Use Changes. *Global Change Biology*, **22**(7), 2505–15. https://doi.org/10.1111/gcb.13272

Tredennick, A. T., Hooten, M. B., Aldridge, C. L., Homer, C. G., Kleinhesselink, A. R., & Adler, P. B. (2016). Forecasting Climate Change Impacts on Plant Populations over Large Spatial Extents. *Ecosphere*, **7**(10), e01525. https://doi.org/10.1002/ecs2.1525

Turco, M., Jerez, S., Augusto, S., Tarín-Carrasco, P., Ratola, N., Jiménez-Guerrero, P., & Trigo, R. M. (2019). Climate Drivers of the 2017 Devastating Fires in Portugal. *Scientific Reports*, **9**(1), 13886. https://doi.org/10.1038/s41598-019-50281-2

Vilà, M., & Sardans, J. (1999). Plant Competition in Mediterranean-Type Vegetation. *Journal of Vegetation Science*, **10**(2), 281–94. https://doi.org/10.2307/3237150

Villalobos, F. J., Sadras, V. O., & Fereres, E. (2016). Plant Density and Competition. In F. J. Villalobos & E. Fereres (Eds.), *Principles of Agronomy for Sustainable Agriculture* (pp. 159–168). Springer International Publishing. https://doi.org/10.1007/978-3-319-46116-8_12

Villarreal-Barajas, T., & Martorell, C. (2009). Species-Specific Disturbance Tolerance, Competition and Positive Interactions along an Anthropogenic

1323 Disturbance Gradient. *Journal of Vegetation Science*, **20**(6), 1027–40.
1324 https://doi.org/10.1111/j.1654-1103.2009.01101.x
1325 Villellas, J., & García, M. B. (2018). Life-History Trade-Offs Vary with Resource
1326 Availability across the Geographic Range of a Widespread Plant. *Plant*
1327 *Biology*, **20**(3), 483–89. https://doi.org/10.1111/plb.12682
1328 Völler, E., Bossdorf, O., Prati, D., & Auge, H. (2017). Evolutionary Responses to
1329 Land Use in Eight Common Grassland Plants. *Journal of Ecology*, **105**(5),
1330 1290–97. https://doi.org/10.1111/1365-2745.12746
1331 Waliser, D., Gleckler, P. J., Ferraro, R., Taylor, K. E., Ames, S., Biard, J., Bosilovich,
1332 M. G., Brown, O., Chepfer, H., Cinquini, L., Durack, P.J., Eyring, V., Mathieu,
1333 P.-P., Lee, T., Pinnock, S., Potter, G. L., Rixen, M., Saunders, R., Schulz, J.,
1334 Thépaut, J.-N., Tuma, M. (2020). Observations for Model Intercomparison
1335 Project (Obs4MIPs): Status for CMIP6. *Geoscientific Model Development*,
1336 **13**(7), 2945–58. https://doi.org/10.5194/gmd-13-2945-2020
1337 Watson, J. E. M., Dudley, N., Segan, D. B., & Hockings, Marc. (2014). The
1338 Performance and Potential of Protected Areas. *Nature*, **515**(7525), 67–73.
1339 https://doi.org/10.1038/nature13947
1340 Wood, S. N. (2011). Fast Stable Restricted Maximum Likelihood and Marginal
1341 Likelihood Estimation of Semiparametric Generalized Linear Models. *Journal*
1342 *of the Royal Statistical Society Series B: Statistical Methodology*, **73**(1), 3–36.
1343 https://doi.org/10.1111/j.1467-9868.2010.00749.x
1344 Wood, S. N. (2017). *Generalized Additive Models: An Introduction with R, Second*
1345 *Edition*. CRC Press.
1346 Wood, S. N., Pya, N., & Säfken, B. (2016). Smoothing Parameter and Model
1347 Selection for General Smooth Models. *Journal of the American Statistical*

Association, **111**(516), 1548–63.
https://doi.org/10.1080/01621459.2016.1180986

Zscheischler, J., Westra, S., van den Hurk, B. J. J. M., Seneviratne, S. I., Ward, P. J., Pitman, A., AghaKouchak, A., Bresh, D. N., Leonard, M., Wahl, T., & Zhang, X. (2018). Future Climate Risk from Compound Events. *Nature Climate Change*, **8**(6), 469–77. https://doi.org/10.1038/s41558-018-0156-3

Appendix S1 – Methodological details and additional results

1. Seedbank parameters

We used previously published data obtained from seed-burial and greenhouse-germination experiments to parameterise the transitions of dewy-pine seeds from and to the soil seedbank and to continuous germination (Table S1). More specifically, following Paniw et al. (2017b), we used data on seeds buried in habitat conditions characteristic of early (i.e., recently burned) or late post-fire stages (i.e., long unburned) to estimate seed survival in the soil (i.e., seedbank stasis; staySB) and the probability of germinating from the seedbank at least two years after burial (outSB). We used estimates from recently burned habitats for anthropogenic populations, which experience constant anthropogenic disturbances mimicking the effects of fire (Paniw et al., 2017b). For natural populations, we used estimates from burned habitats in early post-fire stages (i.e., TSF_2 for staySB and TSF_1 for outSB), and from unburned habitats in later post-fire stages (i.e., from TSF_3 for staySB and from TSF_2 to TSF_4 for outSB). To more accurately describe the observed seedbank dynamics in the first TSFs (i.e., TSF_0 and TSF_1 for staySB and TSF_0 for outSB), we used previously published parameters representing the characteristically high germination rates from the seedbank (outSB) in a fire year (TSF_0), and low germination rates in late TSFs (TSF_5), as well as the very low seedbank stasis (staySB) following a fire (TSF_0 and TSF_1) (Paniw et al., 2017b; Conquet et al., 2023).

To estimate the probability of seeds germinating continuously without contributing to the seedbank (goCont) and its opposite parameter determining the probability of

seeds contributing to the seedbank (goSB), we used data from a growth-chamber germination experiment (see details in Gómez-González et al., 2018). Seeds from 15 individual dewy pines growing in natural or anthropogenic habitats were monitored to obtain the proportion of surviving seeds germinating (goCont) and remaining dormant (goSB = 1 - goCont). We used estimates from the corresponding habitat to parameterise seedbank transitions of our natural and anthropogenic populations. In natural populations, however, continuous germination and contribution to the seedbank only starts in TSF_2 and is extremely low from TSF_5. We therefore fixed the values for goCont and goSB using previously published data (Paniw et al., 2017b; Conquet et al., 2023) for these TSFs to represent these observed processes (Table S1). Because natural populations still experience fires, we defined time-since-fire-specific parameter values for these populations. Additionally, to take advantage of the population-specific data available from the germination experiment for several anthropogenic sites, we defined population-specific goCont and goSB values for anthropogenic populations.

Table S1 – Seedbank parameters obtained from seed-burial and germination experiments. We used previously published data from a seed-burial experiment in recently burned and long unburned dewy-pine habitats to estimate the proportion of seeds remaining in (staySB) or germinating from the seedbank (outSB). Additionally, we used data from a germination experiment on seeds from natural and anthropogenic habitats to estimate the proportion of seeds contributing to the seedbank (goSB) or germinating continuously (goCont). The table contains parameter means and, wherever available, 95% confidence intervals (with binomial standard deviations calculated as $\sqrt{\frac{\mu\times(1-\mu)}{N}}$ where μ is the parameter mean and *N* the

sample size). Asterisks indicate parameter values adapted from previously published values (Paniw et al., 2017b; Conquet et al., 2023), and for which the confidence interval could not be calculated.

Natural populations				
	Seedbank parameters			
Time since fire (TSF)	staySB	outSB	goCont	goSB
TSF_0	0.1*	0.81*	0*	0*
TSF_1	0.05*	0.061 [0.044, 0.077]	0*	0*
TSF_2	0.60 [0.57, 0.63]	0.035 [0.023, 0.046]	0.026 [0.016, 0.037]	0.97 [0.96, 0.98]
TSF_3	0.85 [0.83, 0.86]	0.035 [0.023, 0.046]	0.026 [0.016, 0.037]	0.97 [0.96, 0.98]
TSF_4	0.85 [0.83, 0.86]	0.035 [0.023, 0.046]	0.026 [0.016, 0.037]	0.97 [0.96, 0.98]
TSF_5	0.85 [0.83, 0.86]	0*	0.01*	0.99*
Anthropogenic populations				
	Seedbank parameters			
Site	staySB	outSB	goCont	goSB
Sierra del Retín Disturbed	0.60 [0.57, 0.63]	0.061 [0.044, 0.077]	0.11 [0, 0.28]	0.89 [0.72, 1.0]
Prisioneros	0.60 [0.57, 0.63]	0.061 [0.044, 0.077]	0.29 [0.0071, 0.57]	0.71 [0.99, 0.43]
Bujeo	0.60 [0.57, 0.63]	0.061 [0.044, 0.077]	0.16 [0.060, 0.26]	0.84 [0.74, 0.94]
Montera del Torero	0.60 [0.57, 0.63]	0.061 [0.044, 0.077]	0.18 [0, 0.37]	0.82 [0.63, 1.0]
Sierra Carbonera Disturbed	0.60 [0.57, 0.63]	0.061 [0.044, 0.077]	0.16 [0.060, 0.26]	0.84 [0.74, 0.94]

2. Seedbank parameters correction factors

Accurately estimating seedbank parameters is complex due to the many factors influencing germination and dormancy. Seed mortality is a hidden process that cannot be easily determined in the field without perturbing the populations and is therefore often underestimated. Therefore, to better represent the dewy-pine population dynamics in anthropogenic sites, we computed a correction factor corresponding to the seed aboveground survival (σ_{seed}). σ_{seed} corresponded to the proportion of seeds surviving aboveground and was obtained from data on flower damage (σ_{seed} = 1 – flower damage) (Paniw et al., 2017). As anthropogenic populations never returned to TSF_0, we only used σ_{seed} for TSF_4 (0.33). We corrected the seedbank parameter values in anthropogenic habitats by multiplying all four seedbank parameters (i.e., goCont, outSB, goSB, and staySB) by σ_{seed}. Additionally, previous model calibrations showed the need to further correct several seedbank parameters to mirror the observed dynamics of dewy-pine populations. To do so, we multiplied both goCont and outSB by 0.4 for Sierra Carbonera Disturbed. Moreover, as we estimated plant density within 1-m^2 quadrats, we avoided unrealistically high recruit numbers by capping the number of recruits to the maximum observed number of seedlings per quadrat during the study period in all natural populations and in two anthropogenic populations: Bujeo and Sierra Carbonera Disturbed. In natural populations, this number was TSF specific; however, data was unavailable for some TSFs in some populations. When unavailable for TSF_0, we set the maximum number of recruits to 1.5 times the maximum observed number of seedlings in the populations; in TSF_1, we set it to the maximum observed number of seedlings in the population; and in TSF_2 to the average maximum observed number of seedlings in the population in $TSF_{>0}$. The

correction factors resulted in predicted abundances (out-of-sample predictions) reflecting well observed abundances, size distributions, and aboveground population growth rates (Fig. S1; Fig. S2; Fig. 4 in main text).

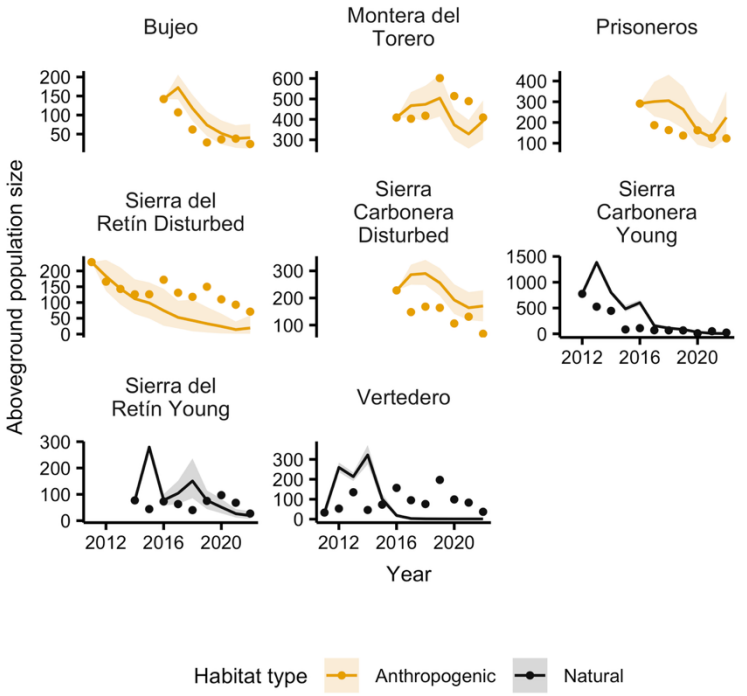

Figure S1 – Observed and projected aboveground population abundance. We projected each natural and anthropogenic population for 500 times across the range of observed years available for each population (maximum range from 2011 to 2022) to perform an out-of-sample validation of our individual-based model parameterization. For each projection, we obtained the average (line) and 25th and 95th (shaded ribbon) percentile of the aboveground population size. We compared these projected values to the observed ones (dots).

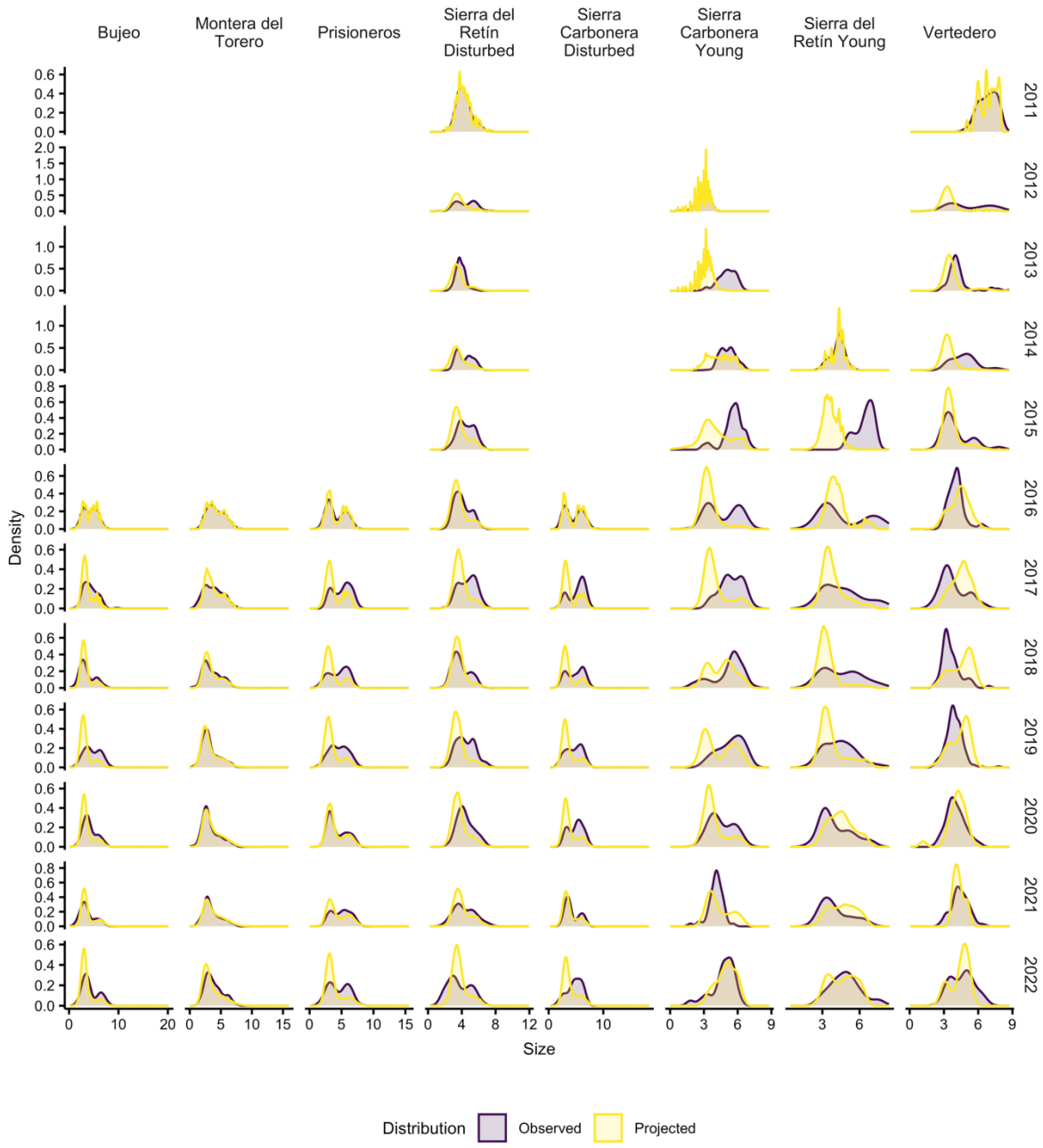

Figure S2 – Observed and projected distributions of individual size across time. We projected each population from the first year it was sampled to 2022 and obtained the site- and year-specific distributions of aboveground individual size, which we compared to the observed distributions. Size is defined as log(number of leaves × length of the longest leaf (cm)).

3. Covariate standardisation and correlation

We standardised all continuous covariates using the approach described by Gelman (2008):

$$\text{covariate}_{\text{scaled}(H)} = \frac{(\text{covariate}_{\text{unscaled}(H)} - \mu_{\text{covariate}_{\text{unscaled}(H)}})}{2 \cdot \sigma_{\text{covariate}_{\text{unscaled}(H)}}} \quad \text{(Equation 1)}$$

where μ and σ are respectively the mean and standard deviation of a given unscaled covariate in a subset of data from a given habitat H (natural or anthropogenic). In comparison with the common standardisation by one standard deviation, this standardisation approach enables the comparison of the effect sizes of both categorical (i.e. habitat) and continuous covariates (i.e. density-dependent variables).

We checked for correlations between covariates using the Pearson correlation coefficient (using the *cor* function from the stats R package; R Core Team, 2022). We considered a pair of variables to be correlated when the absolute value of the correlation coefficient was above 0.5. We included only one of the two correlated variables in a model, choosing the first to be retained in the model selection.

4. Vital-rate model selection

We assessed the nonlinear response of dewy-pine survival, growth, flowering probability, number of flowers, and seedling size to rainfall, maximum daily temperature, time since fire (TSF), aboveground density of large individuals (size >

4.5), and individual size using Generalised Additive Models (GAMs) fitted to demographic data from individual dewy pines growing in natural or anthropogenic habitats. We first assessed whether rainfall and temperature influenced vital rates and in which period. We did this by comparing a null model (i.e., with only year and population random effects, using a random effect basis (bs = “re”) in the mgcv package; (Wood, 2017)) with models including cumulative rainfall or average maximum daily temperature across different periods. As each census was done during the flowering period, we assessed rainfall and temperature effect prior to the annual population census for flowering probability, number of flowers, and seedling size; or in the period between two annual censuses for survival and growth (see Table S2 and Table S3). We considered further lagged climatic effects to be captured by changes in plant size and density.

Table S2 – Periods of average maximum daily temperature and cumulative rainfall considered to assess the effect of temperature and rainfall on dewy-pine vital rates. We investigated the nonlinear response of dewy-pine vital rates to average maximum daily temperature (μ_{maxT}) and cumulative rainfall ($\sum_{rain}$) in various periods of the years prior (for flowering probability, number of flowers, and seedling size; in regular text) or post the annual population census (for survival and growth; in italic).

Period full name	Short name	Start	End	Justification
Previous winter average maximum daily temperature	$\mu_{maxT\_prevWinter}$	January	April	Dewy pines rely almost exclusively on insect prey for nutrients (Paniw et al., 2017a). Long periods of above-average temperatures in winter and spring (approximated by this variable) can result in physiological stress for plants and desiccation of leaf mucilage preventing plants from catching and digest prey insects (Paniw et al., 2018).
Previous fall cumulative rainfall	$\sum_{rain\_prevFall}$	September	November	Rainfall in fall and winter is a key determinant of plant growth and survival in the Mediterranean shrublands (Paniw et al. 2023). For the dewy pine, in particular, plentiful rain translates to more air humidity, which allows the plants to maintain leaf mucilage to catch and digest prey insects (Adamec, 2009). In addition, abundant rainfall may result in higher invertebrate activity and thus more potential food for plants (Paniw et al., 2017b). Too much rain however may result in prey insects being washed off leaves; and this may occur in particular if plants are exposed (i.e., not protected by surrounding shrubs; Brewer et al., 2021).
Previous winter cumulative rainfall	$\sum_{rain\_prevWinter}$	January	April	Same justification as for fall cumulative rainfall. In addition, heavy rainfall in spring may damage or wash away seedlings.

Next summer average maximum daily temperature	$\mu_{maxT\_nextSummer}$	May	September	Extremely high summer temperatures may damage and desiccate plants, preventing them to capture prey with leaf mucilage (Paniw et al., 2018), particularly in anthropogenetic habitats where plants are often more exposed (Brewer et al., 2021) and where prey availability may be lower (Paniw et al., 2018)
Next fall cumulative rainfall	$\sum_{rain\_nextFall}$	September	November	Same justification as for previous fall rainfall, but considering the period between census at time *t* and *t*+1 (which is relevant for plant survival and growth)
Next winter cumulative rainfall	$\sum_{rain\_nextWinter}$	January	April	Same justification as for previous winter rainfall, but considering the period between census at time *t* and *t*+1 (which is relevant for plant survival and growth)
Next fall and winter cumulative rainfall	$\sum_{rain\_nextFallWinter}$	September	April	Same justification as for previous fall/winter rainfall, but considering the period between census at time *t* and *t*+1 (which is relevant for plant survival and growth)

154

155 We selected the best model among the possible rainfall and temperature periods
156 using the Akaike Information Criterion (AIC), through the *model.sel* and *AICtab*
157 functions of the MuMIn (Bartoń, 2022) and bbmle R packages (Bolker, 2022); we
158 used a threshold of $\Delta AIC < 2$ to identify models with no strong difference, and
159 selected the model with the lowest number of degrees of freedom if more than one
160 model were within that threshold. If both models with effects of rainfall and
161 temperature performed better than the null model, we calculated Pearson's
162 correlation coefficient using the *cor.test* function of the stats R package (R Core

Team, 2022) to check whether the two variables were correlated. If they were (i.e., correlation coefficient > |0.5|), we used the AIC and the number of degrees of freedom to select the best model between the one with rainfall and the one with temperature. Conversely, if the two variables were not correlated (i.e., correlation coefficient ≤ |0.5|) We compared the models including one of rainfall and temperature to a model with both climatic variables, including their interaction (Table S3). Finally, we performed a forward selection—using the AIC and the degrees of freedom—, progressively adding aboveground density, size (except for seedling size), and time since fire (TSF; for natural populations only) in the model. While Table S3 only shows splines, we included the linear effects of all covariates in the model selection. We then included interactions between covariates in the model selection if at least one of them was retained in the single effect selection. Additionally, we included terms for site-specific random slopes (e.g., random size effect depending on the site).

Table S3 – Example of the model selection process. We selected the best model to predict a given vital rate (vr) using the Akaike Information Criterion (AIC). We first assessed whether rainfall and temperature affected the vital rate by comparing a null model (with only year and population random effects (**M1**) to models including rainfall or temperature values in various periods of the year (Step 1 for temperature and 2 for rainfall). If both models with temperature and rainfall performed better than the null model, we compared them with a model containing both climatic variables (Step 3), and also included their interaction (Step 4). We then progressively added size, time since fire (TSF), and aboveground density of large individuals (density) to see if their introgression improved the model (Steps 5–7). Finally, we included interactions between covariates when at least one of the two members of the interaction had been previously retained in the model selection (Steps 8–9). For each step, the *Best model according to the AIC* column shows the best model (**M**) according to the AIC. This model is then used as a comparison to the newer models in the next step. Newly added covariates at each time step are shown in green.

Model selection step	Models compared	Best model according to the AIC
1	**M1** = vr ~ s(time, bs = "re") + s(site, bs = "re") **M2** = vr ~ s(μmaxT_prevWinter, k = 3, bs = "cr") + s(time, bs = "re") + s(site, bs = "re")	**M2**
2	**M3** = vr ~ s(time, bs = "re") + s(site, bs = "re") **M4** = vr ~ s(∑rain_prevWinter, k = 3, bs = "cr") + s(time, bs = "re") + s(site, bs = "re") **M5** = vr ~ s(∑rain_prevFall, k = 3, bs = "cr") + s(time, bs = "re") + s(site, bs = "re")	**M5**

3	**M2** = vr ~ s(μmaxT_prevWinter, k = 3, bs = "cr") + s(time, bs = "re") + s(site, bs = "re") **M5** = vr ~ s(∑rain_prevFall, k = 3, bs = "cr") + s(time, bs = "re") + s(site, bs = "re") **M6** = vr ~ s(μmaxT_prevWinter, k = 3, bs = "cr") + s(∑rain_prevFall, k = 3, bs = "cr") + s(time, bs = "re") + s(site, bs = "re")	**M6**
4	**M6** = vr ~ s(μmaxT_prevWinter, k = 3, bs = "cr") + s(∑rain_prevFall, k = 3, bs = "cr") + s(time, bs = "re") + s(site, bs = "re") **M7** = vr ~ s(μmaxT_prevWinter, k = 3, bs = "cr") + s(∑rain_prevFall, k = 3, bs = "cr") + ti(μmaxT_prevWinter, ∑rain_prevFall, k = 3, bs = "cr") + s(time, bs = "re") + s(site, bs = "re")	**M7**
5	**M7** = vr ~ s(μmaxT_prevWinter, k = 3, bs = "cr") + s(∑rain_prevFall, k = 3, bs = "cr") + ti(μmaxT_prevWinter, ∑rain_prevFall, k = 3, bs = "cr") + s(time, bs = "re") + s(site, bs = "re") **M8** = vr ~ s(μmaxT_prevWinter, k = 3, bs = "cr") + s(∑rain_prevFall, k = 3, bs = "cr") + ti(μmaxT_prevWinter, ∑rain_prevFall, k = 3, bs = "cr") + s(size, k = 3, bs = "cr") + s(time, bs = "re") + s(site, bs = "re") **M9** = vr ~ s(μmaxT_prevWinter, k = 3, bs = "cr") + s(∑rain_prevFall, k = 3, bs = "cr") + ti(μmaxT_prevWinter, ∑rain_prevFall, k = 3, bs = "cr") + s(density, k = 3, bs = "cr") + s(time, bs = "re") + s(site, bs = "re") **M10** = vr ~ s(μmaxT_prevWinter, k = 3, bs = "cr") +	**M9**

	s(∑rain_prevFall, k = 3, bs = "cr") + ti(μmaxT_prevWinter, ∑rain_prevFall, k = 3, bs = "cr") + s(TSF, k = 3, bs = "cr") + s(time, bs = "re") + s(site, bs = "re")	
6	**M9** = vr ~ s(μmaxT_prevWinter, k = 3, bs = "cr") + s(∑rain_prevFall, k = 3, bs = "cr") + ti(μmaxT_prevWinter, ∑rain_prevFall, k = 3, bs = "cr") + s(density, k = 3, bs = "cr") + s(time, bs = "re") + s(site, bs = "re") **M11** = vr ~ s(μmaxT_prevWinter, k = 3, bs = "cr") + s(∑rain_prevFall, k = 3, bs = "cr") + ti(μmaxT_prevWinter, ∑rain_prevFall, k = 3, bs = "cr") + s(density, k = 3, bs = "cr") + s(size, k = 3, bs = "cr") + s(time, bs = "re") + s(site, bs = "re") **M12** = vr ~ s(μmaxT_prevWinter, k = 3, bs = "cr") + s(∑rain_prevFall, k = 3, bs = "cr") + ti(μmaxT_prevWinter, ∑rain_prevFall, k = 3, bs = "cr") + s(density, k = 3, bs = "cr") + s(TSF, k = 3, bs = "cr") + s(time, bs = "re") + s(site, bs = "re")	**M12**

7	**M12** = vr ~ s(μmaxT_prevWinter, k = 3, bs = "cr") + s(∑rain_prevFall, k = 3, bs = "cr") + ti(μmaxT_prevWinter, ∑rain_prevFall, k = 3, bs = "cr") + s(density, k = 3, bs = "cr") + s(TSF, k = 3, bs = "cr") + s(time, bs = "re") + s(site, bs = "re") **M13** = vr ~ s(μmaxT_prevWinter, k = 3, bs = "cr") + s(∑rain_prevFall, k = 3, bs = "cr") + ti(μmaxT_prevWinter, ∑rain_prevFall, k = 3, bs = "cr") + s(density, k = 3, bs = "cr") + s(TSF, k = 3, bs = "cr") + s(size, k = 3, bs = "cr") + s(time, bs = "re") + s(site, bs = "re")	**M12**
8	**M12** = vr ~ s(μmaxT_prevWinter, k = 3, bs = "cr") + s(∑rain_prevFall, k = 3, bs = "cr") + ti(μmaxT_prevWinter, ∑rain_prevFall, k = 3, bs = "cr") + s(density, k = 3, bs = "cr") + s(TSF, k = 3, bs = "cr") + s(time, bs = "re") + s(site, bs = "re") **M14** = vr ~ s(μmaxT_prevWinter, k = 3, bs = "cr") + s(∑rain_prevFall, k = 3, bs = "cr") + ti(μmaxT_prevWinter, ∑rain_prevFall, k = 3, bs = "cr") + s(density, k = 3, bs = "cr") + s(TSF, k = 3, bs = "cr") + ti(μmaxT_prevWinter, density, k = 3, bs = "cr") + s(time, bs = "re") + s(site, bs = "re") **M15** = vr ~ s(μmaxT_prevWinter, k = 3, bs = "cr") + s(∑rain_prevFall, k = 3, bs = "cr") + ti(μmaxT_prevWinter, ∑rain_prevFall, k = 3, bs = "cr") + s(density, k = 3, bs = "cr") + s(TSF, k = 3, bs = "cr") + ti(μmaxT_prevWinter, TSF, k = 3, bs = "cr") + s(time, bs = "re") + s(site, bs = "re")	**M15**

	M16 = vr ~ s(μmaxT_prevWinter, k = 3, bs = "cr") + s(∑rain_prevFall, k = 3, bs = "cr") + ti(μmaxT_prevWinter, ∑rain_prevFall, k = 3, bs = "cr") + s(density, k = 3, bs = "cr") + s(TSF, k = 3, bs = "cr") + ti(μmaxT_prevWinter, size, k = 3, bs = "cr") + s(time, bs = "re") + s(site, bs = "re") **M17** = vr ~ s(μmaxT_prevWinter, k = 3, bs = "cr") + s(∑rain_prevFall, k = 3, bs = "cr") + ti(μmaxT_prevWinter, ∑rain_prevFall, k = 3, bs = "cr") + s(density, k = 3, bs = "cr") + s(TSF, k = 3, bs = "cr") + ti(∑rain_prevFall, density, k = 3, bs = "cr") + s(time, bs = "re") + s(site, bs = "re") **M18** = vr ~ s(μmaxT_prevWinter, k = 3, bs = "cr") + s(∑rain_prevFall, k = 3, bs = "cr") + ti(μmaxT_prevWinter, ∑rain_prevFall, k = 3, bs = "cr") + s(density, k = 3, bs = "cr") + s(TSF, k = 3, bs = "cr") + ti(∑rain_prevFall, TSF, k = 3, bs = "cr") + s(time, bs = "re") + s(site, bs = "re") **M19** = vr ~ s(μmaxT_prevWinter, k = 3, bs = "cr") + s(∑rain_prevFall, k = 3, bs = "cr") + ti(μmaxT_prevWinter, ∑rain_prevFall, k = 3, bs = "cr") + s(density, k = 3, bs = "cr") + s(TSF, k = 3, bs = "cr") + ti(∑rain_prevFall, size, k = 3, bs = "cr") + s(time, bs = "re") + s(site, bs = "re") **M20** = vr ~ s(μmaxT_prevWinter, k = 3, bs = "cr") + s(∑rain_prevFall, k = 3, bs = "cr") + ti(μmaxT_prevWinter, ∑rain_prevFall, k = 3, bs = "cr") + s(density, k = 3, bs = "cr") + s(TSF, k = 3, bs = "cr") +	

	ti(density, TSF, k = 3, bs = "cr") + s(time, bs = "re") + s(site, bs = "re") **M21** = vr ~ s(μmaxT_prevWinter, k = 3, bs = "cr") + s(∑rain_prevFall, k = 3, bs = "cr") + ti(μmaxT_prevWinter, ∑rain_prevFall, k = 3, bs = "cr") + s(density, k = 3, bs = "cr") + s(TSF, k = 3, bs = "cr") + ti(density, size, k = 3, bs = "cr") + s(time, bs = "re") + s(site, bs = "re") **M22** = vr ~ s(μmaxT_prevWinter, k = 3, bs = "cr") + s(∑rain_prevFall, k = 3, bs = "cr") + ti(μmaxT_prevWinter, ∑rain_prevFall, k = 3, bs = "cr") + s(density, k = 3, bs = "cr") + s(TSF, k = 3, bs = "cr") + ti(TSF, size, k = 3, bs = "cr") + s(time, bs = "re") + s(site, bs = "re")	
9	**M15** = vr ~ s(μmaxT_prevWinter, k = 3, bs = "cr") + s(∑rain_prevFall, k = 3, bs = "cr") + ti(μmaxT_prevWinter, ∑rain_prevFall, k = 3, bs = "cr") + s(density, k = 3, bs = "cr") + s(TSF, k = 3, bs = "cr") + ti(μmaxT_prevWinter, TSF, k = 3, bs = "cr") + s(time, bs = "re") + s(site, bs = "re") **M23** = vr ~ s(μmaxT_prevWinter, k = 3, bs = "cr") + s(∑rain_prevFall, k = 3, bs = "cr") + ti(μmaxT_prevWinter, ∑rain_prevFall, k = 3, bs = "cr") + s(density, k = 3, bs = "cr") + s(TSF, k = 3, bs = "cr") + ti(μmaxT_prevWinter, TSF, k = 3, bs = "cr") + ti(μmaxT_prevWinter, density, k = 3, bs = "cr") + s(time, bs = "re") + s(site, bs = "re") **M24** = vr ~ s(μmaxT_prevWinter, k = 3, bs = "cr") + s(∑rain_prevFall, k = 3, bs = "cr") +	**M15**

	ti(μmaxT_prevWinter, ∑rain_prevFall, k = 3, bs = "cr") + s(density, k = 3, bs = "cr") + s(TSF, k = 3, bs = "cr") + ti(μmaxT_prevWinter, TSF, k = 3, bs = "cr") + ti(μmaxT_prevWinter, size, k = 3, bs = "cr") + s(time, bs = "re") + s(site, bs = "re") **M25** = vr ~ s(μmaxT_prevWinter, k = 3, bs = "cr") + s(∑rain_prevFall, k = 3, bs = "cr") + ti(μmaxT_prevWinter, ∑rain_prevFall, k = 3, bs = "cr") + s(density, k = 3, bs = "cr") + s(TSF, k = 3, bs = "cr") + ti(μmaxT_prevWinter, TSF, k = 3, bs = "cr") + ti(∑rain_prevFall, density, k = 3, bs = "cr") + s(time, bs = "re") + s(site, bs = "re") **M26** = vr ~ s(μmaxT_prevWinter, k = 3, bs = "cr") + s(∑rain_prevFall, k = 3, bs = "cr") + ti(μmaxT_prevWinter, ∑rain_prevFall, k = 3, bs = "cr") + s(density, k = 3, bs = "cr") + s(TSF, k = 3, bs = "cr") + ti(μmaxT_prevWinter, TSF, k = 3, bs = "cr") + ti(∑rain_prevFall, TSF, k = 3, bs = "cr") + s(time, bs = "re") + s(site, bs = "re") **M27** = vr ~ s(μmaxT_prevWinter, k = 3, bs = "cr") + s(∑rain_prevFall, k = 3, bs = "cr") + ti(μmaxT_prevWinter, ∑rain_prevFall, k = 3, bs = "cr") + s(density, k = 3, bs = "cr") + s(TSF, k = 3, bs = "cr") + ti(μmaxT_prevWinter, TSF, k = 3, bs = "cr") + ti(∑rain_prevFall, size, k = 3, bs = "cr") + s(time, bs = "re") + s(site, bs = "re") **M28** = vr ~ s(μmaxT_prevWinter, k = 3, bs = "cr") + s(∑rain_prevFall, k = 3, bs = "cr") +	

	ti(μmaxT_prevWinter, ∑rain_prevFall, k = 3, bs = "cr") + s(density, k = 3, bs = "cr") + s(TSF, k = 3, bs = "cr") + ti(μmaxT_prevWinter, TSF, k = 3, bs = "cr") + ti(density, TSF, k = 3, bs = "cr") + s(time, bs = "re") + s(site, bs = "re")	
	M29 = vr ~ s(μmaxT_prevWinter, k = 3, bs = "cr") + s(∑rain_prevFall, k = 3, bs = "cr") + ti(μmaxT_prevWinter, ∑rain_prevFall, k = 3, bs = "cr") + s(density, k = 3, bs = "cr") + s(TSF, k = 3, bs = "cr") + ti(μmaxT_prevWinter, TSF, k = 3, bs = "cr") + ti(density, size, k = 3, bs = "cr") + s(time, bs = "re") + s(site, bs = "re")	
	M30 = vr ~ s(μmaxT_prevWinter, k = 3, bs = "cr") + s(∑rain_prevFall, k = 3, bs = "cr") + ti(μmaxT_prevWinter, ∑rain_prevFall, k = 3, bs = "cr") + s(density, k = 3, bs = "cr") + s(TSF, k = 3, bs = "cr") + ti(μmaxT_prevWinter, TSF, k = 3, bs = "cr") + ti(TSF, size, k = 3, bs = "cr") + s(time, bs = "re") + s(site, bs = "re")	

192

5. Vital-rate estimation results

Table S4 – Most parsimonious generalised additive models for dewy-pine vital rates. For natural (n = 3) and anthropogenic (n = 5) populations, we estimated survival (σ), growth of aboveground plants (φ), flowering probability (p_{fl}), number of flowers ($n_{flowers}$), and seedling size (Φ) as a function of monthly average daily maximum temperature in a given period (μ_{maxT_period}), monthly cumulative rainfall in a given period ($\sum_{rain\_period}$), aboveground density of large individuals (density), individual size, and—for natural populations—time since fire (TSF). We selected the best model to predict a given vital rate using the Akaike Information Criterion (AIC). The function $s(x_{edf})$ is the spline smoothing function (i.e. simple effect) of x, and $ti(x, y_{edf})$ is the tensor product smoothing function of x and y. We used a cubic regression spline (bs = "cr" in the mgcv package; Wood, 2011; Wood et al., 2016; Wood, 2017) for all smoothing parameters, with a dimension k = 3 (except for the size effect on the number of flowers, where we used k = 4 to force a decline in the number of flowers of large individuals and avoid an ever-increasing number of flowers). Additionally, all models include a year and site random effect. edf is the corresponding effective degrees of freedom (Wood, 2017), which represents the amount of nonlinearity in the model component (edf = 1 corresponds to a linear fit), and n in the sample size. For the intercept and linear predictors (i.e., outside of s and ti smoothing functions), we report the estimated β-coefficients and the standard error.

Vital rate	Family (link function)	Most parsimonious model	*n*
Natural populations			
σ	Binomial (logit)	$-1.1_{(0.28)} + 0.27_{(0.47)}\mu_{maxT\_nextSummer} + 0.11_{(0.48)}\sum_{rain\_nextFall} + ti(\sum_{rain\_nextFall}, \mu_{maxT\_nextSummer}\ edf=0.88) + s(size\ edf=1.7) + s(TSF\ edf=0.00018) + s(\mu_{maxT\_nextSummer}, site\ edf=1.5, bs = "re") + ti(size, TSF\ edf=2.1) + ti(\sum_{rain\_nextFall}, density\ edf=2.7) - 1.4_{(0.46)}\sum_{rain\_nextFall}*TSF + ti(\mu_{maxT\_nextSummer}, size\ edf=0.74) - 0.26_{(0.096)}\mu_{maxT\_nextSummer}*density + ti(\mu_{maxT\_nextSummer}, TSF\ edf=0.93) + ti(\sum_{rain\_nextFall}, size\ edf=1.7) + s(time\ edf=3.8, bs = "re") + s(site\ edf=0.00010, bs = "re")$	1493
γ	Scaled *t* (identity)	$5.1_{(0.12)} + s(\sum_{rain\_nextFall}\ edf=0.000063) + 1.5_{(0.14)}size + s(TSF\ edf=1.7) - 0.074_{(0.018)}density + s(size, site\ edf=1.6, bs = "re") + ti(\sum_{rain\_nextFall}, TSF\ edf=0.81) + ti(\sum_{rain\_nextFall}, density\ edf=2.1) + ti(size, density\ edf=0.83) + s(time\ edf=0.000019, bs = "re") + s(site\ edf=1.8, bs = "re")$	482
p_{fl}	Binomial (logit)	$-4.0_{(0.57)} + 0.93_{(0.95)}\sum_{rain\_prevFall} + ti(\sum_{rain\_prevFall}, \mu_{maxT\_prevWinter}\ edf=1.5) + 5.5_{(0.44)}size + s(TSF\ edf=0.0000079) + ti(TSF, \mu_{maxT\_prevWinter}\ edf=0.91) + ti(TSF, density\ edf=0.58) + ti(\sum_{rain\_prevFall}, TSF\ edf=0.61) + ti(\sum_{rain\_prevFall}, density\ edf=1.3) + ti(size, density\ edf=1.2) + s(time\ edf=3.8, bs = "re") + s(site\ edf=0.000041, bs = "re")$	1487
$n_{flowers}$	Negative binomial (log)	$2.0_{(0.052)} + s(\mu_{maxT\_prevWinter}\ edf=0.00041) + s(size\ edf=2.8) - 0.40_{(1.4)}TSF + s(time\ edf=0.0013, bs = "re") + s(site\ edf=0.000056, bs = "re")$	185
Φ	Scaled *t* (identity)	$3.4_{(0.073)} + s(\mu_{maxT\_prevWinter}\ edf=0.66) + s(density\ edf=0.49) + 0.16_{(0.079)}TSF + s(density, site\ edf=0.000064, bs = "re") + s(TSF, site\ edf=0.69, bs = "re") + ti(\mu_{maxT\_prevWinter}, density\ edf=1.3) + ti(\mu_{maxT\_prevWinter}, TSF\ edf=0.76) + ti(density, TSF\ edf=0.69) + s(time\ edf=4.8, bs = "re") + s(site\ edf=0.000071, bs = "re")$	745
Anthropogenic populations			
σ	Binomial (logit)	$-0.55_{(0.60)} + s(\sum_{rain\_nextFall}\ edf=0.015) - 1.8_{(0.41)}\mu_{maxT\_nextSummer} + ti(\sum_{rain\_nextFall}, \mu_{maxT\_nextSummer}\ edf=0.00017) + s(size\ edf=1.9) + s(size, site\ edf=3.6, bs = "re") + s(\sum_{rain\_nextFall}, site\ edf=3.2, bs = "re") + ti(\sum_{rain\_nextFall}, size\ edf=0.92) + 0.11_{(0.037)}size*density + s(time\ edf=4.5, bs = "re") + s(site\ edf=3.9, bs = "re")$	6008
γ	Scaled *t* (identity)	$5.0_{(0.13)} + s(\mu_{maxT\_nextSummer}\ edf=0.37) + s(size\ edf=1.6) - 0.028_{(0.0053)}density + s(size, site\ edf=3.9, bs = "re") + s(\mu_{maxT\_nextSummer}, site\ edf=3.9, bs = "re") + s(time\ edf=3.9, bs = "re") + s(site\ edf=3.8, bs = "re")$	3202
p_{fl}	Binomial (logit)	$-4.7_{(0.36)} + s(\sum_{rain\_prevWinter}\ edf=0.50) + s(size\ edf=2.0) + s(density, edf=1.6) + s(size, site\ edf=3.6, bs = "re") + s(\sum_{rain\_prevWinter}, site\ edf=2.4, bs = "re") + s(density, site\ edf=2.7, bs = "re") + s(time\ edf=5.0, bs = "re") + s(site\ edf=3.0, bs = "re")$	6254
$n_{flowers}$	Negative binomial (log)	$1.9_{(0.072)} + s(\sum_{rain\_prevFall}\ edf=0.0012) + s(size\ edf=2.8) + s(\sum_{rain\_prevFall}, site\ edf=4.0, bs = "re") + s(size, site\ edf=3.7, bs = "re") + s(time\ edf=3.0, bs = "re") + s(site\ edf=0.015, bs = "re")$	899
Φ	Scaled *t* (identity)	$3.0_{(0.14)} + s(\mu_{maxT\_prevWinter}\ edf=0.50) - 0.057_{(0.012)}density + s(\mu_{maxT\_prevWinter}, site\ edf=2.9, bs = "re") + s(density, site\ edf=1.9, bs = "re") + ti(\mu_{maxT\_prevWinter}, density\ edf=0.64) + s(time\ edf=5.5, bs = "re") + s(site\ edf=3.9, bs = "re")$	2608

216

Among-site variation in average vital rates and climate effects

Dewy-pine vital rates varied between natural and anthropogenic habitat as well as between sites. Among-site variation was larger in anthropogenic than in natural conditions, possibly because of the among-population differences in the level of anthropogenic disturbance. This variation was especially large for survival rates, which ranged from 0.11 [0.058, 0.20] in Bujeo to 0.80 [0.72, 0.86] in Montera del Torero, while it remained stable at 0.27 [0.17, 0.40] on average in natural populations (Fig. S3).

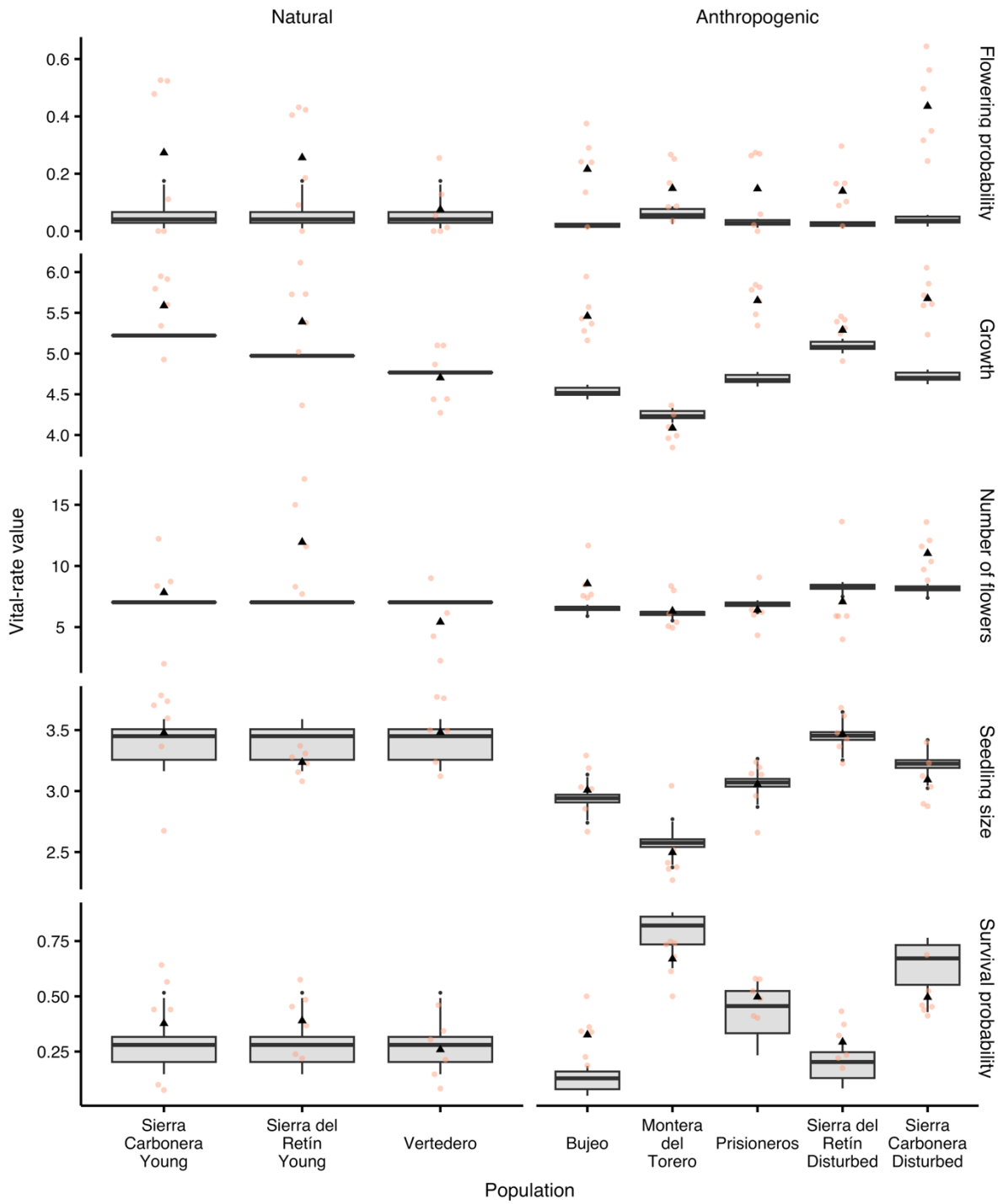

Figure S3 – Among-site variation in average vital-rate values in natural and anthropogenic populations. The boxplots represent the distribution of the average values of predicted site-specific survival, growth, and flowering rates, as well as the number of flowers and seedling size estimated for each year. The whiskers represent the 2.5th and 97.5th percentiles and the black triangle the mean estimate. We kept covariates at their mean values (scaled value = 0) except for the

number of flowers, where we used the mean size of reproducing individuals when doing predictions. The coloured dots represent the observed average vital rates in each population and year.

In anthropogenic habitats, we found among-site disparities in the direction of association between climatic variables and survival, growth, number of flowers per individual, and seedling size (Fig. S4). For instance, the number of flowers was positively associated with increasing rainfall in Montera del Torero population (e.g. from 5.5 [5.0, 6.1] under 100 mm of rain to 7.0 [6.3, 7.8] under 200 mm), but negatively in Sierra del Retín Disturbed (e.g. from 8.7 [7.5, 9.9] to 7.3 [6.4, 8.4]). In contrast, there was no such among-site variation in natural habitats. For example, seedlings were bigger with higher winter temperatures (January–April); seedling size increased from 3.0 [2.8, 3.3] under 16 °C to 3.4 [3.3, 3.6] under 18 °C (Fig. S5).

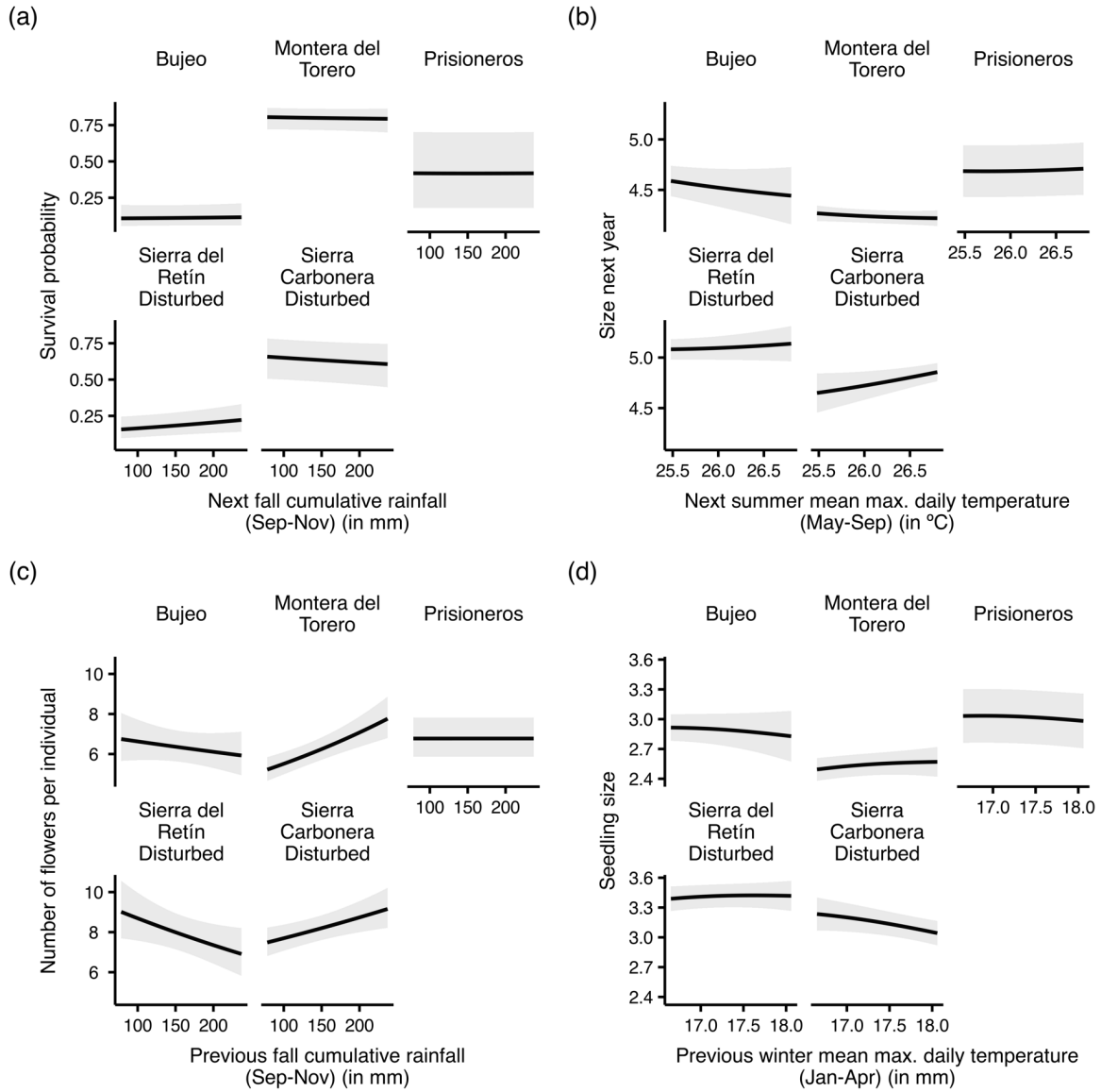

245 **Figure S4 – Among-site variation in the association between climatic**
246 **variables and vital rates in anthropogenic populations.** We predicted the values
247 of (a) survival probability, (b) size in the next year, (c) number of flowers per
248 individual, and (d) seedling size for a range of rainfall and temperature values in
249 each anthropogenic population of dewy pines. The lines represent the average vital-
250 rate value and the shaded ribbon the 95% confidence interval. We kept all other
251 covariates at their mean values (scaled value = 0) except for the number of flowers,
252 where we used the mean size of reproducing individuals.

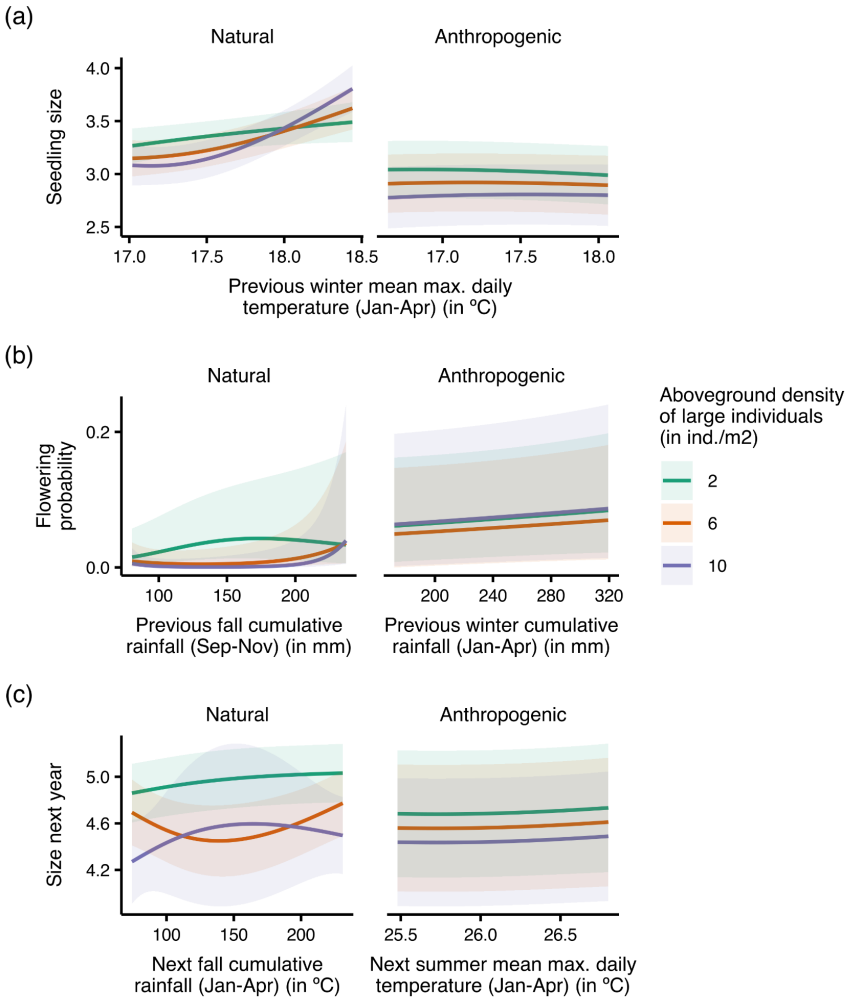

Figure S5 – Density-dependent variation in vital-rate responses to climate. We predicted the values of (a) seedling size, (b) flowering probability, and (c) size in the next year for a range of rainfall and temperature values and three levels of aboveground densities in natural and anthropogenic habitats. The lines represent the average vital-rate value and the shaded ribbon the 95% confidence interval. We kept all other covariates at their mean values (scaled value = 0) except for the number of flowers, where we used the mean size of reproducing individuals.

Vital-rate responses to large aboveground individual density and climate-density interactions

Seedling size decreased with higher numbers of large individuals aboveground (from 3.0 [2.8, 3.3] at 2 ind./m^2 to 2.8 [2.5, 3.1] at 10 ind./m^2 in anthropogenic populations and from 3.4 [3.2, 3.5] to 3.1 [3.0, 3.3] in natural ones; Fig. S5a; Table S5). Density also mediated the association between seedling size and winter temperature in natural populations, with a stronger positive correlation between the two variables with 6 ind./m2 (3.2 [3.1, 3.4] at 17.5 ºC and 3.7 [3.4, 3.9] at 18.5 ºC) than with 2 ind./m2 (3.4 [3.2, 3.5] and 3.5 [3.3, 3.7]) (Fig. S5a; Table S5). Additionally, with high densities in natural populations, flowering probability was low except for high amounts of rainfall (e.g. with 6 ind./m2, 0.19 [0.035, 0.60] for 150 mm of rainfall and 0.37 [0.096, 0.76] for 200 mm; but with 2 ind./m2, 0.71 [0.43, 0.88] and 0.71 [0.38, 0.90]) (Fig. S5b; Table S5), and the pattern was similar for growth (e.g. with 6 ind./m2, 4.5 [4.1, 4.8] for 150 mm of rainfall and 4.6 [4.3, 4.9] for 200 mm; but with 2 ind./m2, 5.0 [4.7, 5.2] and 5.0 [4.8, 5.3]) (Fig. S5c; Table S5).

Vital-rate responses to time since fire and size

As expected from previous work and observations, individuals in natural populations had a short lifespan, as indicated by the decrease in survival with time since fire (TSF) (0.42 [0.28, 0.57] and 0.29 [0.18, 0.42] respectively 3 and 7 years after a fire) and size (0.26 [0.16, 0.40] with a size of 5.0 and 0.22 [0.12, 0.37] with 6.2) (Fig. S6a,b; Table S5). This early decline in survival was accompanied by investment into reproduction from early post-fire stages, with flowering probability decreasing from 0.16 [0.038, 0.48] to 0.051 [0.016, 0.15] respectively 3 and 7 years after a fire and the number of flowers per individual from 10 [8.2, 13] to 7.6 [6.8, 8.4] (Fig. 5c,d; Table S5). Dewy pines growing in natural conditions also appeared to reproduce

290 throughout most of their lifetime, as both flowering probabilities and number of
291 flowers continuously increased with size (individuals had a probability of flowering of
292 0.17 [0.061, 0.38] and 2.9 [2.4, 3.5] flowers with a size of 5.0, which respectively
293 increased to 0.74 [0.47, 0.90] and 7.8 [6.9, 8.7] with 6.2) (Fig. S6e,f; Table S5). In
294 contrast, the largest individuals had the highest survival in anthropogenic habitats
295 (0.61 [0.32, 0.84] and 0.75 [0.46, 0.91] with sizes of 5.0 and 6.2; Fig. S6b; Table S5),
296 but did not invest as much in reproduction with both flowering probability and number
297 of flowers declining after reaching a peak for a size of 7.3 (probability of flowering of
298 0.69 [0.34, 0.91]) and 8.2 (19 [13, 28] flowers) (Fig. S6e,f; Table S5).
299
300 *Vital-rate responses to size-climate interactions*
301
302 In natural populations, small individuals survived best at intermediate rainfall (e.g.
303 0.29 [0.18, 0.43] with 150 mm of rain for an individual of size 3.4) than for high or low
304 amounts of rainfall (0.18 [0.098, 0.30] with 80 mm and 0.26 [0.14, 0.43] with 210
305 mm), while large individuals survived best at low or high rainfall (e.g., for an
306 individual of size 6.6, 0.26 [0.13, 0.45] with 80 mm, 0.20 [0.10, 0.37] with 150 mm,
307 and 0.26 [0.13, 0.45] with 210 mm; Fig. S6g; Table S5). Additionally, survival rates
308 decreased faster with summer temperature for large than for small individuals (from
309 0.60 [0.32, 0.83] at 25 °C to 0.26 [0.13, 0.44] at 26 ºC with a size of 6.6, and from
310 0.57 [0.32, 0.79] to 0.34 [0.22, 0.49] with a size of 3.4; Fig. S6h; Table S5). We also
311 found size dependence in the association between survival and rainfall in
312 anthropogenic populations, where large individuals survived best at intermediate
313 amounts of rain in fall (e.g., for an individual with a size of 6.6, 0.67 [0.37, 0.88] at 80

mm of rain, 0.78 [0.49, 0.93] at 150 mm, and 0.73 [0.44, 0.91] at 210 mm), while small individuals were not affected by changes in rainfall (Fig. S6g; Table S5).

Figure S6 – Vital-rate responses to time since fire, size, and size-climate interactions. We predicted the values of survival and flowering probability as well as

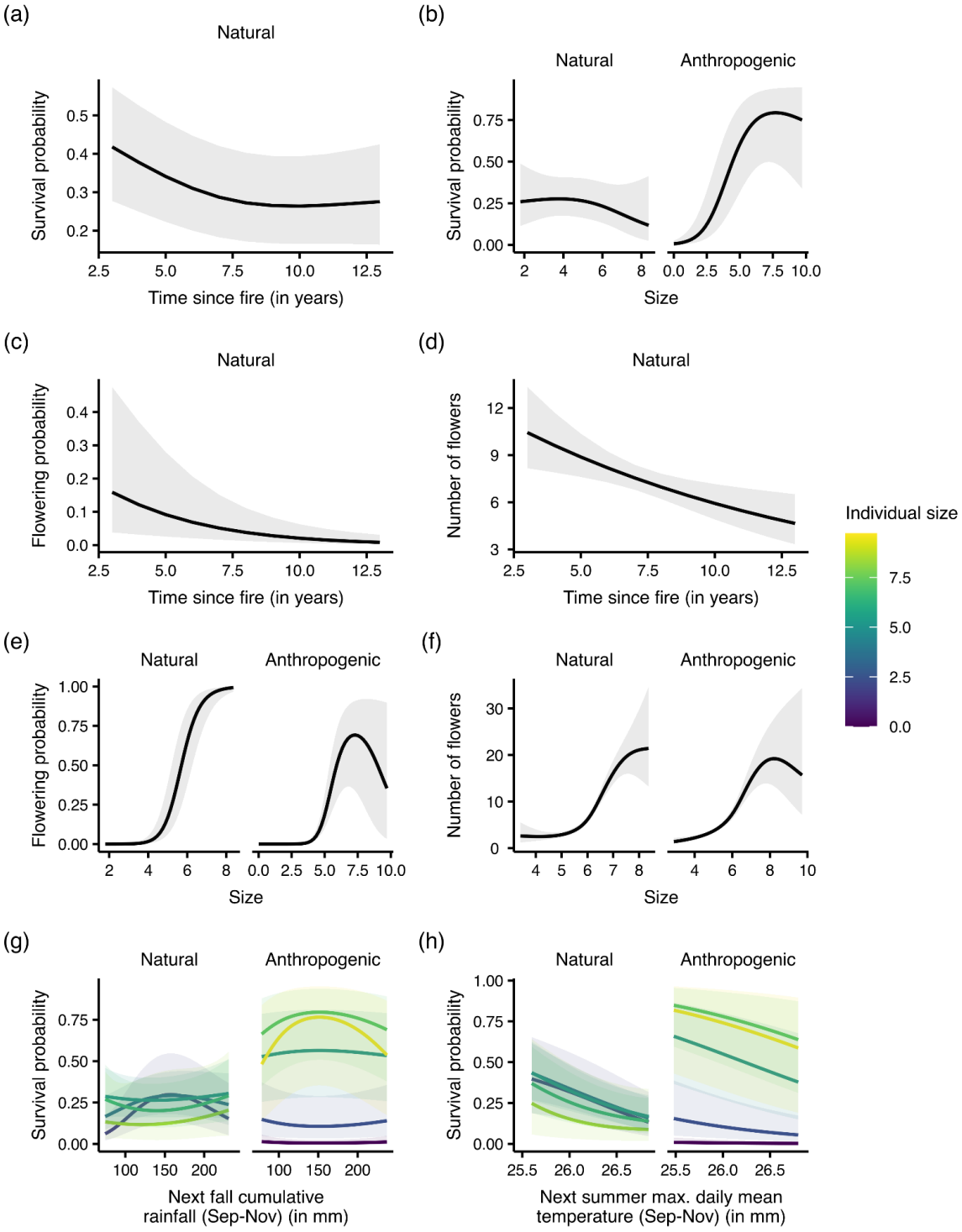

the number of flowers per individual for a range of number of years since the last fire

(time since fire) in natural habitats (a, c, d) and for a range of individual sizes in both natural and anthropogenic habitats (b, e, f). Finally, we predicted the values of survival probability for a range of individual sizes as well as (h) rainfall and (g) temperature values. The lines represent the average vital-rate value and the shaded ribbon the 95% confidence interval. In each case, we kept all other covariates at their mean values (scaled value = 0) except for the number of flowers, where we used the mean size of reproducing individuals.

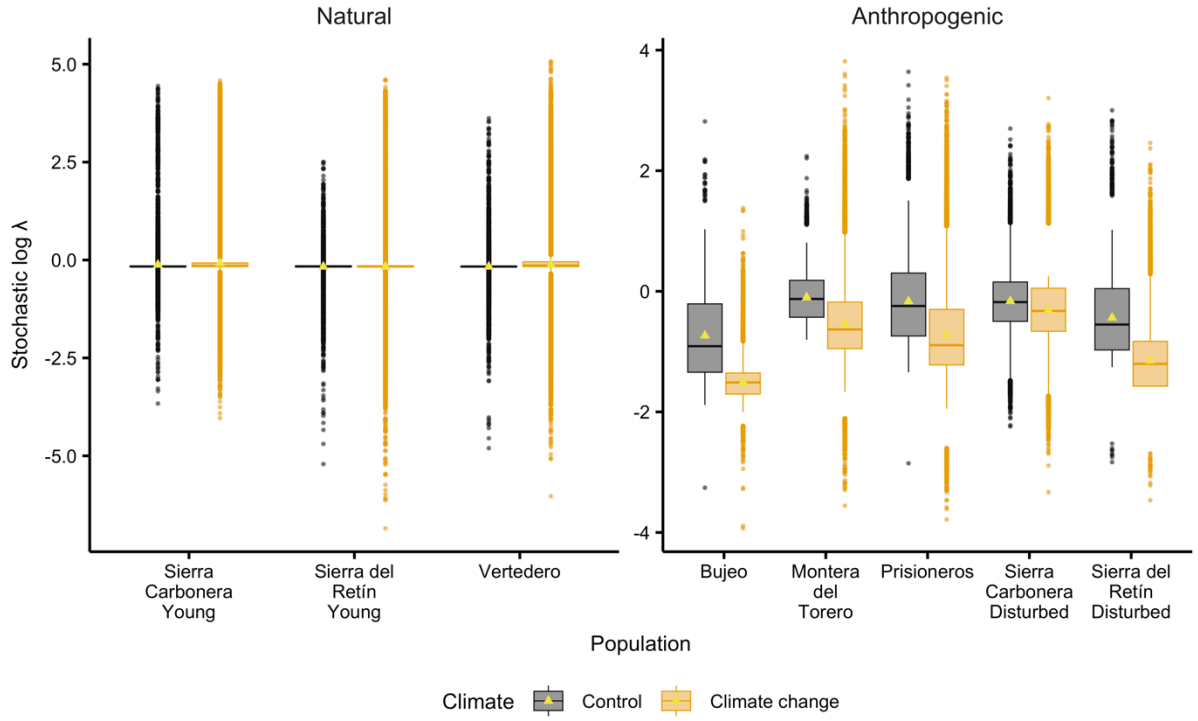

Figure S7 – Site-specific population growth rate. For each population, we calculated the stochastic growth rate log λ_S as the average of all annual log λ in each of 500 projections.

References – Appendix S1

Bartoń, K. (2022). MuMIn: Multi-Model Inference. R. https://CRAN.R-project.org/package=MuMIn

Bolker, B. (2022). Bbmle: Tools for General Maximum Likelihood Estimation. R. https://CRAN.R-project.org/package=bbmle

Conquet, E., Ozgul, A., Blumstein, D. T., Armitage, K. B., Oli, M. K., Martin, J. G. A., Clutton-Brock, T. H., & Paniw, M. (2023). Demographic Consequences of Changes in Environmental Periodicity. *Ecology*, **104**(3), e3894. https://doi.org/10.1002/ecy.3894

Gelman, A. (2008). Scaling Regression Inputs by Dividing by Two Standard Deviations. *Statistics in Medicine*, **27**(15), 2865–73. https://doi.org/10.1002/sim.3107

Gómez-González, S., Paniw, M., Antunes, K., & Ojeda, F. (2018). Heat Shock and Plant Leachates Regulate Seed Germination of the Endangered Carnivorous Plant *Drosophyllum Lusitanicum*. *Web Ecology*, **18**(1), 7–13. https://doi.org/10.5194/we-18-7-2018

Paniw, M., Gil-Cabeza, E., & Ojeda, F. (2017a). Plant Carnivory beyond Bogs: Reliance on Prey Feeding in Drosophyllum Lusitanicum (Drosophyllaceae) in Dry Mediterranean Heathland Habitats. *Annals of Botany*, **119**(6), 1035–41. https://doi.org/10.1093/aob/mcw247

Paniw, M., Quintana-Ascencio, P. F., Ojeda, F., & Salguero-Gómez, R. (2017b). Interacting Livestock and Fire May Both Threaten and Increase Viability of a Fire-Adapted Mediterranean Carnivorous Plant. *Journal of Applied Ecology*, **54**(6), 1884–94. https://doi.org/10.1111/1365-2664.12872

R Core Team. (2022). R: A Language and Environment for Statistical Computing. Vienna, Austria: R Foundation for Statistical Computing. https://www.R-project.org/

Wood, S. N. (2011). Fast Stable Restricted Maximum Likelihood and Marginal Likelihood Estimation of Semiparametric Generalized Linear Models. *Journal of the Royal Statistical Society Series B: Statistical Methodology*, **73**(1), 3–36. https://doi.org/10.1111/j.1467-9868.2010.00749.x

Wood, S. N. (2017). *Generalized Additive Models: An Introduction with R, Second Edition*. CRC Press.

Wood, S. N., Pya, N., & Säfken, B. (2016). Smoothing Parameter and Model Selection for General Smooth Models. *Journal of the American Statistical Association*, **111**(516), 1548–63. https://doi.org/10.1080/01621459.2016.1180986

Appendix S2 – Current and future rainfall and temperature data in dewy-pine populations

1. Current rainfall and temperature data

We modelled the response of dewy-pine vital rates to rainfall and maximum daily temperature using observed daily climatic data at dewy-pine population locations (Table 1) from the E-OBS dataset from the EU-FP6 project UERRA and the Copernicus Climate Change Service (Cornes et al., 2018; accessible at https://surfobs.climate.copernicus.eu/dataaccess/access_eobs.php). We used the ncdf4 R package to process the raw netCDF weather data (Pierce, 2021), and transformed the daily rainfall and maximum daily temperature into monthly cumulative rainfall and average maximum daily temperature. For each population, we then obtained monthly cumulative rainfall and average maximum temperature data from the year prior the first census (i.e., 2010 for Sierra del Retín Disturbed and Vertedero, 2011 for Sierra Carbonera Young, 2014 for Sierra del Retín Young, and 2015 for all other populations). To do so, we averaged the recorded climate values within a buffer of 0.1×1.5 degrees around the GPS location of each population.

Table S1 – Description of dewy-pine populations. Longitude and latitude of population locations are given in decimal degrees.

Population	Habitat type	Description*	Latitude	Longitude	First sampled	Last fire*	% bare ground#
Sierra Carbonera Young	Natural	Little browsed heathland patch (4 fires 1975-2008)	36.209722	-5.36	2012	2011	8.67 (±9.01)
Sierra del Retín Young	Natural	Little browsed heathland patch (1 fire 1975-2008)	36.1769444	-5.8330555	2015	2013	5.01 (±6.38)
Vertedero	Natural	Little browsed heathland patch (1 fire 1975-2008); surrounded by browsed areas but was fenced in after 2009 fire to prevent browsing	36.121667	-5.49	2011	2009	NA
Sierra del Retín Disturbed	Anthropogenic	Moderately browsed heathland patch (1 fire 1975-2008); located in military zone in a regularly cleared area (every 3 years) along a road to avoid wildfire ignitions	36.198056	-5.823611	2011	1996	NA
Prisioneros	Anthropogenic	Located on abandoned quarry; frequent browsing by goats	36.105	-5.4863888	2016	1950	56.80 (±22.09)
Bujeo	Anthropogenic	On a regularly cleared area (every 3 years) along a dirt road to avoid wildfire ignitions; frequent browsing by goats	36.072461	-5.52654	2016	1950	73.87 (±25.47)
Montera del Torero	Anthropogenic	On an old firebreak made by vegetation removal with bulldozers (mechanical uprooting); moderate browsing	36.226389	-5.585278	2016	1950	62.93 (±21.96)

Sierra Carbonera Disturbed	Anthropogenic	In a small uprooted, open patch close to old (abandoned) military premises; moderate browsing	36.106388	-5.3605555	2016	1950	22.67 (±22.99)

*Source: Paniw et al., 2017. See also REDIAM - *Áreas recorridas por el fuego en Andalucía (1975-actualidad);* Browsing was determined based on observations of dung/droppings of ungulates at the study sites during each visit (frequent browsing: droppings found in > 60% of plots on average; moderate browsing: droppings found in 30-60% of plots on average; little browsing: droppings found in < 30% of plots on average)

#Source: Gómez-González et al., 2018. % bare soil cover in a site was calculated as the number of 25 grids (10×10 cm each, arranged in a 50-cm square) that were bare soil. In each site in 2017, 30 of such 50-cm squares were located adjacent to randomly sampled dewy pine plants.

2. Projected rainfall and temperature data

To project dewy-pine populations under climate change, we used projected rainfall and temperature values at dewy-pine population locations from 11 global circulation models (GCM; see Table 2) from the Coupled Model Intercomparison Project 6 (CMIP6; Eyring et al., 2016; Pascoe et al., 2020; Waliser et al., 2020) available from the Earth System Grid Federation (ESFG; Petrie et al., 2021; available at https://aims2.llnl.gov/search). For each model, we selected the best variant using the GCMeval tool (Parding et al., 2020; accessible at https://gcmeval.met.no/). For each GCM, we downloaded data for the intermediate and worst scenario of atmospheric greenhouse gas Representative Concentration

Pathway (RCP), corresponding to a level of radiative forcing reaching 4.5 (RCP 4.5) or 8.5 (RCP 8.5) Watts per square metre (Wm^{-2}) by 2100, respectively. We processed the raw data from each climate projection model using the ncdf4 R package (Pierce, 2021) to obtain monthly cumulative rainfall and average maximum temperature in each population by averaging the values recorded within a buffer of 0.1×1.5 degrees around the population coordinates (i.e., 1.5 times the grid resolution).

Most GCMs comprised projected rainfall and temperature values beyond the values observed in our populations. To avoid predicting vital rates using values of climate variables outside the observed range, we capped these values to the maximum and minimum observed. For example, while the observed maximum cumulative rainfall in fall was 245 mm, six of the considered GCM predicted greater values in some years, ranging from 250 to 463 mm; we transformed these values to the maximum observed (245 mm). This allowed us to investigate the response of dewy-pine populations to increases in the frequency of extreme climatic conditions, rather than changes in absolute rainfall and temperature values.

Table S2 – List of global circulation models used to project dewy-pine populations under climate change.

Source ID	Experiment	Variant	Version	Institution	Modelling centre	Citation
CanESM5	ssp585	r1i1p1f1	20190429	Canadian Centre for Climate Modelling and Analysis, Environment and Climate Change Canada, Victoria, BC V8P 5C2, Canada	CCCma	(Swart et al., 2019)
EC_Earth3	ssp585	r4i1p1f1	20200425	AEMET, Spain; BSC, Spain; CNR-ISAC, Italy; DMI, Denmark; ENEA, Italy; FMI, Finland; Geomar, Germany; ICHEC, Ireland; ICTP, Italy; IDL, Portugal; IMAU, The Netherlands; IPMA, Portugal; KIT, Karlsruhe, Germany; KNMI, The Netherlands; Lund University, Sweden; Met Eireann, Ireland; NLeSC, The Netherlands; NTNU, Norway; Oxford University, UK; surfSARA, The Netherlands; SMHI, Sweden; Stockholm University, Sweden; Unite ASTR, Belgium; University College Dublin, Ireland; University of Bergen, Norway; University of Copenhagen, Denmark; University of Helsinki, Finland; University of Santiago de Compostela, Spain; Uppsala University, Sweden; Utrecht University, The Netherlands; Vrije Universiteit Amsterdam, the Netherlands;	EC-Earth-Consortium	(EC-Earth Consortium (EC-Earth), 2019)

				Wageningen University, The Netherlands. Mailing address: EC-Earth consortium, Rossby Center, Swedish Meteorological and Hydrological Institute/SMHI, SE-601 76 Norrkoping, Sweden		
FGOALS_G3	ssp585	r1i1p1f1	20190818	Chinese Academy of Sciences, Beijing 100029, China	CAS	(Li, 2019)
GFDL_ESM4	ssp585	r1i1p1f1	20180701	National Oceanic and Atmospheric Administration, Geophysical Fluid Dynamics Laboratory, Princeton, NJ 08540, USA	NOAA-GFDL	(John et al., 2018)
GISS_E2_1_G	ssp585	r1i1p1f2	20200115	Goddard Institute for Space Studies, New York, NY 10025, USA	NASA-GISS	(NASA Goddard Institute for Space Studies (NASA/GISS), 2020)
INM_CM4_8	ssp585	r1i1p1f1	20190603	Institute for Numerical Mathematics, Russian Academy of Science, Moscow 119991, Russia	INM	(Volodin et al., 2019)
IPSL_CM6A_LR	ssp585	r1i1p1f1	20190903	Institut Pierre Simon Laplace, Paris 75252, France	IPSL	(Boucher et al., 2019)
MIROC6	ssp585	r1i1p1f1	20191016	JAMSTEC (Japan Agency for Marine-Earth Science and Technology, Kanagawa 236-0001, Japan), AORI (Atmosphere and Ocean Research Institute, The University of Tokyo, Chiba 277-8564, Japan), NIES (National Institute for Environmental Studies, Ibaraki 305-8506, Japan), and R-	MIROC	(Shiogama et al., 2019)

				CCS (RIKEN Center for Computational Science, Hyogo 650-0047, Japan)		
MPI_ESM1_2_LR	ssp585	r10i1p1f1	20190710	Max Planck Institute for Meteorology, Hamburg 20146, Germany	MPI-M	(Wieners et al., 2019)
MRI_ESM2_0	ssp585	r1i1p1f1	20191108	Meteorological Research Institute, Tsukuba, Ibaraki 305-0052, Japan	MRI	(Yukimoto et al., 2019)
NorESM2_MM	ssp585	r1i1p1f1	20191108	NorESM Climate modeling Consortium consisting of CICERO (Center for International Climate and Environmental Research, Oslo 0349), MET-Norway (Norwegian Meteorological Institute, Oslo 0313), NERSC (Nansen Environmental and Remote Sensing Center, Bergen 5006), NILU (Norwegian Institute for Air Research, Kjeller 2027), UiB (University of Bergen, Bergen 5007), UiO (University of Oslo, Oslo 0313) and UNI (Uni Research, Bergen 5008), Norway. Mailing address: NCC, c/o MET-Norway, Henrik Mohns plass 1, Oslo 0313, Norway	NCC	(Bentsen et al. 2019)

3. Current and future climatic trends

Temperatures have increased in the past decades, with an average trend (mean and 95% confidence interval) of 0.033 ºC [0.021; 0.044] per year between

1980 and 2022. This trend will continue and intensify in the future, as climate-change models predict an increase of 0.055 ºC [0.053; 0.057] per year on average between 2015 and 2100 under the RCP 8.5 global change scenario (Moss et al., 2010; van Vuuren et al., 2011; Riahi et al., 2011). Average monthly cumulative rainfall and its variability show opposite trends between the current and projected conditions. Both the yearly mean and variability increased on average between 1980 and 2022 (0.18 [-0.23, 0.59] and 0.083 mm [-0.47, 0.63] per year, respectively) but are predicted to decrease until 2100 according to future projections under the RCP 8.5 scenario (-0.16 [-0.19, -0.13] and -0.11 mm [-0.14, -0.077]). Notably, while the RCP 4.5 global change scenario predicts a more moderate increase in temperature, both scenarios show the same trend for the 30 years of our projections (Fig. S1; Fig. S2a).

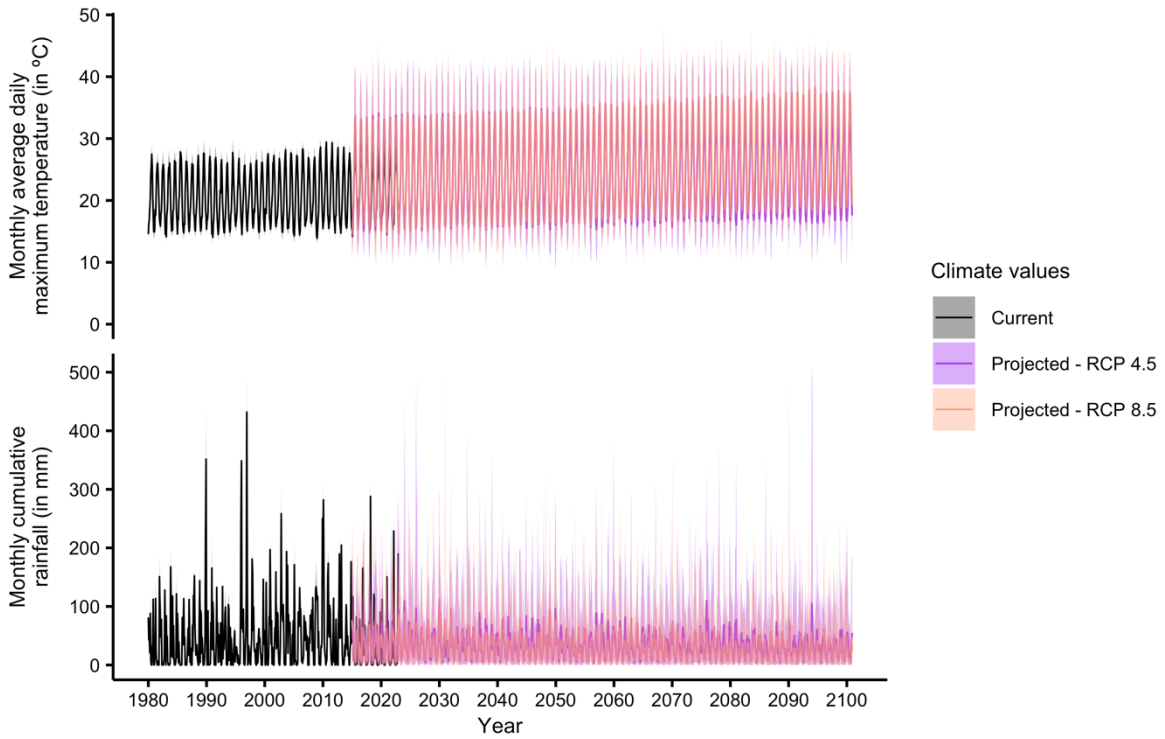

Figure S1 – Current and projected monthly temperature and rainfall data.

We obtained current data on daily maximum temperature and daily rainfall amounts from the E-OBS dataset from the EU-FP6 project UERRA and the Copernicus Climate Change Service. We extracted the projected rainfall and temperature values

under the RCP 4.5 and 8.5 global change scenarios from 11 global change models from the Coupled Model Intercomparison Project 6 (CMIP6; available from the Earth System Grid Federation).

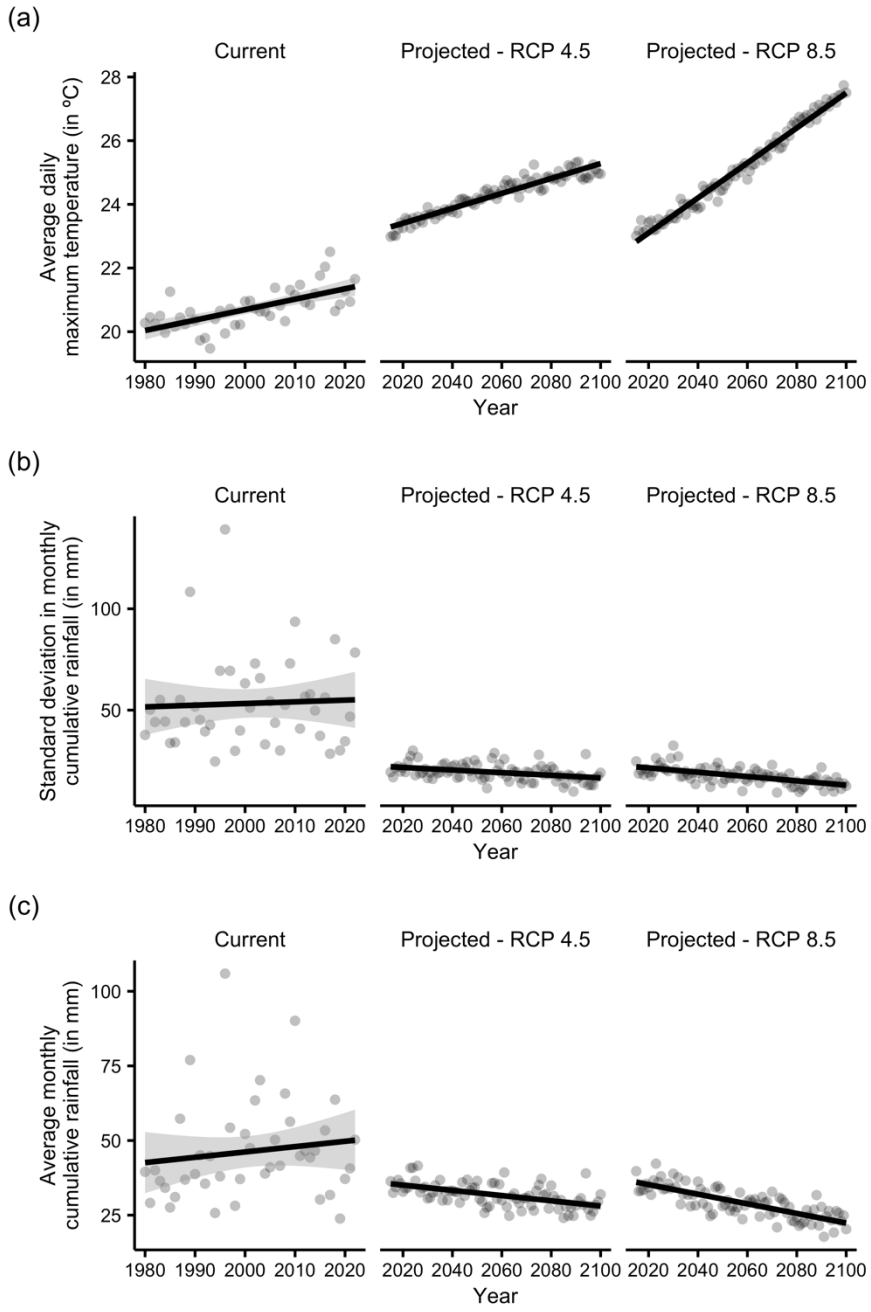

Figure S2 – Current and projected trends in temperature and rainfall. We investigated yearly changes in (a) average daily maximum temperature, (b) standard deviation in monthly cumulative rainfall, and (c) average monthly cumulative rainfall, for the current (1980–2022) and projected conditions (2015–2100) under the RCP

4.5 and 8.5 global change scenarios. Dots represent the observed values and lines and shaded ribbons represent the mean and 95% confidence interval of linear models fitted to each data subset.

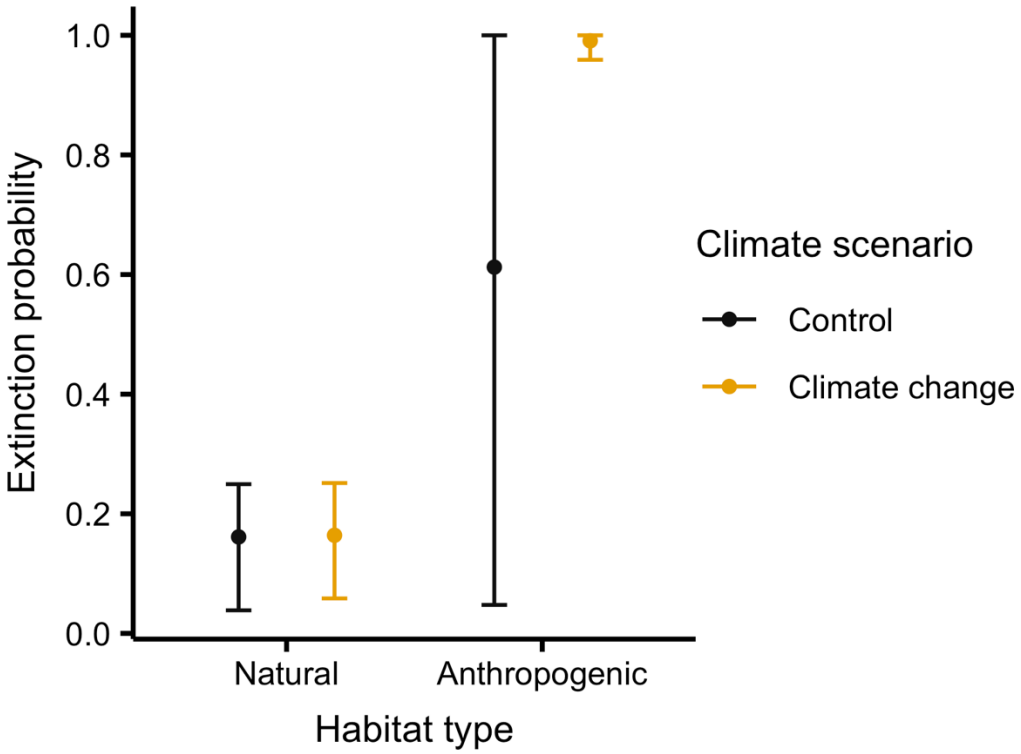

Figure S3 – Demographic consequences of climate change in natural and anthropogenic populations of dewy pines under scenario RCP4.5. We projected each natural and anthropogenic population 500 times for 30 years under a control (keeping temperature and rainfall conditions as currently observed) and two climate-change scenarios (RCP4.5 and RCP8.5). Here, we show results for scenario RCP4.5 (see Figure 5 in the main text for RCP8.5). We computed, for each population, the probability of quasi-extinction ($p_{q\text{-}ext}$). Here we summarise these metrics per habitat type, and the variability in the values therefore correspond to among-population and among-projection differences.

References – Appendix S2

Bentsen, M., Oliviè, D. J. L., Seland, Ø., Toniazzo, T., Gjermundsen, A., Graff, L. S., Debernard, J. B., Gupta, A. K., He, Y., Kirkevåg, A., Schwinger, J., Tjiputra, J., Aas, K. S., Bethke, I., Fan, Y., Griesfeller, J., Grini, A., Guo, C., Ilicak, M., … Schulz, M. (2019). *NCC NorESM2-MM Model Output Prepared for CMIP6 ScenarioMIP ssp585*. Version *20191108*. Earth System Grid Federation. https://doi.org/10.22033/ESGF/CMIP6.8321

Boucher, O., Denvil, S., Levavasseur, G., Cozic, A., Caubel, A., Foujols, M.-A., Meurdesoif, Y., Cadule, P., Devilliers, M., Dupont, E., & Lurton, T. (2019). IPSL IPSL-CM6A-LR Model Output Prepared for CMIP6 ScenarioMIP ssp585. Version *20190903*. Earth System Grid Federation. https://doi.org/10.22033/ESGF/CMIP6.5271

Cornes, R. C., van der Schrier, G., van den Besselaar, E. J. M., & Jones, P. D. (2018). An Ensemble Version of the E-OBS Temperature and Precipitation Data Sets. *Journal of Geophysical Research: Atmospheres*, **123**(17), 9391–409. https://doi.org/10.1029/2017JD028200

EC-Earth Consortium (EC-Earth). (2019). *EC-Earth-Consortium EC-Earth3 Model Output Prepared for CMIP6 ScenarioMIP ssp585.* Version *20200425*. Earth System Grid Federation. https://doi.org/10.22033/ESGF/CMIP6.4912

Eyring, V., Bony, S., Meehl, G. A., Senior, C. A., Stevens, B., Stouffer, R. J., & Taylor, K. E. (2016). Overview of the Coupled Model Intercomparison Project Phase 6 (CMIP6) Experimental Design and Organization. *Geoscientific Model Development*, **9**(5), 1937–58. https://doi.org/10.5194/gmd-9-1937-2016

Gómez-González, S., Paniw, M., Antunes, K., & Ojeda, F. (2018). Heat Shock and

Plant Leachates Regulate Seed Germination of the Endangered Carnivorous Plant *Drosophyllum Lusitanicum*. *Web Ecology*, **18**(1), 7–13.

John, J. G., Blanton, C., McHugh, C., Radhakrishnan, A., Rand, K., Vahlenkamp, H., Wilson, C., Zadeh, N. T., Dunne, J. P., Dussin, R., Horowitz, L. W., Krasting, J. P., Lin, P., Malyshev, S., Naik, V., Ploshay, J., Shevliakova, E., Silvers, L. Stock, C., Winton, M., & Zeng, Y. (2018). *NOAA-GFDL GFDL-ESM4 Model Output Prepared for CMIP6 ScenarioMIP ssp585*. Version *20180701*. Earth System Grid Federation. https://doi.org/10.22033/ESGF/CMIP6.8706

Li, L. (2019). *CAS FGOALS-G3 Model Output Prepared for CMIP6 ScenarioMIP ssp585*. Version *20190818*. Earth System Grid Federation. https://doi.org/10.22033/ESGF/CMIP6.3503

Moss, R. H., Edmonds, J. A., Hibbard, K. A., Manning, M. R., Rose, S. K., van Vuuren, D. P., Carter, T. R., Emori, S., Kainuma, M., Kram, T., Meehl, G. A., Mitchell, J. F. B., Nakicenovic, N., Riahi, K., Smith, S. J., Stouffer, R. J., Thomson, A. M., Weyant, J. P., & Wilbanks, T. J. (2010). The next generation of scenarios for climate change research and assessment. *Nature*, 463, 747–756. https://doi.org/10.1038/nature08823

NASA Goddard Institute for Space Studies (NASA/GISS). (2020). *NASA-GISS GISS-E2.1G Model Output Prepared for CMIP6 ScenarioMIP ssp585*. Version *20200115*. Earth System Grid Federation. https://doi.org/10.22033/ESGF/CMIP6.7460

Paniw, M., Quintana-Ascencio, P. F., Ojeda, F., & Salguero-Gómez, R. (2017b). Interacting Livestock and Fire May Both Threaten and Increase Viability of a Fire-Adapted Mediterranean Carnivorous Plant. *Journal of Applied Ecology*, **54**(6), 1884–94. https://doi.org/10.1111/1365-2664.12872

Parding, K. M., Dobler, A., McSweeney, C. F., Landgren, O. A., Benestad, R., Erlandsen, H. B., Mezghani, A., Gregow, H., Räty, O., Viktor, E., El Zohbi, J., Christensen, O. B., & Loukos, H. (2020). GCMeval – An Interactive Tool for Evaluation and Selection of Climate Model Ensembles. *Climate Services*, **18**(April), 100167. https://doi.org/10.1016/j.cliser.2020.100167

Pascoe, C., Lawrence, B. N., Guilyardi, E., Juckes, M., & Taylor, K. E. (2020). Documenting Numerical Experiments in Support of the Coupled Model Intercomparison Project Phase 6 (CMIP6). *Geoscientific Model Development*, **13**(5), 2149–67. https://doi.org/10.5194/gmd-13-2149-2020

Petrie, R., Denvil, S., Ames, S., Levavasseur, G., Fiore, S., Allen, C., Antonio, F., Berger, K., Bretonnière P.-A., Cinquini, L., Dart, E., Dwarakanath, P., Drukem, K., Evans, B., Franchistéguy, L., Gardoll, S., Gerbier, E., Greenslade, M., Hassell, D., … Wagner, R. (2021). Coordinating an Operational Data Distribution Network for CMIP6 Data. *Geoscientific Model Development*, **14**(1), 629–44. https://doi.org/10.5194/gmd-14-629-2021

Pierce, D. (2021). Ncdf4: Interface to Unidata netCDF (Version 4 or Earlier) Format Data Files. R. https://CRAN.R-project.org/package=ncdf4

Riahi, K., Rao, S., Krey, V., Cho, C., Chirkov, V., Fischer, G., Kindermann, G., Nakicenovic, N., & Rafaj, P. (2011). RCP 8.5—A Scenario of Comparatively High Greenhouse Gas Emissions. *Climatic Change*, **109**(1), 33. https://doi.org/10.1007/s10584-011-0149-y

Shiogama, H., Abe, M., & Tatebe, H. (2019). *MIROC MIROC6 Model Output Prepared for CMIP6 ScenarioMIP ssp585.* Version *20191016*. Earth System Grid Federation. https://doi.org/10.22033/ESGF/CMIP6.5771

Swart, N. C., Cole, J. N. S., Kharin, V. V., Lazare, M., Scinocca, J. F., Gillett, N. P.,

Anstey, J., Arora, V., Christian, J. R., Jiao, Y., Lee, W. G., Majaess, F., Saenko, O. A., Seiler, C., Seinen, C., Shao, A., Solheim, L., von Salzen, K., Yango, D., Winter, B., & Sigmond, M. (2019). *CCCma CanESM5 Model Output Prepared for CMIP6 ScenarioMIP ssp585*. Version *20190429*. Earth System Grid Federation. https://doi.org/10.22033/ESGF/CMIP6.3696

van Vuuren, D. P., Edmonds, J., Kainuma, M., Riahi, K., Thomson, A., Hibbard, K., Hurtt, G. C., Kram, T., Krey, V., Lamarque, J.-L., Masui, T., Meinshausen, M., Nakicenovic, N., Smith, S. J. & Rose, S. K. (2011). The representative concentration pathways: an overview. *Climatic Change*, **109**, 5. https://doi.org/10.1007/s10584-011-0148-z

Volodin, E., Mortikov, E., Gritsun, A., Lykossov, V., Galin, V., Diansky, N., Gusev, A., Kostrykin, S., Iakovlev, N., Shestakova, A., & Emelina, S. (2019). *INM INM-CM4-8 Model Output Prepared for CMIP6 ScenarioMIP ssp585*. Version *20190603*. Earth System Grid Federation. https://doi.org/10.22033/ESGF/CMIP6.12337

Waliser, D., Gleckler, P. J., Ferraro, R., Taylor, K. E., Ames, S., Biard, J., Bosilovich, M. G., Brown, O., Chepfer, H., Cinquini, L., Durack, P.J., Eyring, V., Mathieu, P.-P., Lee, T., Pinnock, S., Potter, G. L., Rixen, M., Saunders, R., Schulz, J., Thépaut, J.-N., Tuma, M. (2020). Observations for Model Intercomparison Project (Obs4MIPs): Status for CMIP6. *Geoscientific Model Development*, **13**(7), 2945–58. https://doi.org/10.5194/gmd-13-2945-2020

Wieners, K.-H., Giorgetta, M., Jungclaus, J., Reick, C., Esch, M., Bittner, M., Gayler, V., Haak, H., de Vrese, P., Raddatz, T., Mauritsen, T., von Storch, J.-S., Behrens, J., Brovkin, V., Claussen, M., Crueger, T., Fast, I., Fiedler, S., Hagemann, S., … Roeckner, E. (2019). *MPI-M MPI-ESM1.2-LR Model Output*

Prepared for CMIP6 ScenarioMIP ssp585. Version *20190710*. Earth System Grid Federation. https://doi.org/10.22033/ESGF/CMIP6.6705

Yukimoto, S., Koshiro, T., Kawai, H., Oshima, N., Yoshida, K., Urakawa, S., Tsujino, H., Deushi, M., Tanaka, T., Hosaka, M., Yoshimura, H., Shindo, E., Mizuta, R., Ishii, M., Obata, A., & Adachi, Y. (2019). *MRI MRI-ESM2.0 Model Output Prepared for CMIP6 ScenarioMIP ssp585*. Version *20191108*. Earth System Grid Federation. https://doi.org/10.22033/ESGF/CMIP6.6929

Appendix S3 – Individual-based model description

The model description follows the ODD (Overview, Design concepts, Details) protocol for describing individual- and agent-based models (Grimm et al., 2006), as updated by (Grimm et al., 2020).

1. Purpose and patterns

The purpose of the model is to predict population growth rates and extinction probabilities of dewy-pine (*Drosophyllum lusitanicum*) populations in natural and anthropogenic habitats in response to projected changes in rainfall and temperature values. We evaluate our model by its ability to reproduce the observed dynamics in the mean changes in aboveground abundance in each population, or at least follow a similar trend.

2. Entities, state variables, and scales

Entities and state variables

The **environment** is a single entity representing the population. Its role is to describe the environment (e.g. climate variables) and keep track of simulated time. Environment state variables correspond to dynamic global variables and are presented in Table 1.

Table 1 – Environment state variables

Variable name	Variable type and units	Range	Meaning
time_sim	Integer; dynamic	≥1	Number of years that passed since the start of the projection
year_obs	Integer; dynamic (e.g. 2020)	≥2016	Current year in the projection
year	Integer; dynamic (e.g. 2020)	≥2016	Year randomly sampled from the available observed years
TSF	Integer; dynamic	≥0	Number of years since the last fire
TSFcat	Categorical; dynamic (0–4)	{0, 1, 2, 3, 4}	Post-fire habitat stage, with any number of years after a fire ≥ 4 corresponding to 4
corr_seed_surv	Probability; dynamic	[0, 1]	Correction factor representing the survival probability of seeds above the ground
summerT	Real number; °C; dynamic	≥0	Average minimum daily temperature in summer (May–September) following the annual survey in May
prevwinterT	Real number; °C; dynamic	≥0	Average minimum daily temperature in winter (January–April) prior to the annual survey in May
fallR	Integer; mm; dynamic	≥0	Cumulative rainfall in fall (September–November) following the annual survey in May
prevfallR	Integer; mm; dynamic	≥0	Cumulative rainfall in fall (September–November) prior to the annual survey in May
prevwinterR	Integer; mm; dynamic	≥0	Cumulative rainfall in winter (January–April) prior to the annual survey in May
extinction	Binary; dynamic	{0, 1}	Current state of the population: extinct (1) or not (0)

Plants are entities representing the aboveground—as opposed to seeds—individual dewy pines in the population. They correspond to individuals from the seedling stage

in the species life cycle. The state variables unique to each plant are presented in Table 2.

Table 2 – Plant state variables

Variable name	Variable type and units	Range	Meaning
ID	Character string; static	NA	Unique identifier of the plant
quadratID	Character string; static	NA	Unique identifier of the quadrat corresponding to the location of the plant
size	Real number; dynamic	≥0	Plant size in the current time step, corresponding to log(number of leaves x length of the longest leaf in cm)
survival	Binary; dynamic	{0, 1}	State of the plant at the next time step: alive (1) or dead (0)
sizeNext	Real number; dynamic	≥0	Plant size in the next time step, corresponding to log(number of leaves x length of the longest leaf in cm)
flowering	Binary; dynamic	{0, 1}	Reproductive state of the plant in the current time step: flowering (1) or not (0)
nbFlowers	Integer; dynamic	≥0	Number of flowers on the plant
nb_seeds	Integer; dynamic	≥0	Number of seeds per flower produced by the plant

Seeds are entities representing individuals before they germinate and become seedlings. Because they are concerned by different processes, we divided seeds between two types of entities: **Seedbank seeds** are entities representing the seeds in the soil seedbank and **produced seeds** are entities representing the individuals that have been produced by aboveground reproducing dewy pines in the current time step. Their state variables are presented in Table 3 and Table 4.

39 **Table 3 – Seedbank seed state variables**

Variable name	Variable type and units	Range	Meaning
ID	Character string; static	NA	Unique identifier of the seed
quadratID	Character string; static	NA	ID of the quadrat corresponding to the location of the seed
size	Real number; dynamic	≥0	Size of the seedling growing from the germinating seed in the next time step, corresponding to log(number of leaves x length of the longest leaf in cm)
outSB	Binary; dynamic	{0, 1}	Seed germination (1) or not (0)
staySB	Binary; dynamic	{0, 1}	Seed dormancy (1) or not (0)

40

41 **Table 4 – Produced seed state variables**

Variable name	Variable type and units	Range	Meaning
ID	Character string; static	NA	Unique identifier of the seed
quadratID	Character string; static	NA	ID of the quadrat corresponding to the location of the seed
size	Real number; dynamic	≥0	Size of the seedling growing from the germinating seed in the next time step, corresponding to log(number of leaves x length of the longest leaf in cm)
goCont	Binary; dynamic	{0, 1}	Seed germination (1) or not (0)
goSB	Binary; dynamic	{0, 1}	Seed entering the seedbank (1) or not (0)

42

Quadrats are two-dimensional squares representing the monitoring units in which plants are censored in a population. Quadrats are only associated with one dynamic state variable, *abLarge*, an integer (≥0) corresponding to the number of plants with a size > 4.5 present in a quadrat.

Scales

The model is spatially explicit and represents a population in a two-dimensional space extending over 40 m^2 divided in 1-m^2 quadrats. These quadrats are discrete units in which individual plants and seeds are distributed, and correspond to the units in which dewy pines are monitored every year—more specifically in four separated transects of ten quadrats each.

The model represents time via discrete time steps, each corresponding to one year, to replicate the annual surveys that take place in May in the various populations.

3. Process overview and scheduling

Process overview

The model covers the life cycle of dewy pines. At each time step, the **environment** updates the environmental variables and simulation time; the **plants** reproduce, survive, and grow; the **seedbank seeds** germinate or stay dormant; and the **produced seeds** germinate or go to the seedbank. The **quadrats** get new aboveground density values.

Schedule summary

Throughout the model, the update of each state variable is done simultaneously for all entities, as each process in a given entity (i.e., environment, seeds, and plants) is assumed to be independent from the processes in another entity.

At each timestep, the model resets the ensemble of **seeds produced** to zero. The population of **plants** is also reset if a fire occurred, as all aboveground individuals are burned. The **environment** then updates the environmental variables (rainfall and temperature) as well as the simulation year and the number of years after the last fire. The latter two are used to update the correction factor representing seed survival (*corr_seed_surv*).

Aboveground **plants** then reproduce (see *Reproduction* submodel); that is, they flower and produce a certain number of flowers, which in turn produce seeds. The number of flowers is capped to the user-selected value if needed. The fate of the **seeds produced** is updated; they can either germinate, contribute to the seedbank, or die (i.e., none of the two former processes). **Produced seeds** that do not die are then assigned an ID, and those that germinate a size, and the maximum ID number is updated.

After reproducing, **plants** survive and grow (*Survival and growth* submodel). The size is capped or adjusted if needed. Seedbank processes take place next (*Seedbank* submodel), with **seedbank seeds** germinating, staying dormant, or dying (i.e., none of the two former processes). Seeds that germinate are attributed a size.

Produced seeds that were assigned to go dormant are added to the seedbank, and those that germinate are added to the aboveground population after capping their number in each **quadrat**.

After each timestep, the population growth rate and mean change in aboveground population abundance are calculated and the yearly individual data is merged to the full data. The **environment** updates the simulation time and the extinction status to 1 if the quasi-extinction threshold is reached, and the size of each surviving **plant** is updated to its size at the next time step. Finally, the aboveground density in each **quadrat** is updated.

Schedule details

The schedule follows the processes of the dewy-pine life cycle during a year from the annual census occurring in May. This census occurs during the flowering period and the model replicates this by starting with the *Reproduction* submodel. The *Survival and growth* and *Seedbank* submodels could come in any order after reproduction took place, as they are independent from each other.

In natural populations, the schedule depends on the fire regime. Reproduction does not happen until the second year after a fire occurs, and only survival and growth, as well as germination or dormancy in the seedbank, are represented in the year of a fire and the following year.

4. Design concepts

1. Basic principles

This model relies on previous knowledge on the life cycle of dewy pines (Paniw et al., 2017; Conquet et al., 2023) to perform a population viability analysis (PVA), a modelling approach commonly used in population ecology. By projecting population dynamics into the future, a PVA aims at assessing the probability of persistence of populations and allows for the introduction of stochasticity in environmental conditions (e.g. fire return, or sampling from a distribution of temperature and rainfall values). While this model is designed for plant populations and does not include any representation of social organisation or individual's decision processes, it allows to take into account demographic stochasticity (by sampling demographic processes from distributions), which is often unaccounted for in PVAs due to the use of simplified population models such as matrix population models (MPM) or integral projection models (IPM).

2. Emergence

Changes in aboveground population size emerge from individual fate, which in turn emerges from the relationship between demographic processes (e.g. survival or reproduction) and individual traits (plant size), density, and environmental variables. Individual traits and density vary with changes in demographic processes affecting individual fate. How the various demographic processes interact to shape individual life histories is imposed by previous empirical observations on the species' life cycle.

Seedbank processes emerge from the simulated sequence of post-fire habitat stages (in natural populations) or from site-specific parameters that do not vary through time parameters (in anthropogenic populations).

3. Adaptation

Individuals do not make any decisions based on objectives in this model.

4. Objectives

Individuals do not use any fitness measure to make decisions.

5. Learning

Learning is not implemented in this model.

6. Prediction

Prediction is not implemented in this model.

7. Sensing

Sensing is not implemented in this model.

8. Interaction

Interactions between individuals in this model are mediated by competition for resources (e.g. light or prey) and facilitation (e.g. provision of shade). These interactions are represented by the effect of density at the beginning of year *t* on demographic processes, and in turn individual fate, from time *t* to *t*+1. Here, density corresponds more specifically to the number of aboveground individuals of size > 4.5 in a given 1-m^2 quadrat, as we expect from observations that individuals further than the quadrat are too far to affect focal plants, and that smaller individuals only have a small effect on other individuals.

9. Stochasticity

Stochasticity occurs at several levels of the model. First, if the user chooses to project the population under current climatic conditions, the sequence of years of the desired length will be created by randomly sampling from the list of observed years. If the user chooses to project the population under future climate-change conditions, this random sampling of observed years is used to obtain the sequence of years to be used as random effects in the submodels, that is, the years representing the variation in demographic processes that is not explained by environmental conditions, individual traits, or density.

Additionally, all demographic processes governing the fate of both aboveground **plants** and **produced and seedbank seeds** are stochastic. For each **plant**, the survival, size (at the next time step or after germinating), flowering status, and

number of flowers are sampled from binomial, scaled Student *t*, and Poisson distributions with parameters obtained from predictions of generalised additive models and depending on the environmental conditions, individual traits, and density. For each **seed**, whether it germinates, stays dormant, or contributes to the seedbank is sampled from a binomial distribution with parameters depending on the site in which the simulation is performed or the time since last fire. The number of seeds per flower for each **plant** is sampled from a Poisson distribution with a fixed mean previously used in population projections for this system (Paniw et al., 2017; Conquet et al., 2023).

Moreover, the location of each seed in the seedbank at the start of the simulation is attributed randomly, with each quadrat having the same probability $\frac{1}{\text{total number of quadrats}}$ to be designated as a seed's location. In subsequent years, all **produced seeds** are assigned to the quadrat of the parent **plant**. This approach allows us to reproduce the lack of active dispersal mechanisms in dewy pines, leading most seeds to fall and establish next to the mother plant.

Finally, when the number of **plants** to add to the population is higher than the capping threshold set by the user, the new individuals to be removed from the recruits are sampled at random.

10. Collectives

There are no collectives in this model.

11. Observation

The two main outputs of this model are (1), for each simulation the yearly population growth rates (log $\lambda = \frac{N_t}{N_{t-1}}$, where N_t is the total population size—above ground and in the seedbank—in year t and $N_{t\text{-}1}$ in year t-1) that can be used to calculate the stochastic growth rate over the whole simulation (log $\lambda_S = \frac{\sum_{t=2}^{T} log\ \lambda_t}{T}$ where T is the number of simulated years), and (2) whether the population went extinct within the number of simulated years, which can be used to obtain the probability of quasi-extinction (proportion of simulations where the population went under the quasi-extinction threshold, i.e., 10 > aboveground individuals and 50 > seeds in the seedbank) across a number of simulations defined by the user.

In addition, the output of the model contains the full individual data across the whole simulation, the mean change in aboveground population abundance (i.e. the population growth rate without taking the seedbank into account), as well as population size and population density (i.e. number of individuals of size > 4.5 per 1-m^2 quadrat).

5. Initialization

For both habitats (natural and anthropogenic) and all scenarios (control and climate change) the initial number of aboveground **plants**, as well as their size and location (**quadrat**) corresponds to that observed in the population and first year chosen by the user for the simulation, as does the density in each **quadrat**. The number of **seeds** present in the seedbank when starting the simulation is defined by the user (by default 10,000 for natural populations and 3,000 for anthropogenic

239 populations), and the **seeds** are initially assigned randomly to their **quadrat**. The
240 number of **produced seeds** and the extinction status are initialised at 0. The
241 sequence of yearly population growth rates, mean change in aboveground
242 population abundance, and population density are initialised with NAs.
243
244 In both scenarios, the required number of years (set by the user) is sampled among
245 the years observed in the full individual data (e.g. 30 samples of years 2016–2021).
246 This sequence of years is used to represent random year variation (i.e., random
247 effects in vital-rate models). However, the sequence of yearly temperature and
248 rainfall values depends on the scenario. Under the control scenario, these values
249 correspond to the observed climate in each year of the sampled sequence. When
250 the population is projected under climate change, the temperature and rainfall values
251 reflect the projected climate values obtained from the global circulation models
252 (GCM) from the first year defined by the user and following a chronological order
253 until the end of the simulation.
254
255 Finally, projecting natural populations requires to initialise a sequence of post-fire
256 habitat stages (0–4). In the first year, this corresponds to the stage observed in the
257 first year of the simulation (defined by the user). The following stages are determined
258 by a Markov chain (Fig. S1; see also Paniw et al., 2017; Conquet et al., 2023), where
259 the transition from the last to the first stage (fire year) depends on the probability of
260 fire return (p), which is set by the user (1/30 by default). The sequence of number of
261 years since the last fire (TSF) is initialised using the observed number in the first

year of the simulation, with the subsequent TSFs being inferred from the sequence of post-fire habitat stages.

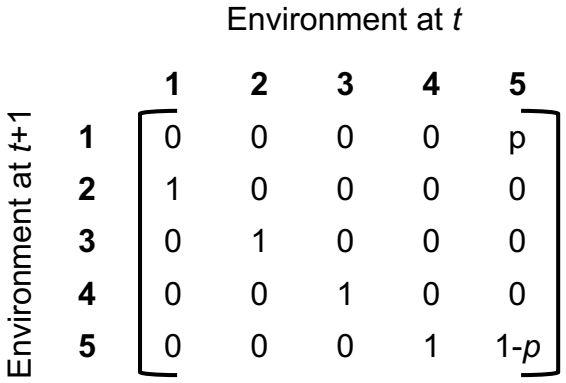

Figure S1 - Markov chain determining the succession of post-fire habitats for the dewy pine population. The first four states (from the fire year to the third year after a fire) constitute the deterministic part of the Markov chain and thus always follow each other in a sequence of 1 to 4 (probability of transition = 1). The fifth state (from the fourth year after a fire) is stochastic, and the transition from this state depends on the fire frequency *p* (i.e., the population will remain in state 5 until a fire occurs).

6. Input data

The model uses as input data individual-based data on dewy pines (aboveground **plants)** in the population chosen by the user. These data have been collected during annual population surveys occurring in May since at least 2016 (earlier for some populations, see Appendix S2). These surveys enabled us to obtain data on individuals' survival, size (log[length of the longest leaf x number of leaves]), reproductive status, and number of flowers (Paniw et al.,, 2017). Additionally, the model uses input data containing values from 2016 to 2050 of (1) average daily

minimum temperature (in ºC) in summer and fall following a census and fall and winter prior to a census, and (2) cumulative rainfall (in mm) in fall and winter following a prior to a census. Details on data sources and preparation can be found in Appendix S2.

7. Submodels

Reproduction

Flowering: Individuals can reproduce from two years after a fire occurred in natural populations (Paniw et al., 2017). The reproductive status of individuals (0 or 1) is drawn from a binomial distribution which probability is predicted from a generalised additive model (GAM) describing the observed relationship between flowering probability and winter mean daily maximum temperature, fall cumulative rainfall, individual size, aboveground density of individuals with size > 4.5, and time since last fire in natural populations (see Appendix S1: Table S5 for the full equation linking the various covariates to flowering probability).

Number of flowers per individual: Reproductive individuals (i.e., flowering = 1) can produce flowers, their number being drawn from a negative binomial distribution which probability is predicted from a generalised additive model (GAM) describing the observed relationship between the number of flowers and winter mean daily maximum temperature, individual size, and time since last fire in natural populations (see Appendix S1: Table S5 for the full equation linking the various covariates to the number of flowers per individual).

Number of seeds per flower: The number of seeds for each flower is drawn from a Poisson distribution with a mean fixed at 9.8, which corresponds to the value used in previous population projections of the dewy-pine system (Paniw et al., 2017; Conquet et al., 2023).

Survival and growth

Survival: Individual survival (0 or 1) is sampled from a binomial distribution which probability is predicted from a generalised additive model (GAM) describing the observed relationship between survival and summer mean daily maximum temperature, fall cumulative rainfall, individual size, aboveground density of individuals with size > 4.5, and time since last fire in natural populations (see Appendix S1: Table S5 for the full equation linking the various covariates to survival).

Growth: The size of surviving individuals in the following year is sampled from a truncated scaled Student *t* distribution with location (i.e. mean), scale (i.e. standard deviation) and degrees of freedom obtained from a generalised additive model describing the observed relationship between individuals' size in the next year and fall cumulative rainfall, individual size, aboveground density of individuals with size > 4.5, and time since last fire in natural populations (see Appendix S1: Table S5 for the full equation linking the various covariates to growth). The minimum or maximum observed sizes were assigned to individuals with infinite size values.

335 *Seedbank*

336

337 Continuous germination and contribution to the seedbank: For each **produced seed**,
338 whether it germinated directly without going to the seedbank (0 or 1) was sampled
339 from a binomial distribution with a mean determined by the probability to germinate
340 when produced (goCont) which depended on time since last fire (in natural
341 populations) or site (in anthropogenic populations) (see Appendix S1: Table S1 for
342 details on the mean values). Among the seeds that will not germinate, seeds that will
343 contribute to the seedbank in the next year (0 or 1) were then sampled from a
344 binomial distribution with a mean determined by 1-goCont. The rest of the seeds
345 were considered dead and removed from the population. In anthropogenic
346 populations, the probabilities of continuous germination and contribution to the
347 seedbank were corrected for seed survival (i.e., multiplied by 0.33) and, in one
348 population (Sierra Carbonera Disturbed), further multiplied by 0.4 to replicate more
349 accurately the observed population dynamics.

350

351 Germination from the seedbank: For each **seedbank seed**, whether it germinated
352 from the seedbank (0 or 1) was sampled from a binomial distribution with a mean
353 depending on time since last fire (in natural populations) or site (in anthropogenic
354 populations) (see Appendix S1: Table S1 for details on the mean values). In
355 anthropogenic populations, the probability of germination from the seedbank was
356 corrected for seed survival (i.e., multiplied by 0.33) and, in one population (Sierra
357 Carbonera Disturbed), further multiplied by 0.4 to replicate more accurately the
358 observed population dynamics.

359

Dormancy: For each **seedbank seed**, whether it remained dormant in the seedbank (0 or 1) was sampled from a binomial distribution with a mean depending on time since last fire (in natural populations) or site (in anthropogenic populations) (see Appendix S1: Table S1 for details on the mean values). In anthropogenic populations, the probability of dormancy was corrected for seed survival (i.e., multiplied by 0.33) to replicate more accurately the observed population dynamics.

Seedling size: The size of a germinating seed is sampled from a truncated scaled Student *t* distribution with location (i.e. mean), scale (i.e. standard deviation) and degrees of freedom obtained from a generalised additive model describing the observed relationship between seedling size and winter mean daily maximum temperature, aboveground density of individuals with size > 4.5, and time since last fire in natural populations (see Appendix S1: Table S5 for the full equation linking the various covariates to seedling size). The minimum or maximum observed sizes were assigned to individuals with infinite size values.

References – Appendix S3

Conquet, E., Ozgul, A., Blumstein, D. T., Armitage, K. B., Oli, M. K., Martin, J. G. A., Clutton-Brock, T. H., & Paniw, M. (2023). Demographic Consequences of Changes in Environmental Periodicity. *Ecology*, **104**(3), e3894. https://doi.org/10.1002/ecy.3894

Grimm, V., Berger, U., Bastiansen, F., Eliassen, S., Ginot, V., Giske, J., Goss-Custard, J., Grand, T., Heinz, S. K., Huse, G., Huth, A., Jepsen, J. U., Jørgensen, C., Mooij, W. M., Müller, B., Pe'er, G., Piou, C., Railsback, S. F., Robbins, A. M., … DeAngelis, D. L. (2006). A Standard Protocol for Describing Individual-Based and Agent-Based Models. *Ecological Modelling*, **198**(1), 115–26. https://doi.org/10.1016/j.ecolmodel.2006.04.023

Grimm, V., Railsback, S. F., Vincenot, C. E., Berger, U., Gallagher, C., DeAngelis, D. L., Edmonds, B., Ge, J., Giske, J., Groeneveld, J., Johnston, A. S. A., Milles, A., Nabe-Nielsen, J., Polhill, J. G., Radchuk, V., Rohwäder, M.-S., Stillman, R. A., Thiele, J. C., & Ayllón, D. (2020). The ODD Protocol for Describing Agent-Based and Other Simulation Models: A Second Update to Improve Clarity, Replication, and Structural Realism. *Journal of Artificial Societies and Social Simulation*, **23**(2), 7. https://doi.org/ 10.18564/jasss.4259

Paniw, M., Quintana-Ascencio, P. F., Ojeda, F., & Salguero-Gómez, R. (2017). Interacting Livestock and Fire May Both Threaten and Increase Viability of a Fire-Adapted Mediterranean Carnivorous Plant. *Journal of Applied Ecology*, **54**(6), 1884–94. https://doi.org/10.1111/1365-2664.12872

Appendix S4 – Results from sensitivity analyses

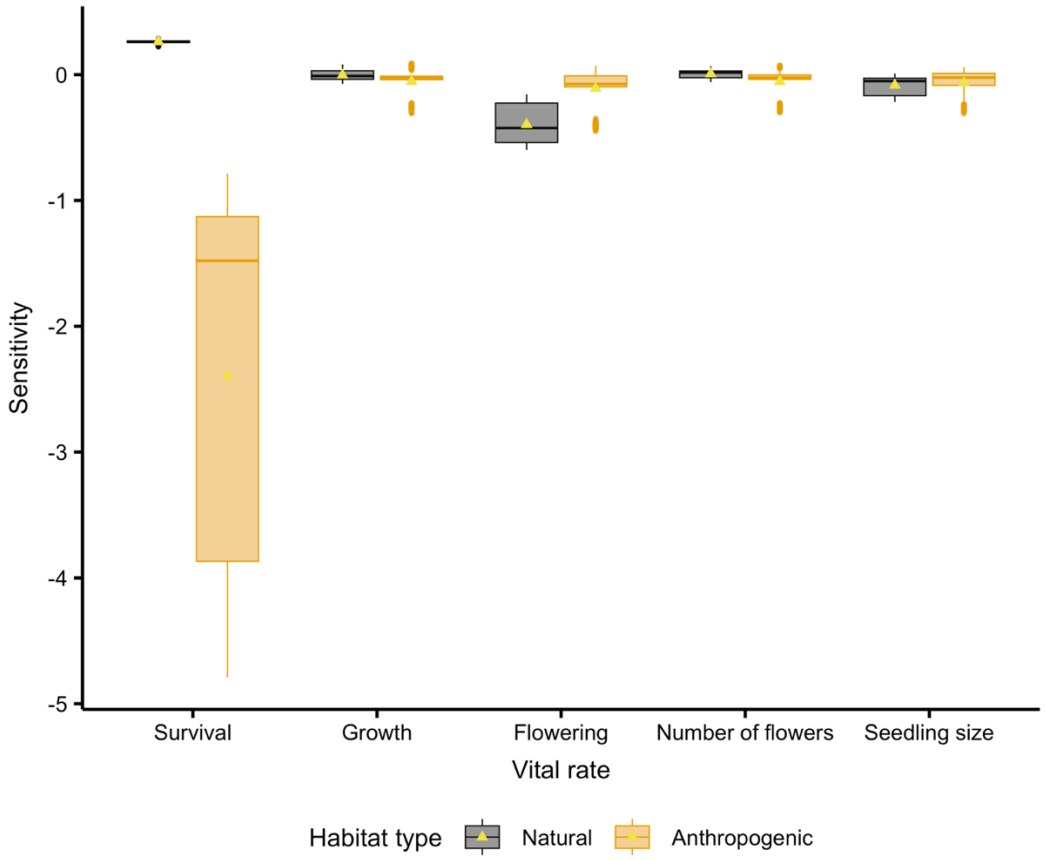

Figure S1 – Sensitivity of stochastic population growth rate across 30 years (log λ_S) to climate-change effects in different vital rates. We projected each natural and anthropogenic population 100 times for 30 years by changing temperature and rainfall values as projected under the RCP 8.5 climate-change scenario in specific vital rates while keeping climatic drivers at their past observed values for the remaining vital rates. We then calculated % changes in log λ_S compared to a control scenario where climatic drivers are at their past observed values for all vital rates (500 log λ_S for each population). We calculated 500 sensitivity values for each population by randomly sampling 100 log λ_S_control from the 500 available and comparing them to the 100 available log λ_S_perturbed. Here we summarise these changes per vital rate, with the triangles representing averages across populations and sensitivity simulations.

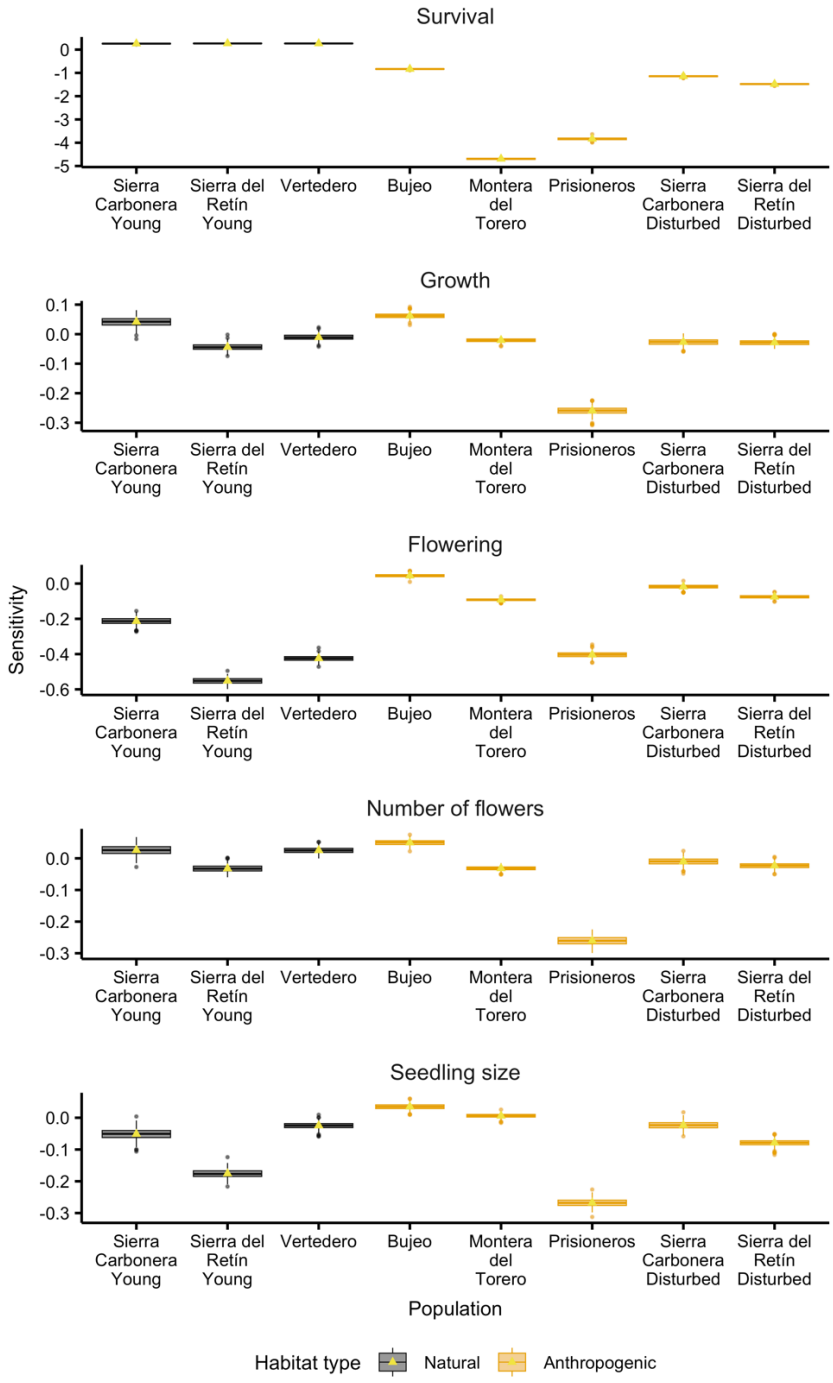

Figure S2 – Sensitivity of stochastic population growth rate across 30 years (log λ_S) to climate-change effects in different vital rates across populations. We projected each natural and anthropogenic population 100 times for 30 years by changing temperature and rainfall values as projected under the RCP 8.5 climate-change scenario in specific vital rates while keeping climatic drivers at their past observed values for the remaining vital rates. We then calculated %

changes in log λ_S compared to a control scenario where climatic drivers are at their past observed values for all vital rates (500 log λ_S for each population). We calculated 500 sensitivity values for each population by randomly sampling 100 log λ_S_control from the 500 available and comparing them to the 100 available log λ_S_perturbed. Here we summarise these changes per vital rate and population, with the triangles representing averages across 500 sensitivity values.